PURPOSE-LED
PUBLISHING™

TOPICAL REVIEW

Plasma power-to-X (PP2X): status and opportunities for non-thermal plasma technologies

View the article online for updates and enhancements.

Topical Review

Plasma power-to-X (PP2X): status and opportunities for non-thermal plasma technologies

Jing Sun[1], Zhongping Qu[1], Yuting Gao[1], Tianyu Li[1], Jungmi Hong[2], Tianqi Zhang[2], Rusen Zhou[1,2], Dingxin Liu[1], Xin Tu[3], Guoxing Chen[4], Volker Brüser[5], Klaus-Dieter Weltmann[5], Danhua Mei[6], Zhi Fang[6], Ana Borras[7], Angel Barranco[7], Shaojun Xu[8], Chuanlong Ma[9], Liguang Dou[10], Shuai Zhang[10], Tao Shao[10], Guangliang Chen[11], Dawei Liu[12], Xinpei Lu[12], Zheng Bo[13], Wei-Hung Chiang[14], Krasimir Vasilev[15], Michael Keidar[16], Anton Nikiforov[17], Ali Rouhollah Jalili[24], Patrick J Cullen[2,18], Liming Dai[19], Volker Hessel[20], Annemie Bogaerts[21], Anthony B Murphy[22], Renwu Zhou[1,*] and Kostya (Ken) Ostrikov[23]

[1] State Key Laboratory of Electrical Insulation and Power Equipment, Centre for Plasma Biomedicine, School of Electrical Engineering, Xi'an Jiaotong University, Xi'an, Shaanxi 710049, People's Republic of China

[2] School of Chemical and Biomolecular Engineering, University of Sydney, Sydney, NSW 2006, Australia

[3] Department of Electrical Engineering and Electronics, University of Liverpool, Liverpool L69 3GJ, United Kingdom

[4] Fraunhofer Research Institution for Materials Recycling and Resource Strategies IWKS, Brentanostraße 2a, 63755 Alzenau, Germany

[5] Leibniz Institute for Plasma Science and Technology, INP Greifswald e.V., 17489 Greifswald, Germany

[6] College of Electrical Engineering and Control Science, Nanjing Tech University, Nanjing, Jiangsu 211816, People's Republic of China

[7] Nanotechnology on Surfaces and Plasma Laboratory, Materials Science Institute of Seville, CSIC-US, C/Americo Vespucio 49, 41092 Seville, Spain

[8] School of Electrical and Automation Engineering, Hefei University of Technology, Hefei 230009, People's Republic of China

[9] Catalytic and Plasma Process Engineering, Department of Chemical Engineering, McGill University, Montreal, Quebec H3A 0C5, Canada

[10] Beijing International S&T Cooperation Base for Plasma Science and Energy Conversion, Institute of Electrical Engineering, Chinese Academy of Sciences, Beijing 100190, People's Republic of China

[11] Department of Materials Engineering, Huzhou University, Huzhou 313000, People's Republic of China

[12] State KeyLaboratory of Advanced Electromagnetic Engineering and Technology, School of Electronic and Electrical Engineering, Huazhong University of Science and Technology, Wuhan, Hubei, People's Republic of China

[13] State Key Laboratory of Clean Energy Utilization, College of Energy Engineering, Zhejiang University, Hangzhou, Zhejiang 310027, People's Republic of China

[14] Department of Chemical Engineering, National Taiwan University of Science and Technology, Taipei 10607, Taiwan

[15] College of Medicine and Public Health, Flinders University, Bedford Park, SA 5042, Australia

[16] Department of Mechanical and Aerospace Engineering, George Washington University, Washington, DC 20052, United States of America

---

* Author to whom any correspondence should be addressed.

[17] Research Unit Plasma Technology (RUPT), Department of Applied Physics, Ghent University, Sint-Pietersnieuwstraat 41, B4, 9000 Ghent, Belgium

[18] PlasmaLeap Technologies, Marrickville, NSW 2204, Australia

[19] School of Chemical Engineering, University of New South Wales (UNSW), Sydney, NSW 2052, Australia

[20] School of Chemical Engineering, The University of Adelaide, Adelaide, SA 5005, Australia

[21] Research Group PLASMANT, Department of Chemistry, University of Antwerp, Universiteitsplein 1, Wilrijk B-2610, Belgium

[22] CSIRO Manufacturing, Lindfield, NSW 2070, Australia

[23] School of Chemistry and Physics and Centre for Materials Science, Queensland University of Technology (QUT), Brisbane, Queensland 4000, Australia

[24] School of Chemistry, University of New South Wales (UNSW), Sydney, NSW 2052, Australia

E-mail: renwu.zhou@xjtu.edu.cn

Abstract

This article discusses the 'power-to-X' (P2X) concept, highlighting the integral role of non-thermal plasma (NTP) in P2X for the eco-friendly production of chemicals and valuable fuels. NTP with unique thermally non-equilibrium characteristics, enables exotic reactions to occur under ambient conditions. This review summarizes the plasma-based P2X systems, including plasma discharges, reactor configurations, catalytic or non-catalytic processes, and modeling techniques. Especially, the potential of NTP to directly convert stable molecules including CO_2, CH_4 and air/N_2 is critically examined. Additionally, we further present and discuss hybrid technologies that integrate NTP with photocatalysis, electrocatalysis, and biocatalysis, broadening its applications in P2X. It concludes by identifying key challenges, such as high energy consumption, and calls for the outlook in plasma catalysis and complex reaction systems to generate valuable products efficiently and sustainably, and achieve the industrial viability of the proposed plasma P2X strategy.

Keywords: plasma power-to-X, non-thermal plasma, gas conversion, plasma catalysis, renewable energy

1. Introduction

Power-to-X (P2X) represents a burgeoning and promising innovation for the imminent renewable energy landscape. While the term P2X lacks a universal definition [1], here we define the term P2X covers processes for converting renewably sourced electricity ('P') to value-added chemicals or fuels ('X'), especially energy carriers such as H_2, syngas, methanol and ammonia [2]. Additionally, we consider the source of 'X' to be readily available resources such as water, air (N_2 and O_2), CO_2, and methane (CH_4). This approach broadens the adaptability of sustainable energy systems by facilitating energy storage, transportation, and subsequent conversion processes that rely heavily on electricity generated from renewable energy. P2X offers a pathway to the decarbonization of global industry and society by replacing fossil fuels in numerous industrial production processes, helping to curb greenhouse gas emissions. One of its goals is to harness both the economic and environmental potential of renewable electricity [3].

Currently, the core technology behind P2X is electrochemistry, which has been extensively studied. It uses renewable electricity to transform water or seawater into hydrogen and oxygen/chlorine [4, 5], NO_x or N_2 into ammonia [6, 7], and CO_2 into CO [8], syngas and formic acid [9]. However, in certain applications, the 'power' in electrochemistry is insufficient to activate stable molecules effectively, leading to low reactivity or poor water solubility of the reactants, such as N_2, as well as competition with the hydrogen evolution reaction (HER). As a result, electrochemistry exhibits relatively low productivity. For instance, in ammonia synthesis from N_2 and water, productivity typically ranges between 10^{-9} and 10^{-11} mol cm^2 s^{-1}, which makes reliable detection challenging and, barring a few exceptions, results in very low selectivity, below 1% [10]. Importantly, we need to understand how exactly to use the 'power' of renewable electricity, which, according to the conventional definition, is the energy divided by time. The more energy used over the shorter time, the higher the power. In this case, electrochemistry features relatively low powers as it utilizes energy over longer process durations.

Non-thermal plasma (NTP) technology, on the other hand, offers unique opportunities to gainfully utilize much higher powers, in particular because of the possibility to generate highly reactive plasma discharges over much shorter periods

J. Phys. D: Appl. Phys. **57** (2024) 503002

Topical Review

Table 1. Comparison of plasma [19–23], electrochemical [24–28], thermal [29, 30], photochemical [31–34], and biological [35–38] processes for gas or liquid conversions.

Process	Energy consumption	Product rate	Capital cost	Operating cost	Flexibility	CO_2·footprint
Plasma	High	High	Low	High	High	Low
Electrochemical	Medium	Medium	Low	Medium	Medium	Low
Thermal	High	High	Medium	High	Low	High
Photochemical	Medium	Low	High	Low	Medium	—
Biological	—	Low	High	High	Low	—

(e.g. even in the nanosecond range), while using relatively low amounts of energy. The ability of NTP to massively accelerate chemical reactions at near-ambient conditions has attracted strong attention across several scientific and technological fields. Consequently, NTP is regarded as a highly promising scenario for P2X, which we define as the *Plasma Power-to-X*, or *PP2X,* with the additional 'P' referring to NTP. Plasma, commonly referred to as 'the fourth state of matter' alongside solid, liquid, and gas, is a partially ionized gas consisting of various reactive species such as electrons, diverse ions, radicals, excited atoms, vibrationally and electronically excited molecules, and neutral ground state molecules [11]. NTP is generated by applying electricity, typically high voltage, to a gas. This process energizes highly mobile electrons via the applied electric field, which then activates ground-state gas molecules through the excitation, ionization, and dissociation processes. This chain of reactions generates a large variety of reactive species and enables chemical reactions, including thermodynamically unfavorable ones, to occur under ambient temperature and pressure [12]. The unique thermal nonequilibrium nature of NTP (electron temperatures are typically much higher than the temperatures of ions and neutral species) makes it particularly promising for gas conversion applications. The highly energetic electrons (with typical energies in the 1–10 eV range) can effectively activate ground-state gas molecules (e.g. N_2, CO_2 and CH_4), breaking down their stable bonds or reducing their energy barriers without heating the entire gas bulk or adding extra chemicals/solvents. In this regard, NTP presents a highly promising approach to overcome the constraints of other existing electricity-driven technologies. Therefore, it is crucial to assess the plausible contributions of NTPs within the realm of renewable P2X technologies, and to map the directions for further advances in the near future, and this is the key aim of this review.

To understand the role of plasma technology in gas and liquid conversion processes beyond P2X, we compared it with other methods, including thermal, photochemical, and biological processes, each utilizing different energy sources like heat, light, and biological energy. Table 1 shows a qualitative overview of common conversion processes, noting that varying standardized frameworks across technologies make precise comparisons challenging. Thus, only relative comparisons are made here. Photochemical and biological processes directly use solar energy, while other methods rely on electricity or heat, leading to some energy losses during the conversion process. Plasma and electrochemical processes can draw from diverse energy sources, such as solar, wind,

and tidal energy, providing flexibility. However, NTP technology remains highly energy-intensive, hindering its commercial applications. Thermal processes are generally mature but still heavily rely on fossil fuels, resulting in significant CO_2 emissions. Encouragingly, researchers have begun exploring solar energy for heat generation. While most technologies deliver high conversion rates and yields, photochemical and biological processes tend to lag behind. Plasma and thermal processes have relatively high operation costs, mainly due to the high energy consumption, while biochemical processes remain relatively costly due to their complexity and specialized requirements.

1.1. Scope and structure of the review

This review focuses on exploring the opportunities and challenges associated with NTP discharges in the context of renewable P2X technologies. It offers an overview of the current approaches and the potential of plasma-based gas conversion to produce eco-friendly chemicals and fuels (figure 1). In the second section, we introduce nonthermal plasma-based P2X systems, including different types of plasma discharges, along with the corresponding reactor designs and plasma catalysis processes. Section 3 is dedicated to examining direct NTP-assisted gas conversions (involving CO_2, CH_4, air/N_2), providing any available experimental evidence of their significance. In section 4, we discuss the applications of hybrid P2X technologies, which involve various combinations of NTP with other techniques, such as electrocatalysis and photocatalysis. Section 5 analyzes future scenarios for energy and chemical production, and how the plasma technology could forge new routes for renewable P2X. We conclude the review by highlighting the areas within plasma science, chemical engineering, and chemistry that are promising to ensure further technological advances toward a sustainable global economy and society.

It is important to highlight some aspects not fully covered in this review but still worth noting. First, PP2X is crucial not just for manufacturing chemicals and fuels but also for producing various 'X' components like catalysts, electrodes, and support structures [13–15]. For instance, plasma polymerization [16], an eco-friendly method that forms polymers using plasma without harmful solvents, exemplifies this by creating carbon-based catalysts and supports. This process bypasses traditional waste treatment methods, reflecting the rapid evolution of the field. Second, 'X' can also be sourced from readily available resources like biomass, plastic materials, and

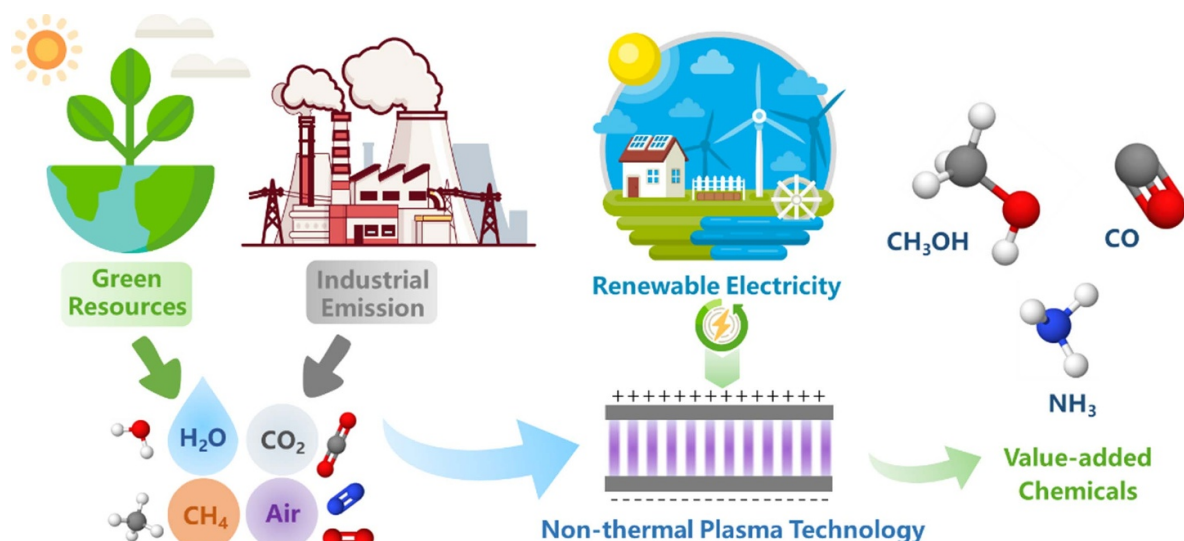J. Phys. D: Appl. Phys. **57** (2024) 503002

Topical Review

Figure 1. Schematics of non-thermal plasma power-to-X (PP2X) approach for diverse applications.

waste products [17]. Third, while plasma technology has broad applications, its productivity and energy efficiency vary by process. For instance, electrolysis may outperform plasma in hydrogen production, but nitrogen fixation benefits significantly from plasma technology. This study focuses on the NTP applications that offer unique advantages over electrochemistry. Lastly, thermal plasmas like microwave plasma are highly energy-efficient (up to 80%–90% at reduced pressures) but operate at extremely high temperatures above 3000 K [18]. Thus, their discussion falls outside this NTP-focused review.

2. NTP systems

NTP gas discharges are widely recognized for their ability to operate under ambient conditions. The gas breakdown typically necessitates a substantial electric field, achieved by applying an electric potential difference across two electrodes, thus forming the discharge zone in the gaps. This potential might comprise direct current (DC), alternating current (AC), or pulsed energy.

By modifying electrode geometries, configurations or power sources, various types of NTPs can be generated for use in plasma-based energy applications. In a gas-phase system, the primary NTP types for gas conversion include dielectric barrier discharge (DBD) and gliding arc (GA). When a liquid is introduced to the plasma system (gas–liquid systems), gas-phase generated plasmas interact with the liquid (*i.e.* in a pre-existing bubble, over a liquid surface, or when the latter is in the form of water sprays and droplets). This interaction significantly influences the chemical composition of the species produced directly in the liquid due to varying breakdown strengths in the gas phase and solution phase. The main types of NTP in gas–liquid systems include atmospheric-pressure plasma jet (APPJ), plasma-bubble discharges and surface discharges. In addition, the integration of NTP with

heterogeneous catalysts through plasma catalysis is drawing increased attention due to the strong interplay of plasmas and catalysts often leading to pronounced synergistic effects.

This section will focus on NTP systems in terms of plasma discharge types with the corresponding reactors, power sources and plasma catalysis setups, discussing their working principles and typical operating conditions, highlighting their strengths and weaknesses, as well as the modeling aspect of progress and challenges with a few examples of how they have been applied in P2X.

2.1. Discharge types

Here we introduce typical types of NTPs commonly utilized in P2X applications for gas conversion. These include DBD and GA for gas phase systems, as well as gas–liquid discharges (GLDs).

2.1.1. Dielectric barrier discharge (DBD). DBD is a non-uniform plasma generated by applying an electric field (i.e. AC) between two electrodes, with at least one covered by a dielectric barrier, which will limit the amount of charge transported between the electrodes and thus reduce the electric current [39, 40]. This feature prevents the discharge from transitioning into a thermal plasma mode. The DBD can be configured using two parallel plates or concentric cylindrical electrodes (refer to figure 2). A typical cylindrical reactor consists of an inner electrode connected to a power supply, surrounded by a dielectric tube, providing a gap of a few millimeters; the outer electrode is often a mesh or foil that is covered around the tube as ground. The cylindrical configuration is more applicable for gas conversion, where the working gas flows in from one side and is gradually converted along its way through the gap between the inner electrode and dielectric tube, resembling a plug flow reactor, and flows out from the other side.
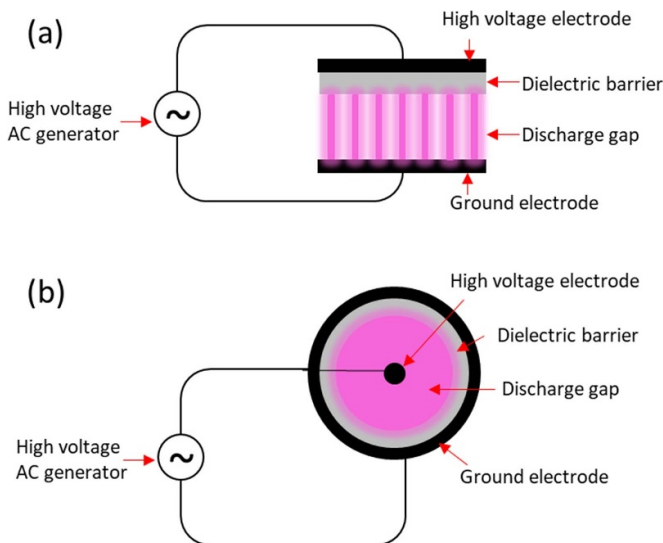
Figure 2. Typical reactor setup of BDD with (a) parallel plane electrodes or (b) concentric cylindrical electrodes. Reproduced from [19]. CC BY 3.0.

Figure 3. Schematic of gliding arc systems. (a) Conventional 2D gliding arc plasma [41]; (b) reverse vortex flow gliding arc plasma [43].

The simple design of the DBD reactor, together with its mild operation conditions (ambient pressure and temperature), makes it easy to scale it up for commercial applications. Moreover, the DBD reactor is well-suited for incorporating catalysts within the plasma discharge area, enabling enhanced control over the selectivity of value-added products through plasma catalysis. Further details will be discussed in section 2.2. While DBD plasmas exhibit generally acceptable conversion efficiency, the energy efficiency in the plasma-assisted chemicals production is lower compared to other plasma systems.

2.1.2. Gliding arc (GA). A GA discharge refers to a transient arc discharge generated between two flat diverging electrodes with applied high-voltage electricity [39]. In a conventional GA reactor in figure 3(a), the arc is initiated and then moves along the electrodes from the shortest inter-electrode distance to the larger inter-electrode distance (in the Z direction) propelled by the gas blast until it extinguishes. Subsequently, a new arc forms immediately from the shortest inter-electrode distance and the generation process is repeated [41].

To enhance the gas conversion efficiency of this conventional two-dimensional GA discharge, the design of three-dimensional reactors, such as the reverse vortex flow (RVF) GA or rotating GA (RGA), can be employed. In the three-dimensional configuration, more gas can pass through the arc discharge zone, increasing the residence time of the feed gas. Figure 3(b) illustrates the RVF GA, where a stable arc discharge is initiated between the top and bottom electrodes and rotates around the Z-axis. The reverse vortex effect prolongs the residence time of the reacted gas within the plasma discharge region and promotes a more uniform discharge compared to the conventional GA setup [42, 43].

The mild operation conditions of the GA discharge make it also appropriate for industrial applications. Furthermore, GA
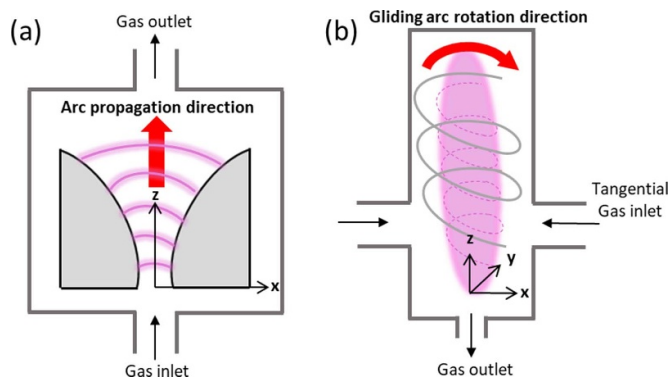
exhibits a relatively high energy efficiency for many gas conversion applications. However, due to the fairly high gas temperature ($T_e = 1.4$–2.1 eV and $T_g = 1000$–3000 K), the conversion is considered to be mainly thermal [44]. Moreover, it is hard to further improve the gas conversion performance, as the existing reactor designs seem to be already quite optimized [20], and it is difficult to combine a GA with a catalyst.

2.1.3. Gas–liquid discharge (GLD). GLD involves interactions between NTP and water or other liquids. This process has been extensively studied for its diverse applications, including water purification [45], medical and biotechnological uses [46], and the synthesis of chemicals and nanomaterials [47]. Recently, GLD technology has emerged as a promising environment-friendly method for converting gases into valuable liquid products, expanding its range of applications [48, 49]. In GLD, the chemical reactivity arises from the presence of highly reactive chemical species and solvated electrons that are generated during the interactions between the plasma and the liquid medium [50]. Various configurations have been employed to achieve GLDs, as shown in figure 4. These configurations can be broadly categorized into three main groups:

(1) direct discharges in liquids;
(2) discharges in the gas phase over a liquid:
   - Without direct electrical coupling with the liquid;
   - With a conductive liquid as an electrode;
   - At the plasma–liquid interface (surface discharges);

(3) discharges in multiphase environments including:
   - Gas phase plasmas with dispersed liquid sprays or foams;
   - Gas phase plasmas in bubbles inside liquids.

NTP discharges are commonly produced in liquid media using high-voltage pulses in pin-to-pin or pin-to-plate configurations, as illustrated in figure 4(a). These discharges typically require a rapid breakdown process, which is often achieved through microsecond voltage pulses [52]. However, this high breakdown voltage requirement can lead to electrode
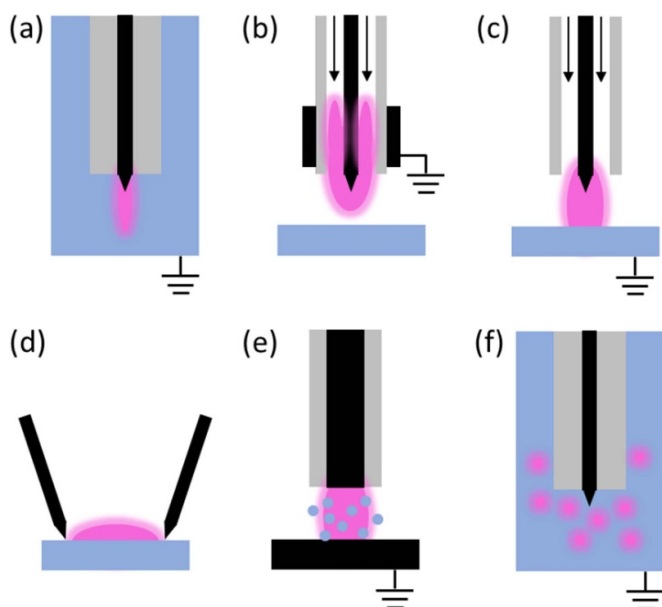
Figure 4. Schematic of different discharges used in plasma–liquid interactions: (a) direct discharge in liquid, (b)–(d) gas phase discharges and (e) and (f) multiphase discharges. In more detail: (b) plasma jet without direct contact with liquid, (c) gas phase plasma with liquid electrode, (d) surface discharge, (e) gas phase plasma with dispersed liquid phase (aerosols) and (f) discharges in bubbles. Here, blue color denotes liquid, pink—plasma, grey—dielectric, black—metal electrodes. Reproduced from [51]. © IOP Publishing Ltd. All rights reserved.

corrosion and increased power consumption. In this type of GLD, only electron impact dissociation and thermal dissociation of water are typically considered as the mechanisms for radical production. The calculated stable final products are H_2O_2, H_2, and O_2, with densities of H• and •OH reaching up to 8.5×10^{24} m^{-3}. These results align well with the liquid phase measurements and the associated theoretical model [53]. Due to the limited reactive species generated in this GLD type, its application in the P2X field has been constrained.

The second type of GLD involves gas phase discharges occurring over a liquid surface, with the liquid acting as a collector for the species generated by the gaseous plasma (figure 4(b)). The liquid phase can be utilized as an electrode (figures 4(c) and (d)). While it is relatively easy to initiate plasma over the liquid surface using this approach, it often results in unstable discharges and intem transfer of gaseous plasma species into the liquid medium. Figure 4(e) presents the third type of GLD, where liquid enters the plasma volume as molecules or small droplets (aerosols). The direct contact between water and plasma in this configuration generates a larger quantity of H species, which can provide more protons to produce substances such as ammonia, methanol, and ethanol. Another configuration for the third type of GLD is sketched in figure 4(f) and is known as plasma-bubble discharges. These discharges are generated within the liquid phase by introducing pre-existing bubbles. This approach can lower the breakdown voltage to some extent and enhance the mass transfer of reactive species from the gas phase to the liquid phase [48]. Recent studies reveal an increasing interest in bubble

discharges or plasma bubbles, showcasing their broad range of applications and potential for achieving more efficient chemical reactions with the reactive species generated underwater [54, 55].

In figure 5, the intricate interactions between plasmas and water are summarized, specifically focusing on an air plasma as an example, although various other gas mixtures are also significant. The diagram considers several processes, including gas phase chemistry, transport of species across multiple phases, mass and heat transfer, interfacial reactions, and liquid phase chemistry. The gas–liquid interface, a critical zone of interaction, showcases major processes such as diffusion and sputtering and additional processes such as evaporation and electrolysis. In the liquid phase, dissolved species such as hydrogen peroxide and various nitrogen oxides participate in further chemical reactions, contributing to processes like water treatment and forming reactive molecules like peroxynitric acid. It is important to note that different radicals penetrate different depths based on their lifetimes, resulting in varying thicknesses of the interfacial layer for different processes and species. GLDs are widely applied across multiple domains, such as CO_2 reduction, nitrogen fixation, and waste treatment. In CO_2 reduction, GLDs activates CO_2 molecules under ambient conditions, efficiently converting them into chemicals like oxalic acid [56]. For nitrogen fixation, GLD enables low-temperature activation of nitrogen and hydrogen, enhancing sustainable ammonia production [57]. In waste treatment, GLD not only breaks down pollutants but also generates valuable chemicals, illustrating its dual benefits in both environmental purification and resource recovery [58].

2.1.4. Comparison of different plasma types. In the realm of plasma technology, a comparative analysis between GA, DBD and GLD plasmas exhibits distinctive properties and efficiencies, especially in gas conversion application. Table 2 summarizes how each type of discharge, distinguished by its discharge power, power supply configuration, pressure, and other variables, produces plasmas with different energy densities and temperatures.

GA plasma operate effectively at atmospheric pressure and showcases good energy efficiency. Its main limitation lies in the low conversion rates, around 10%, primarily due to the short gas residence time and the need for high gas flow rates. Despite these constraints, post-plasma catalysis (PPC) significantly enhances its conversion and efficiency. The relatively high gas temperature of GA limits the direct integration of catalysts. In contrast, DBD plasma, characterized by a higher reduced electric field, directs a larger portion of electron energy to electronic excitation, making it less efficient for vibrational excitation compared GA plasmas. The electric field GA plasmas is generally lower, leading to lower electron energy, which is more conducive to vibrational excitation of molecules like CO_2. While the simplicity and mild operational conditions (ambient pressure and temperature) of DBD reactors make them easily scalable for commercial use. Additionally, DBD reactors are conducive to integrating catalysts directly into the plasma discharge area, allowing
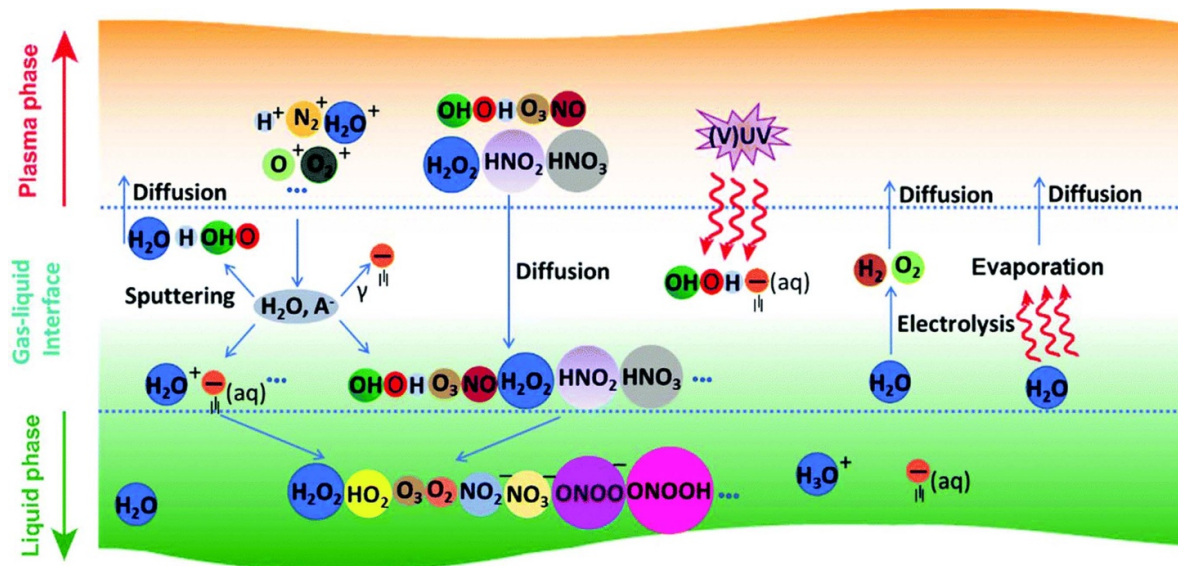
J. Phys. D: Appl. Phys. **57** (2024) 503002

Topical Review

Figure 5. Schematic of the most important transfer processes at the plasma–liquid interface. Reproduced from [59] with permission from the Royal Society of Chemistry.

Table 2. Properties of plasma in different reactor types [19, 51, 60–66].

Discharge type	DBD	GA	GLD-in liquid	GLD-over liquid
Electron energy (eV)	1–30	1.4–2.1	1	1–3
Electron density (cm^{-3})	10^{12}–10^{15}	10^{14}–10^{15}	10^{24}–10^{26}	10^{16}–10^{21}
Gas temperature (K)	300–500	1000–3000	1000–7000	300–400
Pressure (bar)	1	1	$<10^4$	1
Reduced electric field (Td)	1–500	50	/	<100
Key feature	Easy to combine with catalysts	Relatively higher energy efficiency	Not applicable in PP2X	H and OH radicals generated at gas–liquid interface

for better control over the selectivity of value-added products through plasma catalysis.

The GLD system, particularly when interacting with water, generates more reactive species, notably OH radicals, crucial for forming various liquid products like methanol and for biomedical applications. The plasma community can also benefit from coupling GLD with established work in the field of electrochemistry, photolysis, biocatalysis as discussed in detail in section 4. Integrating plasmas with liquids, is promising; however, understanding of reactive species densities and transfer at the gas–liquid interface remains limited. This complex interface poses scientific challenges and opportunities, particularly in fields like plasma medicine, materials synthesis, and environmental management. Advancements in plasma-induced chemistry in liquids, addressing broader societal issues in energy, environment, and health, require coordinated efforts in diagnostics and modeling.

2.2. Plasma catalysis

Plasma catalysis, also known as plasma-assisted catalysis, plasma-catalysis coupling, or plasma-driven/enhanced catalysis, refers to the integration of plasma discharges with catalytic materials to create a highly interactive system, enhancing the performance of plasma-activated reactions such as ammonia synthesis [67], CH_4 conversions [68], CO_2 hydrogenation [69] and water-gas shift reaction [70]. Typically using non-thermal and atmospheric pressure plasmas, plasma catalysis allows reactions to occur at lower environmental temperatures and higher rates [71]. Catalysts are crucial in increasing reaction selectivity and speeding up chemical processes by providing lower-energy pathways. This combination of plasmas and catalysts extends the applicability of PP2X approach, facilitating the efficient conversion of low or negative-value materials like CO_2, CH_4 and biomass into carbon-neutral fuels, opening new avenues for renewable P2X technology.

The effectiveness of a catalyst in chemical reactions relies heavily on its structural, physical, and chemical properties. Reactions take place between the species adsorbed onto the surface of the catalytic material, either interacting with other adsorbed species (Langmuir–Hinshelwood (L–H) reactions) or with species present in the gas phase (Eley–Rideal (E–R) reaction) [72]. These active adsorption sites determine the mechanisms that provide pathways with lower energy requirements for the reactions to occur.

Research on plasma catalysis can be traced back more than sixty years ago. One of the earliest notable studies dates back to 1954, where a low-pressure DC discharge of ammonia was

investigated, leading to the observation of hydrazine formation. The study involved coating the walls of the discharge tube with platinum, which catalytically enhanced the yield of hydrazine by removing hydrogen atoms [73].

In 1992, Mizuno *et al* published a ground-breaking work on atmospheric pressure plasma catalysis [74]. Their study focused on the synthesis of methanol (CH_3OH) from CH_4 and CO_2 in a DBD reactor. The catalyst used was ZnO–CrO_3, which significantly improved the efficiency of the synthesis. Over the following decades, extensive research has been conducted on atmospheric pressure, NTP catalysis, resulting in significant progress in understanding the underlying processes. This research has provided valuable insights and knowledge in terms of the configuration and interaction between plasma and catalysts. In this section, we will briefly discuss plasma catalysis, emphasizing its configuration and the interaction between plasma and catalysts. We will explore specific examples related to this topic in sections 3 and 4.

2.2.1. Configurations for coupling plasma with a catalyst.

Most research on plasma catalysis has been reported with DBD plasma reactors in a packed-bed configuration, where packing materials are typically beads (of a few mm diameters) coated by catalysts. The DBD configuration is preferred for plasma catalysis due to its numerous advantages, including a high density of energetic electrons, low processing temperature, continuous operation, easy integration with catalysts, and cost-effectiveness in terms of operation and maintenance. In general, plasma and catalysts can be configured in two main ways. The first approach involves placing catalysts directly within the plasma discharge region, often referred to as in-plasma catalysis (IPC) or a one-stage plasma-catalytic system (figure 6(a)). The second approach is to position catalysts downstream of the plasma, known as PPC or a two-stage arrangement (figure 6(b)). PPC can be expanded to incorporate multiple catalysts placed in sequence, enabling a multistage plasma catalysis process that facilitates versatile treatment of various gas stream compositions (figure 6(c)) [75]. So far, this 'chained' catalyst configuration has been used for volatile organic compounds (VOCs) removal [21], but its application in PP2X processes has been limited. However, it holds promise as a feasible method to address complex gas mixtures in future applications. The method of introducing catalysts into plasma reactors plays a crucial role in determining the nature of plasma catalyst interactions. In DBD reactors, catalysts are commonly packed between the electrodes. The particle size, quantity applied, and packing method can significantly influence the performance of plasma-catalyst processing, as observed in the case of dry reforming of CH_4 with CO_2 in a DBD reactor [76]. However, packed-bed reactors of this type have inherent drawbacks, including difficulties in scaling up and high pressure drops caused by the packing.

Several studies have explored the utilization of ceramic monoliths that are either coated or impregnated with catalysts. One study [77] examined ceramic honeycombs and foams
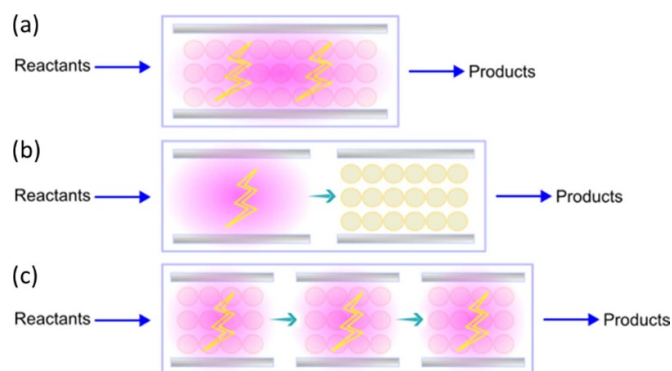

Figure 6. Typical configurations of plasma coupled with catalysts: (a) one-stage plasma catalytic system; (b) two-stage plasma catalytic system; (c) multi-stage plasma catalytic system.

subjected to both A.C. and D.C. discharges and found that the size of the microporous channels influences the formation of surface microdischarges within the pores. Another study [78] demonstrated that employing alumina ceramic foams coated with Ni and Rh can effectively regulate the discharge temperature in a DBD reactor and enhance the chemical reactions involved in the dry reforming of CH_4 with CO_2.

Nevertheless, incorporating a catalyst directly into the discharge region of certain plasma reactors, especially GA discharges, has posed challenges. To address this issue, Schmidt-Szaloskwi *et al* [79] introduced an innovative approach using a fluidized bed for methane conversion. This method involves introducing gaseous reactants from the bottom of the reactor, which lifts the powdered catalyst into the discharge region located between the electrodes, thereby facilitating effective gas-surface interactions. In a similar approach, Lee and Sekiguchi [80] employed a fluidized bed configuration in a GA reactor to directly convert methane into higher hydrocarbons. Additionally, Wang *et al* [81] utilized a comparable setup in a DBD reactor for the dry reforming of methane (DRM).

To date, there have been limited investigations into catalysis for plasma–liquid systems, particularly in P2X applications. Only a few studies [82] have demonstrated the synergistic effects of coupling water plasma bubbles with ions (such as Fe (III)–S (IV)) in liquid for antibiotics degradation. These reports have revealed that the synergetic mechanism operates through self-perpetuating chain reactions, including the oxy-sulfur radical cycle, Fe (II)/Fe (III) cycle, and Fenton reaction. These findings have opened up a potential new avenue for future research on catalysis in plasma–liquid systems. They offer greater opportunities for the application of plasma technology, specifically GLD, in P2X processes.

2.2.2. Plasma-catalyst interactions.

Plasma catalysis has garnered increasing interest due to its potential applications in various energy and environmental fields. However, the underlying mechanisms of plasma-catalyst interactions remain incompletely understood. These interactions are intricate, as
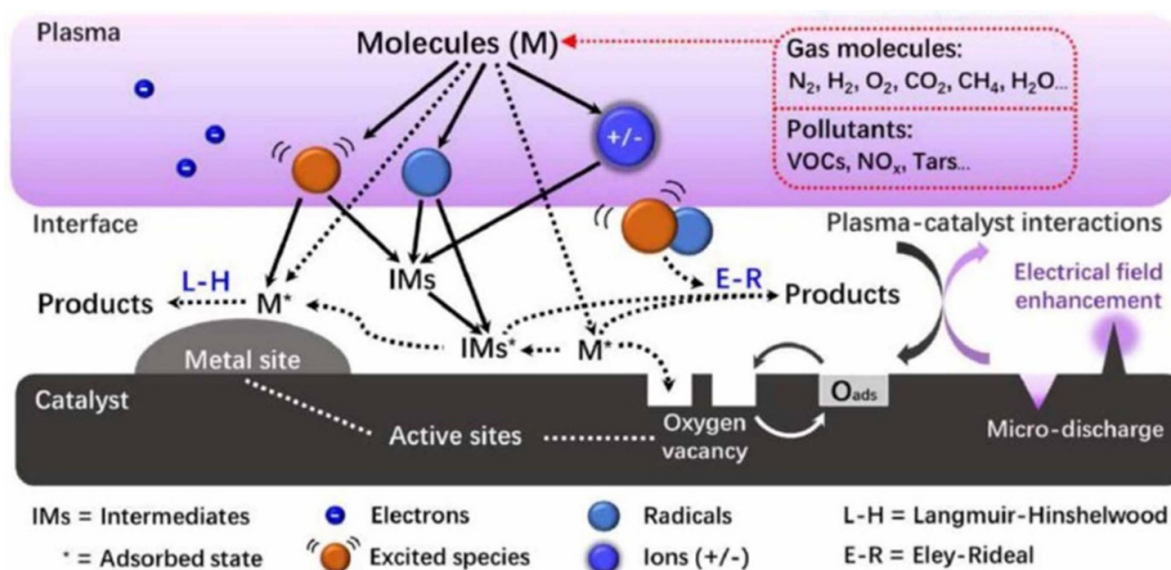
Figure 7. Important mechanisms and species in the plasma and at the catalytic surface, indicating the complexity of plasma catalysis. Reproduced from [83]. © The Author(s). Published by IOP Publishing Ltd. CC BY 4.0.

the catalyst can influence the plasma both chemically and physically, while the plasma, in turn, can affect the properties and catalytic mechanisms of the catalysts. Similar to conventional catalytic processes like thermal catalysis and electrocatalysis, a prerequisite for a reaction to take place on the plasma-exposed catalyst surface is the adsorption of reactants onto that surface.

Figure 7, extracted from 'The 2020 plasma catalysis roadmap' [83], provides a visual representation outlining the primary species, reactions, and processes involved in plasma catalysis within a one-stage plasma-catalytic system. Various plasma species—such as electrons, ions, and radicals—are produced under excitation in high voltage fields and interact with gas molecules including N_2, H_2, O_2, CO_2, CH_4, H_2O, as well as pollutants like VOCs and NO_x. These species are adsorbed and transformed into intermediates on the catalytic surface, which is equipped with metal and active sites essential for converting these intermediates into final products. The interface is distinguished by critical processes such as adsorption and specific reaction pathways, particularly the Langmuir–Hinshelwood and E–R mechanisms, which significantly enhance reaction efficiency. Moreover, the effectiveness of the system is further amplified by electrical field enhancements and micro-discharges that dynamically influence the catalytic reactions. This interaction between the plasma and the catalyst produces a synergistic effect that optimizes the overall process performance.

Unlike thermal catalysis or other conventional catalysis, where ground-state molecules are primarily activated by heat, plasma catalysis involves a rich mixture of species including vibrationally and electronically excited molecules, atoms, ions, radicals, and electrons, offering a more diverse set of reactive entities in the gas phase. This leads to a significantly broader range of chemical reactions. The interactions between plasmas and catalysts rely on various mechanisms, such as heat and charge transfers, as well as alterations in electric fields. Consequently, the composition and properties of the support materials (such as dielectric beads) must be considered, as they can influence the available chemical reaction pathways. Additionally, plasma impacts the catalytic surface by inducing heating, charging, and modifying the structure and morphology of the catalyst. While the temperature's influence on different plasma catalysis processes has been investigated, it is commonly assumed that the surface temperature is close to the temperature of the plasma gas.

Understanding the complex physicochemical interactions between plasmas and catalysts is vital but challenging. These interactions involve various physical phenomena such as discharge formation, species transport in pores, electric field enhancements, charging, heating, and modification of the catalyst surface, all of which are tightly coupled with plasma chemistry [84]. To gain deeper insights into plasma chemical reactions, especially those involving surface-adsorbed species, it is crucial to establish close correlations between experimental observations and theoretical modeling. This approach will enable us to guide the design of plasma reactors, optimizing species transportation to the catalyst surface, shaping the electron energy distribution function to enhance plasma chemistry, and improving catalyst design to create a more favorable environment for surface reactions involving active species present in the plasma. To advance the field of plasma catalysis and conduct thorough fundamental studies, it is imperative to enhance existing methodologies and develop new diagnostic techniques and experimental setups. These efforts will help overcome current limitations.

Currently, the use of *in situ* diagnostics for studying plasma-catalyst interactions is still in its early stages. The available *in situ* measurements for plasma catalysis are limited to two main techniques: (i) fast imaging using intensified charged-coupled device cameras to observe the morphology of

plasma filaments on catalytic surfaces; (ii) broadband infrared absorption using Fourier transform infrared spectroscopy, with options including diffuse reflectance infrared Fourier transform spectroscopy [85], transmission [86–88], or attenuated total reflectance [89] configurations; and (iii) *in-situ* Raman spectroscopy [90] which is intensively used to obtain information about surface processes. These methods allow the monitoring of infrared-active adsorbed molecules on materials exposed to plasma.

2.3. Plasma modeling

In addition to the *in situ* diagnostics, the development of 0D chemical kinetics models or 2D/3D fluid dynamics models and density functional theory (DFT) calculations to understand the reaction pathways on the catalyst surface are also essential. These models should incorporate both plasma and surface chemistries to optimize the plasma discharges and catalysts. Despite the difficulties posed by the intricate nature of plasmas in interaction with reactive surfaces, significant advances have been made in plasma modeling, including (i) modeling the impact of solid reactor materials on plasma [91] and (ii) integrating plasma chemistry with surface reactions [84].

Among possible modeling techniques, zero-D plasma chemistry model was used to identify the important intermediates and pathways regarding various gas conversion applications as shown in one example of figure 8 for NO_x synthesis [92]. GlobalKin [93, 94] and ZDPlaskin [95] have been heavily used in recent years for this purpose, combined with Boltzmann equation solver such as ELENDIF [95] or BOLSIG+ [96]. Numerous studies and investigations using this global modeling revealed crucial information and understanding of different gas conversion process enhanced by various plasma discharges. However, as discussed in section 2.2.2, the complexity of plasma-surface interaction in plasma catalysis, remained as a significant challenge compared to what has been developed for sophisticated gas phase discharge models or pure chemical catalysis models under thermal equilibrium condition [83].

Hong *et al* [97], for the first time, considered the discharge plasma surface reaction and molecular vibrational excited states in the model, and combined the kinetic model with the spatiotemporal-dependent discharge model to obtain a more accurate model for the synthesis of NH_3 from atmospheric-pressure N_2–H_2, which provides theoretical guidance for the industrial synthesis of ammonia. Zhang *et al* [49] modeled the plasma discharge process by ZDPlaskin to compare the electron loss fraction and electron collision rate over time with different catalysts to select the most suitable catalyst. Wang *et al* [92] investigated the NO*X* synthesis process in a dual-power sliding arc reactor by ZDPlaskin modeling, which elucidated the roles of various particles and their vibrationally excited states in the NO_x synthesis process, and provided a guide on how to further improve the sliding arc technology to form NO_x. Ramakers *et al* [98] have elucidated the fundamental plasma chemistry of CO_2 conversion in a novel sliding arc plasma gas
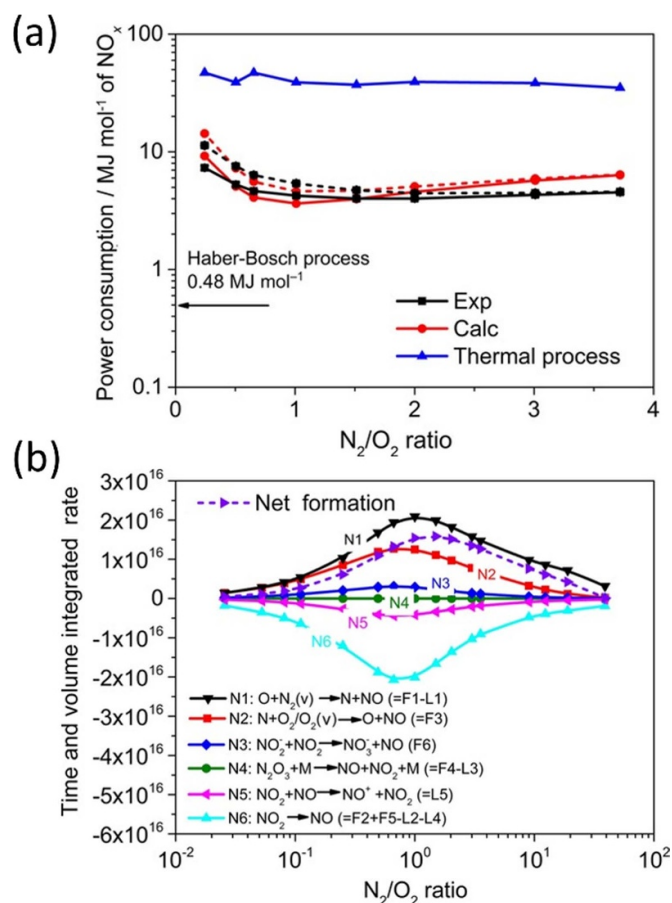

Figure 8. (a) Experimental and calculated energy consumption of NO_x formation; (b) time and volume integrated net rates of the various NO formation processes as a function of N_2/O_2. [92] John Wiley & Sons. © 2017 Wiley-VCH Verlag GmbH & Co. KGaA, Weinheim.

pedal (GAP) by means of the ZDPlaskin model, and the simulations show that vibrationally excited carbon dioxide contributes significantly to the dissociation of carbon dioxide. In conclusion, ZDPlasKin is a computational tool for simulating the kinetics of plasma chemical reactions and the evolution of active particles, which plays an important role in explaining the trend of the evolution of active particles, predicting chemical reactions, and optimizing plasma discharge devices.

To describe the surface interaction in the model especially the reactivity of the given adsorption and E–R interaction, which are considered to be predominant against L–H interaction in general plasma catalysis, is represented simply by a sticking coefficient without strong theoretical or experimental supporting information for different many surface conditions [99]. However, recent approach combined with DFT study enabled improvement in dealing with different surface reactions. The calculated adsorption energy and bonding strength gave a clue about the preferences of adsorption of different gas species as well as the accurate activation energy for L–H interactions on specific catalyst/support [49, 91, 100].

Cui *et al* [101] demonstrated the synergistic effect between Cu/γ-Al$_2$O$_3$ catalysts and CO_2/H_2 plasma by DFT, and the results showed that the interfacial sites of Cu_{13} clusters and

J. Phys. D: Appl. Phys. **57** (2024) 503002

Topical Review

γ-Al$_2$O$_3$ supports have a bifunctional effect: they not only activate the CO$_2$ molecules, but also adsorb the key intermediates strongly to further promote their hydrogenation. Han *et al* [102] investigated the mechanism of methanol conversion in cold plasma by DFT, and the results showed that the main obstacle to the conversion of methanol to hydrogen or ethylene glycol is the dissociation of methanol. The results showed that the main obstacle to the conversion of methanol to hydrogen or ethylene glycol was the dissociation of methanol. Kim *et al* [103] investigated NTP-activated carbon dioxide hydrogenation in Pd2Ga/SiO$_2$ alloy catalysts. Experimental studies combined with DFT calculations showed that vibrationally excited carbon dioxide reacted directly with hydrogen adsorbed on the palladium sites, while the formation of formate was accelerated due to the neighboring gallium sites. DFT plays a key role in understanding the process of plasma-based energy conversion, providing the basis for optimizing plasma energy conversion processes, revealing reaction pathways and principles, and guiding the design of catalysts.

It is also worthwhile to note the contribution of microkinetic model combined with DFT study from Mehta *et al* [104] which answers one of the long-awaited questions in plasma catalysis by demonstrating the crucial importance of vibrationally excited N$_2$ species and possible shift of volcano curve of optimized catalyst for plasma catalysis of ammonia production. Yet, it is found that the contribution of vibrationally excited species cannot universally enhance plasma-surface interactions such as CH$_4$ dissociation on catalytic surface [105, 106]. Apart from this progress a fundamental challenge of defining surface area of catalyst, active site density, and discharge volume with irregular or powder form of catalyst remains.

On the other hand, 2D/3D plasma fluid modeling or particle-in-cell-Monte Carlo collision (PIC-MCC) simulations helps to give information on more physical aspect of plasma characteristics. Particularly for studying the time evolution of plasma with enhanced local electric field effect (figure 9) in different geometries [107–109] and plasma formation in catalyst pore [110]. However, in order to visualize and provide more realistic simulation results, the catalytic reactivity element regarding surface reactions will be much needed. Because the chemical changes on the surface such as oxidation or coverage by adsorbate of metallic electrode may significantly influence the physical characteristics of the plasma discharge [99, 108, 111].

Catalysts (or catalytic-packing) can influence the behavior of plasmas in various ways. Catalytic-packing can induce local electric field enhancement at contact points between beads, and can also change discharge behavior (from volumetric filaments to more surface discharges) in packed-bed DBD reactors. Packed-bed DBD reactors have a 3D geometry, which makes their modeling quite challenging. Therefore, 3D modeling of packed-bed DBD reactors is currently not feasible within limited calculation time. Van Laer and Bogaerts [112] developed two complementary 2D fluid models, a 'contact point' model and a 'channel of voids' model, to approximate 3D modeling, which are used to explain the reaction characteristics of 3D packed-bed DBD reactors. The
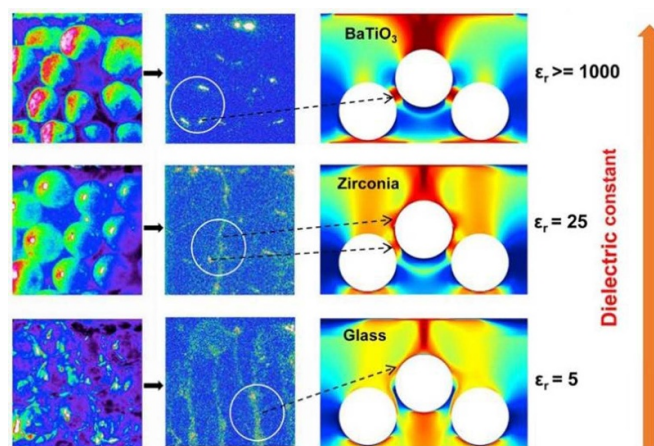

Figure 9. Simulated electron density distribution in a packed bed reactor with influence of different dielectric material packing where experimental imaging of the micro-discharges are provided for comparison. Reprinted from [108], Copyright (2018), with permission from Elsevier.

combination of these two models can explain two important features of packed-bed DBD reactors: (1) the contact between beads, which leads to local electric field enhancement due to polarization effects, and (2) the voids between particles, allowing gas to propagate from one side of the discharge gap to the other [112]. The effects of the dielectric constant, beads size, and gap size of catalytic-packing on electric field enhancement, electron temperature, and electron density were also studied [113, 114]. The model shows that ionization in the pores seems to occur more easily when the dielectric constant is smaller. The polarization of the left sidewall of the pore cancels counteracts that of the right wall when the dielectric constant is larger, reducing the net electric field and preventing the plasma from passing through the channel between the pores, and thus resulting in lower electron temperature and electron impact ionization within the pores. Similar effects were also observed for smaller particles, where the modeling also predicts lower electron density due to electron loss on the surface of the particles, and more pronounced electric field enhancement due to many contact points [114].

In addition to the plasma behavior in packed-bed reactors, another key issue is whether the plasma can penetrate into the pores of the catalyst, as it determines the surface area of the catalyst exposed to the plasma, thereby determining the available surface area for plasma catalysis. In order to understand whether the plasma can penetrate such small pores in depth, PIC-MCC simulations must be applied. Zhang and Bogaerts [115] studied the mechanism of plasma streamer propagation in catalyst pores ranging from nm to μm by using a 2D PIC/MCC. The so-called Debye length is an important criterion for plasma penetration into catalyst pores, i.e. when the diameter of the pore is greater than the Debye length, the plasma streamer can penetrate into the pore. The Debye length depends on the electron density and temperature in the plasma streamer light, but under typical DBD conditions in air, the Debye length is usually between 100 nm and 1 μm. Model predictions suggest that the larger pore size and the applied

J. Phys. D: Appl. Phys. **57** (2024) 503002

Topical Review

voltage, the easier it is to form plasma inside the pores [78]. Hensel *et al* [77, 116] also observed this phenomenon, identifying the pore size and the applied voltage as key parameters for microdischarge formation [77]. They demonstrated that when the aperture is 0.8 μm, discharge occurs only on the surface of the medium (so-called surface discharge), while when the aperture is 15 μm, the discharge mode transitions above the threshold voltage (i.e. 8.6 kV) and microdischarge occurs inside the pores by experiment. In addition, they studied the physical properties of microdischarges under different pore sizes, discharge powers, and gas mixtures, and reported that the starting voltage for microdischarge formation decreases as the pore size increases [117].

The approach utilizing machine learning (ML) has been suggested to establish structure-function relationships in plasma catalysis [83] as in broad catalysis research area to investigate stable(meta) structures, assist operando simulation, and perform critical analysis of experimental measurements [118]. Based on the deep learning approach, a recent model provided a reasonable prediction for new input plasma condition as in reference kinetic model for both CH_4/Ar and N_2/H_2 pulsed discharge [119]. As in encouraging progress in many areas, ML might be useful to accelerate the data integration and optimization process for plasma-catalysis by bridging gaps between scattered numerous models and measurements.

3. NTP-assisted gas conversion

NTP-assisted gas conversion in the P2X field refers to the use of NTP technology to convert various types of gas into other chemical products, including hydrogen, ammonia, and synthetic fuels. These converted products serve as energy carriers or feedstocks for chemical production. Compared to conventional thermal conversion methods, NTP-assisted gas conversion offers notable advantages such as high efficiency, high yield, and low emissions. Consequently, this technology shows great promise in decarbonizing energy systems and mitigating greenhouse gas emissions.

This section offers an in-depth analysis of key gases used in PP2X processes, including CO_2, CH_4, and N_2 (Air). We will explore their unique properties and characteristics, alongside the reaction mechanisms of these gases in plasma or plasma-catalysis systems. Our goal is to provide a comprehensive understanding of the gas conversion processes to facilitate their effective implementation in a PP2X system.

3.1. CO₂ conversion

Recently, the pressing concern of climate change has gained immense urgency, demanding immediate action to curb greenhouse gas emissions and minimize their impact on the environment. One effective approach to tackle this challenge involves harnessing renewable energy sources and advancing technologies capable of transforming CO_2 into valuable products. The conversion of CO_2 into high-value chemicals and fuels, however, presents a significant obstacle due to the remarkable stability of the molecule, necessitating a substantial amount of
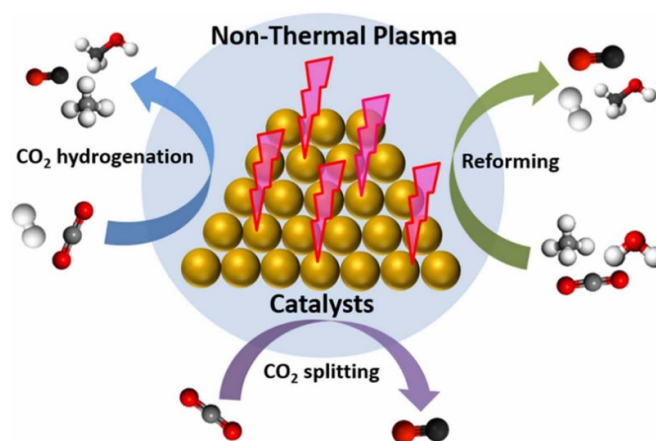

Figure 10. NTP catalysis for CO_2 conversion. Reproduced from [122]. © The Author(s). Published by IOP Publishing Ltd. CC BY 4.0.

energy to break its double carbon–oxygen bonds (O=C=O) [120]. Nevertheless, NTP offers a promising solution to this problem. By operating under specific conditions of low temperature and atmospheric pressure, NTP facilitates rapid and efficient reactions. This remarkable efficiency is attributed to the ability of the plasma electrons, with energy of 1–10 eV, to activate CO_2 by ionization, excitation, and dissociation processes [121].

The fundamental principle of NTP-assisted CO_2 conversion revolves around dissociating the CO_2 molecule into smaller constituents, such as CO and O_2, while utilizing the energy provided by the plasma. Subsequently, these newly formed CO and O_2 can serve as building blocks for the synthesis of other valuable chemicals like methanol or syngas.

However, several obstacles must be overcome to establish NTP-assisted CO_2 conversion as a practical technology for P2X applications. These challenges encompass enhancing the energy efficiency of the process, devising cost-effective and durable plasma reactors, and developing novel catalysts and processes to optimize the conversion of CO_2 into specific target products. This section explores the use of NTP in diverse CO_2 conversion processes, as illustrated in figure 10. It covers topics such as CO_2 splitting/decomposition, CO_2 hydrogenation, and CO_2 reforming (reduction with water). Furthermore, the section examines the prospects of the PP2X approach in promoting a sustainable and low-carbon economy.

3.1.1. CO₂ splitting. The conversion of CO_2 to CO and O_2 has garnered significant attention due to the crucial role of CO as a vital chemical building block in the synthesis of diverse fuels and chemicals [120, 123]. To accomplish this conversion, different types of plasma sources have been employed. Among these sources, DBD [124, 125], MW [126–128] and GA plasmas [98, 129, 130] have emerged as the most utilized methods for the efficient transformation of CO_2 into CO and O_2.

When the average electron temperature of the NTP ranges between 1 and 2 eV, or the reduced electric field (E/N) is

within 20–40 Td, approximately 97% of the total plasma energy can be effectively utilized to excite CO_2 vibrationally, resulting in CO_2 dissociation through vibrational excitation (R1) [131], which is considered one of the most efficient ways to convert CO_2. However, in the case of DBD plasmas, the reduced electric field is typically high, exceeding 100 Td. Consequently, the energy efficiency for CO_2 splitting is typically below 15% because the electron impact dissociation of CO_2 (R2) becomes dominant over CO_2 dissociation [132],

$$e + CO_2 \rightarrow e + CO_2(v^*) \rightarrow CO + O \qquad (R1)$$
$$e + CO_2 \rightarrow CO + O + e. \qquad (R2)$$
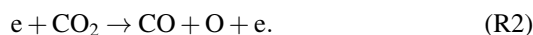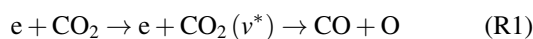
NTP-assisted CO_2 decomposition is influenced by several operational parameters, including specific energy input (SEI), dilution gas, dielectric material, gap distance, gas temperature, electrode material, and reactor configuration. Multiple studies [120, 124, 133–137] have reported on the significance of these parameters. Among them, SEI stands out as the most critical factor affecting both energy efficiency and CO_2 conversion rate. Recent study [134] found that increasing SEI leads to higher conversion rates, reaching up to 35%. However, energy efficiency decreases with higher SEI. At 35% conversion, energy efficiency is only 2%. A higher energy efficiency of 8% can be achieved at an SEI of 25 J cm^{-3}, but with a lower conversion rate. Thus, there is a clear trade-off between the conversion rates and energy efficiency. Optimization depends on the specific application and boundary conditions, allowing for the prioritization of either factor or a compromise between the both. Increasing the discharge power is known to improve CO_2 conversion [133]. Mei and Tu observed that increasing the discharge power in a DBD reactor led to an increase in micro-discharges and the formation of additional reaction channels, thereby enhancing CO_2 conversion [133]. Earlier research indicated that adjusting the discharge frequency had a minimal impact on the conversion of CO_2 when the discharge power remained constant [133, 134]. It was further observed that the fluctuation of frequency between 6 and 75 kHz did not show a significant effect on both CO_2 conversion and energy efficiency [134]. The study by Mei and Tu [133]. investigated the influence of CO_2 flow rate on conversion and efficiency. They found that the optimal CO_2 conversion rate of 22.4% occurred at a flow rate of 25 ml min^{-1}. However, increasing the flow rate reduced CO_2 residence time in the plasma, resulting in lower conversion. For instance, when the flow rate increased from 25 to 125 ml min^{-1}, conversion decreased from 22.4% to 12.6%. Interestingly, higher flow rates improved energy efficiency from 2.3% to 6.6%. Another study [133] also reported that as the discharge gap increased from 2.5 to 3.5 mm in a DBD reactor, the CO_2 conversion rate decreased from 22.1% to 16.8%, resulting in a 25% decrease in energy efficiency at a constant SEI. By enlarging the discharge gap, the residence time of the reactants in the plasma increased, positively affecting CO_2 conversion. However, widening the discharge gap decreased the power density (defined as discharge power divided by discharge volume) at a constant discharge power due to the increased
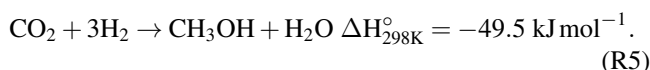
plasma volume. Brandenburg *et al* [137] systematically investigated a stackable planar and easily up-scalable volume DBD reactor by varying the electric parameters for the conversion of CO_2. The role of the different geometrical parameters on the discharge performance was studied. It was shown that a higher dielectric permittivity and a thinner dielectric enabled a lower threshold voltage and a higher discharge power for the same voltage amplitude. The distinct dependence of the energy yield of CO formation on the mean reduced electric field strength could not be concluded from the measurements. In another work [136], the results of electrical and chemical characterization of coaxial DBD reactors show a threefold increase in CO_2 conversion as well as energy efficiency of CO formation when the operating pressure is increased from 1 to 2 bar. At fixed voltage amplitude there is an optimum pressure in which both the CO_2 conversion and energy efficiency have the highest values.

During the process of plasma splitting CO_2 to generate CO, a common challenge arises in balancing the conversion of CO_2 and energy efficiency. However, a promising solution to this trade-off is the integration of plasmas with catalysts. This approach presents a viable pathway to enhance both the conversion of CO_2 and energy efficiency simultaneously, offering improved performance across these crucial indicators. In a recent study [138], the introduction of a packing of dielectric ZrO_2 beads into a DBD reactor was found to double the CO_2 conversion and energy efficiency compared to using plasma alone for CO_2 splitting. This enhancement can be attributed to the increased local electric field and electron energy near the contact points of the beads, leading to a lower breakdown voltage, as supported by 2D fluid modeling. Another work [139] reported a maximum CO_2 conversion of 22.6% by fully packing ferroelectric $BaTiO_3$ pellets into the discharge gap of a DBD reactor. By introducing γ-Al_2O_3 or 10 wt% Ni/γ-Al_2O_3 catalyst upstream of the $BaTiO_3$ bed, the CO_2 conversion and energy efficiency were increased, with the best performance observed in the upstream packing configuration, minimizing reverse reactions. The presence of Ni active species on the catalyst surface contributed to the enhanced CO_2 conversion, which was corroborated through argon plasma treatment of the reacted Ni catalyst. A more recent study [140] investigated plasma-catalytic CO_2 splitting using metal-doped CeO_2 catalysts (Fe, Co, Ni, Cu, Cr, V, Mn, or Mo). Mo-doped CeO_2 showed the highest activity due to increased oxygen vacancies resulting from strong Mo–CeO_2 interaction and the oxygen-deficient, Ar-rich calcining atmosphere. Stable oxygen vacancies were maintained through interactions between active gas-phase O and adsorbed O on vacancy sites, facilitating desorption as O_2 molecules and vacancy recovery. Other authors [136] used pure CeO_2 coatings on glass beads as the catalyst for investigations of CO_2 splitting at elevated pressures. It has been found that the energy yield of CO generation obtained at 2 bar with a CeO_2-coated packed bed in the discharge volume is four times higher than in the empty reactor at 1 bar. Furthermore, the addition of N_2 and Ar during the plasma process improved CO_2 conversion, particularly with N_2, by promoting new reaction routes induced by metastable species. Notably, N_2 acted as an O scavenger,

by enhancing forward chemical equilibrium and inhibiting the reverse reaction to form CO_2. Zhang *et al* [141] introduced an effective approach by combining a GA discharge plasma with a TiO_2 photocatalyst for CO_2 dissociation, revealing a synergistic effect. The study investigated two different modes of the plasma catalysis (IPC and PPC) and analyzed potential mechanisms. The results demonstrate that the IPC configuration produces synergistic effects, leading to a significant increase in CO_2 conversion by 138% and energy efficiency by 133% at a flow rate of $2\,l\,min^{-1}$. The activation effect of plasma, generating energetic electrons that create electron–hole pairs on the catalyst surface, is believed to be the primary contributor to the observed synergistic effects in plasma catalysis, as evidenced by the negligible impact of PPC on reaction performance.

To sum up, the conversion of CO_2 into CO and O_2 using plasma technology, such as DBD, MW, and GA plasmas, is a process of growing interest due to its potential in producing valuable chemicals. This process involves high-energy electrons in the plasma colliding with CO_2 molecules, leading to vibrational excitation and subsequent dissociation of CO_2. However, achieving energy efficiency is a significant challenge, particularly with DBD plasmas where high electric fields can reduce efficiency. Operational factors like SEI, gas composition, and reactor design critically influence the balance between CO_2 conversion rate and energy usage. Recent advancements include integrating plasmas with catalysts such as ZrO_2, $BaTiO_3$, and metal-doped CeO_2, which has shown to enhance both conversion and efficiency, indicating a synergistic interaction between plasma and catalysis. Furthermore, the addition of gases such as N_2 and Ar to the process has been found to improve CO_2 conversion by opening new reaction pathways.

3.1.2. CO_2 hydrogenation.

3.1.2. CO$_2$ hydrogenation.　Extensive investigations [142–145] have been conducted on the conversion of CO_2 using molecular H_2 through CO_2 hydrogenation. The direct route of this process predominantly yields three primary types of C1 chemicals: CH_4 (R3), CO (R4), and CH_3OH (R5) [146],

$$CO_2 + 4H_2 \rightarrow CH_4 + 2H_2O \quad \Delta H^{\circ}_{298K} = -252.9\ kJ\,mol^{-1} \tag{R3}$$

$$CO_2 + H_2 \rightarrow CO + H_2O \quad \Delta H^{\circ}_{298K} = 41.2\ kJ\,mol^{-1} \tag{R4}$$

$$CO_2 + 3H_2 \rightarrow CH_3OH + H_2O \quad \Delta H^{\circ}_{298K} = -49.5\ kJ\,mol^{-1}. \tag{R5}$$

CH_4 is a significant fuel source and plays a crucial role in energy production, while CO acts as a vital chemical building block for the synthesis of various platform chemicals and synthetic fuels using established methods such as the Fischer–Tropsch (FT) process and methanol synthesis. The conversion of CO_2 to CH_3OH through hydrogenation stands out as a promising pathway for CO_2 utilization. CH_3OH has significant value as a fuel substitute, additive, and raw material for high-value chemical synthesis. Additionally, methanol shows great potential as a hydrogen carrier, ideal for efficient storage and transportation. However, the reduction of carbon is hindered by its high oxidation state, which necessitates an

eight-electron process. This limitation significantly affects the reaction kinetics and generally requires a catalyst with both high rates and selectivity.

3.1.2.1. Reverse water gas shift reaction (RWGS).

3.1.2.1. Reverse water gas shift reaction (RWGS).　The RWGS reaction generates CO, which offers significant versatility as it can be utilized in both methanol synthesis and downstream FT processes to produce chemicals and fuels. However, RWGS is an endothermic process (R4), necessitates high temperatures for operation, while the conversion of reactants is limited by equilibrium to approximately 23% at 300 °C and 1 MPa [147]. The non-equilibrium nature of NTP can help overcome kinetic barriers in reactions, enabling low-temperature occurrence of the highly endothermic RWGS reaction. The high reaction rate and fast reaching of the steady-state allow quick discharge start-up and shutdown, thus reducing the energy costs compared to thermal processes.

Zeng and Tu [144] studied the effect of the H_2/CO_2 molar ratio on the RWGS reaction in a DBD reactor. They observed that increasing the H_2/CO_2 molar ratio from 1:1 to 4:1 led to a nearly linear rise in CO_2 conversion. The CO yield was also significantly improved with an increased H_2/CO_2 ratio, although the CO selectivity remained unchanged. Another study [142] explored the impact of Ar on the plasma-assisted RWGS reaction. The authors observed a substantial increase in CO_2 conversion, from 18.3% to 38.0%, when the Ar content in the gas mixture was raised from 0 to 60 vol% at a constant discharge power of 30 W and a fixed H_2/CO_2 molar ratio of 4:1. The presence of metastable Ar species in the discharge created new reaction pathways for CO_2 dissociation, resulting in the improved CO_2 conversion.

Catalysts for RWGS utilize well-dispersed nanoparticles supported on a metal-oxide substrate to maximize the interfacial area. Two main CO formation pathways have been proposed: the redox mechanism observed in Cu-based catalysts, where CO_2 oxidizes Cu^0 to produce CO and Cu^+ [148] and the formate decomposition mechanism, where CO_2 is hydrogenated into formate (HCOO–) before cleavage of the C=O bond [149]. Effective RWGS catalysts require dual functionality for hydrogenation and C=O bond scission. For example, Zhu *et al* [123] investigated the impact of plasmas on the RWGS reaction using an Au/CeO_2 catalyst. The study demonstrated that the introduction of plasma resulted in a CO_2 conversion rate of approximately 25.5%, exceeding the thermodynamic equilibrium value of approximately 22% at a temperature of 400 °C. Sun *et al* [88] used a Pd/ZnO catalyst in a tubular DBD reactor and found CO_2 conversion almost doubled (36.7%) compared to using only plasma or plasma with ZnO. The enhanced conversion over Pd/ZnO was attributed to strong metal-support interactions at the Pd–ZnO interface and abundant H species on its surface, whereas, in the plasma + ZnO system, CO_2 splitting to CO was dominant due to the absence of these interactions and active H species.

3.1.2.2. Hydrogenation of CO_2 to methanol.

3.1.2.2. Hydrogenation of CO$_2$ to methanol.　The process of the conversion of CO_2 and hydrogen into methanol is not only
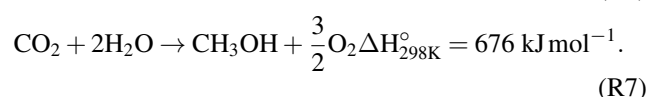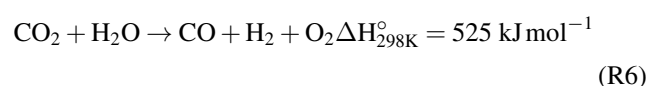
exothermic but also reduces volume (R5). This process is thermodynamically favored at low reaction temperatures and high pressures, typically ranging from 30 to 300 atm. Notably, NTP presents a highly promising pathway for achieving direct CO_2 hydrogenation to methanol under low temperatures and ambient pressure. Extensive research has explored the influence of packing material properties, reaction parameters, and reactor configurations within a plasma system to enhance the efficiency of CO_2 conversion [150]. Recent studies have concentrated on plasma-driven catalytic processes aimed at achieving high selectivity in the synthesis of methanol from CO_2 hydrogenation at room temperature and atmospheric pressure.

The work [151] reported the first successful synthesis of methanol from CO_2 and H_2 using a DBD reactor, while no reaction occurred at ambient conditions in the absence of plasma. The innovative water-electrode design was demonstrated to enhance both the conversion of CO_2 and the yield of methanol. Moreover, the incorporation of $Cu/\gamma\text{-}Al_2O_3$ in the plasma system substantially enhanced methanol production performance compared to plasma-only hydrogenation, achieving an impressive methanol yield of 11.3%, a methanol selectivity of 53.7%, and a CO_2 conversion rate of 21.2% (measured offline, not with online GC). In further work, Cui *et al* [101] investigated the combined experimental and computational aspects of plasma-catalytic CO_2 hydrogenation to CH_3OH using a $Cu/\gamma\text{-}Al_2O_3$ catalyst, revealing a synergistic effect between the catalyst and CO_2/H_2 plasma. The DFT analysis demonstrated the significance of interfacial sites on the Cu_{13} cluster and $\gamma\text{-}Al_2O_3$ support, enabling the activation of CO_2 molecules and adsorption of crucial intermediates for efficient hydrogenation. Moreover, reactive plasma species governed surface reactions through the E–R mechanism, resulting in the accelerated hydrogenation and enhanced intermediate production. Similarly, Men *et al* [152] employed a highly dispersed Pt-based catalyst (Pt/film/In_2O_3), achieving a remarkable CO_2 conversion rate of 37.0% and a high methanol selectivity of 62.6% (measured offline). This performance enhancement can be attributed to the catalyst's ability to facilitate the activation of adsorbed CO_2, leading to the formation of methoxy species, which serve as crucial intermediates in the hydrogenation of CO_2 to methanol.

3.1.2.3. Hydrogenation of CO_2 to CH_4. Hydrogenation of CO_2 into methane by the Sabatier reaction (R3) offers a sustainable alternative to natural gas, potentially creating a carbon-neutral fuel economy. Typically, a 4:1 H_2/CO_2 ratio yields optimal methane selectivity and CO_2 conversion [144]. The methanation process is enhanced by lower temperatures and high pressures and recently, the use of NTP for low-temperature CO_2 hydrogenation to methane has gained growing interest [153]. For instance, vibrationally excited CO_2 can adsorb onto the catalyst surface, reducing the energy barrier compared to ground-state CO_2 and aiding the creation of reactive intermediates on the catalyst surface [154]. In contrast, thermal catalysis requires CO_2 to be adsorbed and activated by the catalyst surface before surface reactions occur, necessitating high temperatures [155].

A study by Biset-Peiró *et al* [156] demonstrated this by comparing a Ni–CeO_2/Al_2O_3 catalyst's performance under thermal and NTP conditions. They achieved a 70% CO_2 conversion and a 96% methane yield under NTP conditions at approximately 150 °C. In contrast, similar results required temperatures over 350 °C with thermal conditions. Similar results were observed [157] using a $Ru/\gamma\text{-}Al_2O_3$ catalyst. The authors found that increasing the discharge frequency and H_2/CO_2 ratio, along with introducing Ar, enhanced CO_2 conversion and methane selectivity. The maximum CO_2 conversion and CH_4 selectivity were 23.20% and 97.38%, respectively, at the optimized discharge conditions. In plasma catalysis research, CO_2 methanation studies are relatively sparse, primarily focusing on nickel (Ni) catalysts [155], which are often used in thermal catalysis due to their high activity, selectivity, and cost-effectiveness [158].

3.1.3. CO_2 reduction with H_2O. In addition to H_2 and CH_4 (see section 3.2), H_2O can also serve as hydrogen sources for converting CO_2 into valuable products, with water being particularly intriguing due to its abundance, low cost, and potential for mimicking natural photosynthesis when combined with renewable energy. Although the reduction of CO_2 with water for producing syngas (R6) or oxygenates (R7) is environmentally friendly and sustainable, these reactions are highly endothermic and thermodynamically unfavorable, thus requiring high temperatures. Nonetheless, NTP presents an attractive option for enabling CO_2 reduction with water at low temperatures and ambient pressure [159],

$$CO_2 + H_2O \rightarrow CO + H_2 + O_2 \, \Delta H^{\circ}_{298K} = 525 \text{ kJ mol}^{-1}$$
$$\text{(R6)}$$

$$CO_2 + 2H_2O \rightarrow CH_3OH + \frac{3}{2}O_2 \, \Delta H^{\circ}_{298K} = 676 \text{ kJ mol}^{-1}.$$
$$\text{(R7)}$$

In the absence of a catalyst, DBD discharge of CO_2/H_2O primarily generates reactive species such as OH, CO, O, and H. However, the OH radicals tend to recombine with CO molecules, leading to the production of CO_2 and H atoms, which reduces CO_2 conversion. Additionally, H atoms react with O to form H_2O instead of CH and CHO species, which are crucial intermediates for the synthesis of oxygenated products [160]. Chen *et al* [159] explored the simultaneous dissociation of CO_2 and H_2O (1:1) through surface-wave microwave discharge, resulting in the production of syngas with a H_2/CO ratio close to 1. Moreover, experiments using Ar/H_2O instead of CO_2/H_2O indicated that the presence of CO_2 in the gas mixture enhanced H_2 generation from H_2O at a low SEI.

To address the issue of selectivity towards oxygenated hydrocarbons in CO_2 reforming with H_2O, recent research has focused on developing catalytic reforming systems for CO_2/H_2O plasma. Ma *et al* [161] used a $Ni/\gamma\text{-}Al_2O_3$ catalyst in a DBD reactor to significantly improve the yields of H_2 and CO to 13.8% and 5.6%, respectively, compared to NTP-only conditions. They also found that the introduction of Ar generated reactive Ar species, reducing the recombination of

H_2 and O_2, thereby enhancing H_2O conversion. Additionally, Zhao *et al* [162] reported an elevated ethanol production rate of 15.60 μmol $g_{cat}^{-1}h^{-1}$ using a Cu/ZnO/Al$_2$O$_3$ catalyst under NTP conditions, surpassing the rates achieved in thermal systems (3.02 μmol $g_{cat}^{-1}h^{-1}$ with the catalyst) and NTP-only conditions (3.5 μmol $g_{cat}^{-1}h^{-1}$).

Recently, an innovative approach for CO_2 conversion in water, utilizing CO_2 discharge within microchannels, has been reported by Zhou *et al* [56], leading to enhanced plasma–liquid interactions and a notable increase in oxalate and H_2O_2 production. The method achieved more than 99% liquid selectivity for oxalic acid, highlighting its effectiveness for sustainable CO_2 upcycling and contributing significantly towards the realization of the Power-to-Chemicals concept using renewable energy sources. Further addition of CH_4 in the feeding CO_2 gas can facilitate hydrocarbon chain growth up to C40 in the solid state (including oxygenated products), predominantly when CH_4 exceeds CO_2 in the feedstock [163].

The use of a CO_2/H_2O gas mixture shows promise for sustainable hydrogen production, with H_2O offering a cost-effective alternative to H_2. However, the limited number of studies on combined CO_2/H_2O conversion in plasmas and inconsistent findings in the literature highlight the complexity of this process. Some research indicates that even small amounts of H_2O may reduce CO_2 conversion rates and increase energy costs due to potential quenching of CO_2 vibrational levels [160, 164–166]. Variations in the impact of H_2O across different plasma setups emphasize the need for further exploration and parameter optimization. The intricate interplay between H_2O addition, pressure conditions, and energy efficiency requires ongoing research efforts to fully unlock the potential for sustainable hydrogen generation. Intriguing possibilities, such as methanol formation in specific microwave plasma studies, underscore the multifaceted nature of these interactions. As we pursue more sustainable and efficient hydrogen production methods, continuous research and innovative approaches are crucial to unravel the complexities of CO_2/H_2O conversion in plasmas for practical applications in the PP2X approach.

3.1.4. Summary.
Plasma-based methods offer significant promise for CO_2 conversion due to their versatility in supporting various reactions, low operational costs, and the possibility of operation without rare earth metals. Plasmas are particularly advantageous in terms of modularity, scalability with plant output, and compatibility with renewable electricity sources. The ability of plasma discharges to be easily switched on and off makes them ideal for converting intermittent renewable energy into base chemicals or fuels, thereby aiding in peak shaving and grid stabilization.

However, challenges persist in enhancing the energy efficiency, conversion rates, and product selectivity of plasma-based CO_2 conversion. The energy efficiency largely hinges on the plasma reactor type and operating conditions, with the most efficient dissociation pathway being strong vibrational excitation at low gas temperatures. The current research indicates that in certain plasmas, CO_2 conversion mainly occurs

through thermal reactions, and achieving high energy efficiency requires avoiding certain backward reactions through rapid gas quenching. Additionally, improvements in reactor design, fluid dynamics, and plasma-catalyst interactions are crucial for better conversion rates and selectivity, particularly for targeted compounds. The scalability and handling of complex gas mixtures, as well as integrating plasma technology with other processes like light-induced water transformation, are areas requiring further exploration to fully realize the potential of plasma in CO_2 conversion.

3.2. CH$_4$ conversion

Methane (CH_4) is abundant in nature, has a high heating value, and a relatively low carbon footprint compared to coal, making it a promising energy resource. However, methane reforming remains one of the major challenges of this century. Plasma-based CH_4 reforming is a relatively new and rapidly developing field. In this section, we discuss four methane reforming pathways: methane decomposition, DRM, partial oxidation of methane, and steam methane reforming, as illustrated in figure 11.

3.2.1. Methane decomposition.
Plasma-assisted methane decomposition refers to the introduction of methane or a mixture of methane and inert gases under the action of plasma, resulting in the formation of elemental carbon and hydrogen, or the generation of higher hydrocarbon compounds. The reactors used in this process vary. Baldissarelli *et al* [167] utilized DC plasma to dissociate CH_4, yielding carbon black and carbon nanotubes. The results indicate that under conditions without catalytic activity, CH_4 undergoes decomposition to form carbon black. In the presence of Ni/Ce–Al$_2$O$_3$ catalysts, carbon nanotubes are produced. As carbon nanotubes grow on the catalyst surface, the active metal components of the catalyst migrate upward, forming metal caps. Upon complete coverage of the active metal components by carbon, catalyst deactivation occurs. Li *et al* [168] employed a mixture of CH_4 and Ar for discharge, utilizing arc plasma for methane decomposition. Experimental results reveal that the residence time and gas flow rate of the feed gas during plasma-assisted CH_4 decomposition influence the production of elemental carbon. Additionally, during methane decomposition, methyl and C_2 radicals are generated first, serving as precursors to elemental carbon. Ghanbari *et al* [169] conducted experimental studies on the catalytic conversion of CH_4 to H_2 using a nanosecond pulse DBD plasma reactor. The presence of Ni–K$_2$O/Al$_2$O$_3$ catalysts significantly enhances CH_4 conversion, H_2 yield, H_2 selectivity, and energy efficiency. Noble metal-based catalysts effectively suppress coking during methane decomposition and prevent rapid catalyst deactivation. Khalifeh *et al* [170] employed DBD plasma coupled with Pt–Re/Al$_2$O$_3$ catalysts for methane decomposition. Experimental results demonstrate that when discharge power is below 10 W, both energy efficiency and CH_4 conversion rate are high, with minimal carbon deposition on the catalyst and electrode surfaces.

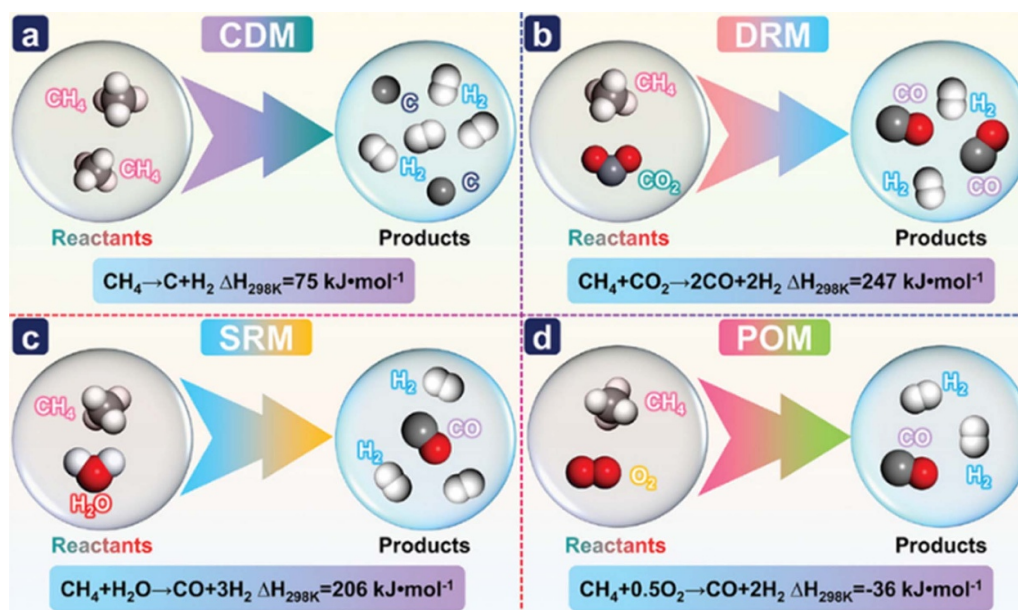J. Phys. D: Appl. Phys. **57** (2024) 503002

Topical Review

Figure 11. Four pathways for methane reforming. Reproduced from [62]. CC BY 4.0.

In addition to elemental carbon and hydrogen gas, methane decomposition can produce higher hydrocarbon compounds, primarily C_2 compounds. Zhang *et al* [171] employed sliding arc plasma generation and mixed nitrogen gas into the CH_4 gas feed, ultimately producing C_2 hydrocarbons. The results indicate that N_2 can promote the dissociation of CH_4, and the formation of C_2 hydrocarbons is influenced by CN and C_2 radicals.

3.2.2. Dry reforming of methane (DRM). DRM is one of the attractive methods for the utilization of greenhouse gases (e.g. CH_4, CO_2) to produce valuable fuels (e.g. syngas, refer to R8). Unlike traditional methods that rely on hydrogen (H_2) as a source, CH_4 can serve as an ideal substitute due to its high hydrogen density and availability from various sources like biogas, flared gas, natural gas, landfill gas, and shale gas [172].

The molar ratio of CH_4/CO_2 affects the reactant conversion, energy efficiency, and product distribution, especially the H_2/CO ratio. A case study [173] indicated that when the CH_4/CO_2 molar ratio was increased from 3:7 to 7:3, the conversion rate of CH_4 was reduced from 16.2% to 8.6%. However, this increase simultaneously boosted the conversion of CO_2 by 53% and increased H_2/CO molar ratio from 0.24 to 3.3 when using a GA reactor. The promise of the plasma catalysis lies in its ability to address the compromise between conversion and energy efficiency in DRM reactions. Extensive research has been done on a range of catalysts for plasma-catalytic DRM to enhance reactant conversion and control product selectivity. Nickel-based catalysts are frequently employed in plasma DRM reactions to produce syngas. For example, Long *et al* [174] utilized a cold plasma jet for DRM over a Ni/Al_2O_3 catalyst, resulting in enhanced reactant conversion, syngas yield, and energy efficiency compared to plasma alone, with H_2 and CO yield increases of 18% and 11%, and energy yield improving from 2.9 to 3.7 mmol kJ^{-1}.

Similarly, Wang *et al* [81] examined Ni/γ-Al_2O_3 in a DBD reactor for DRM, noting significant conversion increases for CH_4 and CO_2, from 11% and 21% with plasma only, to 33% and 22.5%, under the same conditions, indicating effective plasma-catalysis synergy. Furthermore, other metals like Co, Mn, Fe, Cu, La, and Pd have also been used in plasma-catalytic DRM reactions. Zeng *et al* [175] observed that Ni/γ-Al_2O_3 and Mn/γ-Al_2O_3 catalysts significantly improved CH_4 conversion in the plasma-assisted DRM, while all the catalysts had little effect on the CO_2 conversion. Ni/γ-Al_2O_3 catalyst provided the highest CH_4 conversion (19.6%) and showed the best syngas production activity among all the examined metals (Ni, Co, Cu and Mn). Although promoters are often used to boost catalyst activity and stability in thermal catalytic DRM, their application in plasma-catalytic DRM has been less studied. Zeng *et al* [176] noted that promoted Ni/Al_2O_3 catalysts behave differently in low-temperature plasma DRM compared to high-temperature thermal catalysis, attributing this to the temperature-dependent nature of the promoters. The K-promoted catalyst (Ni–K/Al_2O_3) was found to improve the conversion of CO_2 and CH_4, yield of H_2 and CO, and energy efficiency of the plasma process, recording the highest conversions for CO_2 (22.8%) and CH_4 (31.6%). Wang *et al* [177] studied Ce-promoted Ni-supported activated carbon (NiCe*x*C) catalysts in plasma DRM, finding NiCe1C as the best catalyst with remarkable conversions of CO_2 (53.7%) and CH_4 (55.6%), and notable H_2 (50.0%) and CO (53.2%) selectivity. The presence of CeO_2 resulted in a higher number of basic sites with increased basicity on the catalyst, thereby enhancing the adsorption capability for reactants, notably for acidic CO_2 gas. Recently, Mei *et al* [178] investigated three γ-Al_2O_3 supported catalysts, prepared using an enhanced impregnation technique, for plasma-catalytic DRM in a DBD reactor. The conversion of CO_2 and CO selectivity were found to be strongly related to the basicity of the catalyst. Among the

catalysts, Ag/γ-Al$_2$O$_3$ achieved the highest CO$_2$ (21.4%) and CH$_4$ (27.6%) conversions, while Ni/γ-Al$_2$O$_3$ exhibited the highest selectivity for liquid products.

3.2.3. Methane partial oxidation. In plasma-assisted methane partial oxidation, pure O$_2$ is commonly used as the oxidant [179]. However, excessive oxygen can completely oxidize CH$_4$ to CO$_2$, so controlling the feed ratio of methane to oxygen is particularly important. Partial oxidation of methane can generate various products, including synthesis gas and CH$_3$OH. The dissociation energy of CH$_4$ is relatively high (9 eV), requiring continuous collisions with high-energy electrons in the plasma for complete dissociation, which is a challenging process [180]. However, the introduction of O$_2$ can promote the dissociation of CH$_4$, and reactive oxygen species (ROS) generated in the plasma, such as O$^-$, O$_2$ $^-$, and O$_2^{2-}$, can break the C–H bonds, forming CH$_x$ [181]. These radicals can adsorb stably on the catalyst surface, leading to the formation of CH$_3$OH via the L–H reaction [182, 183]. Chawdhury *et al* [184] successfully achieved CH$_4$ partial oxidation to CH$_3$OH by combining a DBD reactor with CuO/γ-Al$_2$O$_3$ catalyst, demonstrating a significant synergistic effect that notably improved CH$_4$ conversion and CH$_3$OH selectivity. Under optimal experimental conditions, the CH$_3$OH selectivity was approximately 34%. The main intermediates in the plasma are methyl and ROS. Additionally, CH$_3$OH, HCO, and HCOOH are formed in the plasma reactor.

3.2.4. Steam methane reforming. Plasma-assisted steam methane reforming introduces water into the basis of dry reforming, incorporating more hydrogen and oxygen elements into the reaction process, which may alter the reaction pathways of methane reforming. Zhu *et al* utilized plasma-catalytic technology [185], employing a sliding arc reactor to generate thermal plasma for methane steam reforming to produce hydrogen, using Ni/CeO$_2$/Al$_2$O$_3$ as the catalyst. The process achieved conversion rates close to thermodynamic equilibrium, with complete selectivity towards CO and CO$_2$, and a methane conversion rate of 90%. Unlike the mainstream DBD reactor-based approaches for the other three plasma-assisted methane reforming routes, there are more reports on systems utilizing thermal plasmas. This may be because methane steam reforming is an endothermic process, and although plasma can alter its energy equation, it cannot bypass its inherent endothermic nature, thus requiring plasma reactors to operate at higher temperatures. Liu *et al* [186] studied the relationship between plasma temperature and product selectivity and yield during steam methane reforming reactions using a DBD reactor. The results indicate that reactant conversion rates are primarily influenced by thermochemical factors. As the plasma temperature increases, the methane conversion rate increases while the water conversion rate decreases, with electron-induced chemistry having minimal impact on product distribution. Thermochemistry also has a significant effect on product selectivity. Montoro-Damas *et al* [187] employed a DBD reactor to generate plasma for methane steam reforming and used isotopically labeled hydrogen in the reaction,

using D$_2$O and CH$_4$ as reactants. The results show that hydrogen gas (H$_2$, HD, D$_2$), methane (CH$_4$, CH$_3$D, and CH$_2$D$_2$), and water (D$_2$O, DHO) molecules all contain both H and D atoms. However, the H/D ratio within molecules varies with changes in plasma current and gas residence time, while overall reaction yields and process energy efficiency are also correlated with experimental parameters. The results demonstrate that intermediates produced under plasma conditions generate water and methane, significantly reducing the overall efficiency of the reforming process.

3.2.5. Summary. Current challenges in plasma technology for methane reforming include low selectivity for desired products and low energy efficiency, estimated at 12%–15%. Improvements in NTP technology require enhanced reactor designs, like reducing electrode gaps and optimizing GA reactors for better gas interaction with plasma. Additionally, using high-voltage discharges in NTP to generate active species and incorporating gases like N$_2$ and O$_2$ can improve selectivity and energy efficiency.

Advancing this field involves several key strategies. It is essential to develop new micro-kinetic models for plasma-catalysis that capture the complexity of chemical reactions, including plasma species on catalyst surfaces, to improve selectivity towards the desired products. Extending reactor models to consider physical dimensions and phenomena like surface charging is also critical. Reusing heat from this process to preheat incoming gas can further improve efficiency. Combining plasma with photocatalysts and exploring ultra-short pulse nanosecond technology in DBD reactors could enhance efficiency, though uniform discharge in larger volumes remains a challenge needing further research.

3.3. N$_2$ fixation

Nitrogen fixation is a process by which atmospheric nitrogen (N$_2$) is converted into a form that can be used by plants and animals, such as ammonium (NH$_4^+$) or nitrate (NO$_3^-$). It is an important process for sustaining life on Earth, as it provides a constant source of nitrogen to ecosystems and helps maintain the nitrogen cycle [188]. Nitrogen fixation holds considerable value in agriculture due to its vital role in fertilizer production, a crucial aspect of cultivating crops. Furthermore, this process assumes a pivotal position in the advancement of P2X applications. By enabling the production of synthetic ammonia, it becomes a fundamental step that facilitates the creation of an appealing chemical energy carrier that can be efficiently stored and transported, thereby contributing to the progress of a low-carbon energy system [189, 190].

The Haber–Bosch (H–B) process, widely used for current industrial ammonia production, faces sustainability challenges due to high energy consumption, greenhouse gas emissions, and the need for large-scale operations [191]. Researchers are actively seeking an environmentally friendly and energy-efficient alternative. The industrial opportunity of plasma-based nitrogen (N) fixation, as opposed to chemical and biological N-fixation, has been reviewed [192]. The use of

J. Phys. D: Appl. Phys. **57** (2024) 503002

Topical Review

renewable energy and abundant Earth resources (air, water) marks the potential for increasing sustainability in the products ammonia and nitric acid; with applications in fertilizers and energy [193]. Sustainability assessment by life cycle assessment and techno-economic analysis confirmed the positive impact of plasma-assisted processing on the environmental profile, the importance of process design, economy model (support by cost internalization), and supply chain model [194–198].

Nitrogen fixation through atmospheric pressure NTP has two types: reduction and oxidation of nitrogen [199, 200]. These reactions have different mechanisms and pathways, leading to diverse research focus. Foundation work has been made concerning reactor engineering (proposition of GA reactor as production tool), plasma catalysis, and containerized modular production for the plasma-assisted synthesis for N fixation [201–203]. This section provides an overview of recent studies on atmospheric pressure NTP nitrogen fixation technology, highlighting the reduction and oxidation of nitrogen through NTP, and summarizing the research focus and current advancements under various reaction conditions.
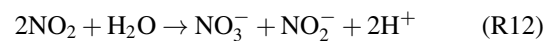
3.3.1. N_2 oxidation. Nitrogen oxidation in plasma involves N_2 and O_2, resulting in nitrogen oxide generation, including NO_2, NO, N_2O_5, and N_2O species. If the reaction occurs at the plasma–liquid interface, the resulting nitrogen oxide products can be absorbed by liquid water, producing NO_2^- and NO_3^-. Given that air contains approximately 78% nitrogen and 21% oxygen, and is inexpensive and easily accessible, many plasma-based nitrogen oxidation reactions utilize air as a reactant. NO_x, which is a common product of these reactions, has numerous important applications, including its use in agricultural fertilizers and the industrial production of nitric acid. Importantly, NTP for NO_x production has a lower limit of energy consumption than the H–B process [204], along with the accessibility of air makes it a highly promising nitrogen fixation technology with wide-ranging potential.

Atmospheric pressure NTPs cannot generate NO directly by breaking the chemical bonds of N_2 and O_2, unlike thermal plasmas, due to the much lower gas temperature in NTP. Instead, NTPs activate and dissociate N_2 and O_2 molecules through electron collisional and vibrational excitation (R8) [205]. The Zeldovich mechanism describes how excited-state nitrogen molecules react with O atoms to produce excited-state nitrogen atoms and NO molecules. These nitrogen atoms then react with O_2 molecules to generate O atoms and NO (R9) and (R10) [206]. The resulting NO can further react with O to produce NO_2. Additionally, O atoms can react with O_2 molecules to form ozone. When ozone is present, NO can also be oxidized to NO_2,

$$N_2 + e \rightarrow N_2^* + e \qquad (R8)$$

$$N_2^* + O \rightarrow NO + N^* \qquad (R9)$$

$$N^* + O_2 \rightarrow NO + O. \qquad (R10)$$
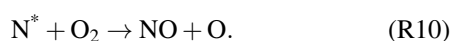
NO and NO_2 can react with water to produce nitrite ions and protons (R11). Meanwhile, NO_2 can undergo dissociation to produce NO_3^- and NO_2^- in water (R12). The presence of OH radicals is inevitable, and they can form H_2O_2 in the liquid phase or react with each other to produce H_2O and O atoms (R13). OH radicals also act as oxidizing agents and participate in reactions with nitrogen oxides in water, leading to the formation of nitrate and nitrite ions. Specifically, OH radicals can oxidize N atoms, NO, and NO_2, resulting in the formation of NO, HNO_2, and HNO_3 (R14)–(R16) [206]. Via experiments, Wandell *et al* [207] confirmed that OH plays a significant role in converting gas-phase NO and NO_2 into water-soluble ions, and O atoms from water may contribute to the formation of NO and NO_2. Moreover, when comparing N_2/O_2/Ar mixtures and air, it has been observed that the production of ROS significantly increases the generation of NO_2,

$$NO + NO_2 + H_2O \rightarrow 2NO_2^- + 2H^+ \qquad (R11)$$

$$2NO_2 + H_2O \rightarrow NO_3^- + NO_2^- + 2H^+ \qquad (R12)$$

$$OH + OH \rightarrow H_2O + O \qquad (R13)$$

$$OH + N \rightarrow NO + H \qquad (R14)$$

$$OH + NO \rightarrow HNO_2 \qquad (R15)$$

$$OH + NO_2 \rightarrow HNO_3. \qquad (R16)$$

Recent studies have explored various discharge types, such as DBD, microwave discharge, spark discharge, and GA discharge, to create plasma and facilitate nitrogen fixation through oxidation reactions that occur at the gas phase or the interface between gases and liquids [208]. For example, Pei *et al* [208] compared the nitrogen fixation performance of different discharges and identified the electric field strength and temperature product (χ) as a key factor in energy consumption. Strategies to reduce energy consumption were proposed, such as cooling, using short-time high-current pulses, or extending the discharge length to decrease χ value. Other authors [209] used a microwave plasma tube and vortex gas flow to minimize energy loss, finding that NO_x production correlated with gas flow rate and power, with optimal conditions at high flow rates and power. They achieved the highest NO_x yield (3.8%) and the lowest energy consumption (2 MJ mol^{-1}), which is promising for upscaling. Additionally, the most effective NO_x production occurred in an oxygen-rich environment with a nitrogen-to-oxygen ratio of 1:1. Bogaerts and co-workers also studied NO_x production in various types of GA reactors, such as a classical GA [92], a GA plasma [210], and a RGA [211]. The latter allowed to reach record-high NO_x yields of 5.5%, at an energy consumption of 2.5 MJ mol^{-1}, which could further be improved by using an effusion nozzle (to avoid back-reactions, by quenching; as demonstrated by the detailed modeling) [212] or by using higher pressures, where it was possible to reach an energy consumption of only 1.8 MJ mol^{-1} [213].

Zhang *et al* [206] employed a nanosecond pulse spark discharge and achieved high energy efficiency and NO_x concentration, highlighting the dependence of reaction pathways on the plasma parameters and the residence time of reactive species. More than 50% of NO species was generated through chain reactions of O and N with vibrationally excited N_2 and

J. Phys. D: Appl. Phys. **57** (2024) 503002

Topical Review

O_2 molecules, and most NO_2 molecules were formed by further oxidation of NO species. Abdelaziz and Kim [214] studied the effects of gas temperature, humidity, and oxygen concentration on nitrogen fixation in nanosecond-pulsed DBD. Temperature minimally affected discharge characteristics but significantly influenced product selectivity. Lower temperatures favored nitrate and nitrite formation, while higher temperatures favored NO production. Additionally, higher oxygen concentrations promoted nitrogen fixation by increasing the oxidation state of nitrogen. In a related study, Wandell *et al* [207] utilized a nanosecond-pulsed power supply and gas–liquid flow reactor to examine nitrogen oxide and H_2O_2 production in an Ar/N_2 gas mixture. They observed a notable rise in nitrogen oxide production with increasing N_2 concentration, while the production rate of H_2O_2 slightly decreased. Using a low-power pulsed spark plasma jet, Vervloessem *et al* [215] obtained the low energy consumption of $0.42\,MJ\,mol^{-1}$ for NO production, directly from air. Recent study [216] employed an innovative plasma bubble reactor to produce liquid-phase NO_x (e.g. nitrate and nitrite). This research aimed to enhance the energy efficiency of nitrogen fixation by fine-tuning the reactor and electrode configurations to regulate discharges (DBD and spark) at the interface between plasma and water. Additionally, a dual reactor arrangement was employed while the dynamics of the bubbles involved in the process was effectively controlled.

Despite extensive research in the plasma catalysis field, only limited studies have focused on N_2 oxidation, particularly for atmospheric pressure NTPs. Recent study [217] reported on the impact of support materials on NO_x synthesis in a DBD reactor. γ-Al_2O_3, with its smallest particle size, demonstrated superior performance in terms of NO_x concentration and energy consumption. Additionally, the study revealed that incorporating 5% WO_3/γ-Al_2O_3 further enhanced NO_x concentration by approximately 10% compared to γ-Al_2O_3. However, it decreased the selectivity towards NO, suggesting the potential occurrence of thermal oxidation of NO to NO_2 through surface oxygen species. Recent study [91] further demonstrated the significance of high-valence nitrogen in the nitrogen fixation process, particularly in the production of liquid-phase nitrate (NO_3^-). The authors employed a bubble DBD discharge combined with TiO_2 supported by 5% graphene oxide (GO) catalyst, successfully enhancing the catalytic oxidation activity, ultimately resulting in an increase of over 100% in nitrate (NO_3^-) yield with a selectivity of 93%. This achievement was attributed to the synergistic physico-chemical interaction between the TiO_2@5% GO catalyst and the plasma. Characterization of the catalyst and investigation of the plasma kinetics model confirmed the enhanced generation of nitrite products, particularly N_2O_5, as the primary reactive species, especially under low-temperature DBD plasma conditions.

3.3.2. N_2 reduction. NTP-assisted nitrogen reduction is to synthesize ammonia by reacting nitrogen gas with hydrogen-containing substances. Ammonia is a vital industrial chemical worldwide and is a crucial fertilizer for crops,

contributing to the global food supply. Additionally, it is considered a promising carbon-free hydrogen source and energy storage medium. NTP-assisted synthesis of ammonia has recently advanced significantly, with deeper understanding gained regarding the optimum reaction conditions, reactors, reactants, and catalysts [218]. The nitrogen source for NTP-assisted synthesis of ammonia is typically nitrogen gas or air, while hydrogen can come from various sources, including H_2, H_2O, and organic matter such as methane and ethanol. However, the use of organic matter as a hydrogen source negatively impacts the environment due to by-products like carbon accumulation and CO_2. Considerable efforts have been devoted to the design of the plasma reactors, development of catalysts, and investigation of reaction mechanisms for NTP-assisted nitrogen reduction. This section will summarize the N_2 and H_2 as well as N_2 and H_2O reaction systems for ammonia synthesis.
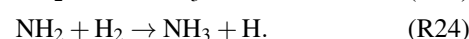
3.3.2.1. N_2–H_2 reaction system. Previous studies on ammonia synthesis from N_2 and H_2 have primarily focused on plasma reactions, with less attention given to the source of hydrogen. Although the exothermic nature of reaction (R17) favors low temperatures, the dissociation of N_2 necessitates a high energy input,

$$N_2\,(g) + 3H_2\,(g) \leftrightarrow 2NH_3\,(g)\,;\,\Delta H = -92.44\,kJ\,mol^{-1}. \tag{R17}$$
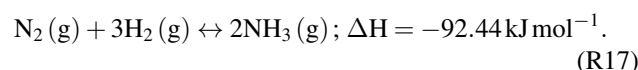
Reactions (R18)–(R24) represent the primary reaction mechanism in the plasma-assisted ammonia synthesis. The dissociation of N_2 and H_2 occurs first, with N_2 dissociation being rate-limiting due to its high dissociation energy of 9.8 eV [61, 222]. By the plasma activation, N_2 is exposed to electrons that cause the dissociation of nitrogen molecules into highly reactive N atoms. There are two forms of excitation that N_2 molecules undergo: vibrational and electronic. Vibrational excitation requires less energy at 0.29 eV, while electronic excitation requires 6.17 eV (for excitation to the $v = 1$ level; excitation to higher levels requires more energy). Both values are lower than the dissociation energy of N_2,

$$N_2 + e \rightarrow 2N + e \tag{R18}$$

$$H_2 + e \rightarrow 2H + e. \tag{R19}$$
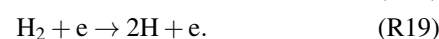
Following the dissociation reactions, NH radicals are formed and considered the most significant intermediates in the process [223]. The concentration of NH radicals has a significant impact on the ammonia production rate, with a higher concentration resulting in a higher yield of NH_3 [72]. NH_3 is subsequently produced through stepwise addition reactions with H and H_2,

$$N + H \rightarrow NH \tag{R20}$$

$$NH + H \rightarrow NH_2 \tag{R21}$$

$$NH + H_2 \rightarrow NH_2 + H \tag{R22}$$

$$NH_2 + H \rightarrow NH_3 \tag{R23}$$

$$NH_2 + H_2 \rightarrow NH_3 + H. \tag{R24}$$

The reaction mechanism discussed above is for gas-phase NH$_3$ synthesis, but surface reactions become important with catalysts. The key issue is if vibrationally excited N$_2$ dissociates on the catalyst surface or in the plasma. Hong *et al* [97] found that gas phase reactions need less energy, but recent findings by van 't Veer *et al* [224] suggest that the latter route dominates. To be more specific, the H and N atoms contribute to ER reactions, forming NH(s), but the subsequent NH$_3$ formation occurs by LH steps [225].

The feed gas ratio of N$_2$ and H$_2$ is crucial for ammonia production. The stoichiometric ratio is optimal for energy efficiency, as reported by Gómez-Ramírez *et al* [223] and other researchers [226, 227]. However, some studies suggest that a higher N$_2$/H$_2$ ratio is better for ammonia production [222, 228, 229]. Peng *et al* [230] proposed a plausible explanation that a high hydrogen content environment with less intensive discharges (e.g. low voltage and frequency) promotes the formation of NH radicals due to higher average electron density and temperature, and consequently achieving high ammonia production. In contrast, the production of more active nitrogen species that react with hydrogen and lead to the increased ammonia production in intensive plasma discharges is facilitated by a nitrogen-rich environment. To attain optimal results, the residence time is a significant factor to consider. Several studies, including the research conducted by Peng *et al* [222] and other sources, have found that increasing the flow rate from 0 to 5 l min^{-1} leads to a rise in the energy efficiency. However, Gómez-Ramírez *et al* [223] also noted this correlation but observed a decrease in N$_2$ conversion. This is because high flow rates result in shorter residence times, which in turn leads to a lower extent of ammonia decomposition due to plasma.

The production of ammonia in the N$_2$–H$_2$ plasma system can be affected by adding noble gases [231]. In a study by Hong *et al* [232], argon was added to the feed gas stream consisting of N$_2$ and H$_2$ in a pack-bed DBD reactor. The addition of 10 sccm Ar resulted in an increase in discharge power, uniformity, and gas temperature, leading to higher ammonia production rates. The authors observed a rise in N$^+$ in the optical emission spectra, which they attributed to the potential reaction between Ar$^+$ and N$_2$. They also suggested that noble gases could act as an extra source of N atoms that enhance the production of NH$_3$ [233]. In their research using DC glow discharge plasma, de Castro *et al* [234] examined the effect of helium addition and found that it led to a 45% increase in ammonia production when 8% helium was added. They attributed this increase to the modification of the tungsten wall surface caused by the addition of helium, which they identified as the key factor that enhanced N–H recombination. Additionally, the authors suggested that addition of helium significantly affected the electron temperature and mass spectrometry measurements. As a result, the measured ammonia production rates increased, which could be attributed to these changes.

Recent research on the synthesis of ammonia from N$_2$ and H$_2$ has focused on a catalytic synergistic approach, which has led to an increasing interest in the catalytic effect of the catalyst

and its physical properties on the discharge process. In particular, DBD has emerged as one of the most common forms of discharges in N$_2$ and H$_2$ plasma synthesis of ammonia, as it can be easily coupled with catalysts. The most widely used catalytic material is the porous oxide carrier type, which typically takes the form of M/C, where M is a transition metal element like Ni, Co, Ru, Fe, or Cu, and C is a carrier substance such as γ-Al$_2$O$_3$ or MgO. On the effect of the physical properties of the catalyst on the discharge process, Gorbanev *et al* found that transition metal catalysts performed much better than plasma alone or Al$_2$O$_3$ supports, but there is not much difference between different transition metal catalysts [235], in line with their earlier model predictions about the role of radicals and E–R mechanisms at the catalyst surface [236]. Moreover, it was recently found that the catalyst also affects the plasma by changing the physical characteristics of the plasma, rather than playing a real chemical catalytic effect [237]. The porous metal oxide is often employed as the primary material for filling DBD beds. Wang *et al* [221] designed a novel DBD reactor and used Al$_2$O$_3$ loaded with different transition metals (Fe, Ni, Cu) as the catalysts for ammonia synthesis. The dominant catalytic active sites were found to be the chemical properties of the catalyst surface, and Ni/Al$_2$O$_3$ demonstrated the highest effectiveness with a synthesis rate of 471 μmol g^{-1} h^{-1}, a 100% improvement over plasma alone, attributed to metal sites and weak acidic sites promoting NH$_3$ by facilitating the formation of NH$_2$ intermediates on the surface (figure 12(c))

Similarly, Iwanmoto *et al* [238] also found that Ni/Al$_2$O$_3$ catalyst was significantly more active than Fe/Al$_2$O$_3$ and Ru/Al$_2$O$_3$, with the latter two showing lower catalytic activity than unloaded alumina. The study suggested the activation of nitrogen atoms was the main obstacle to ammonia decomposition on Ni, making Ni/Al$_2$O$_3$ a good choice due to its high activity. Liu *et al* [239] investigated the synthesis of ammonia using a bimetallic catalyst in addition to a single-metal one. They found that Co–Ni/Al$_2$O$_3$ had the highest ammonia synthesis rate of 1500 μmol g^{-1} h^{-1}. The addition of the Co–Ni bimetallic catalyst reduced catalyst surface acidity, facilitating ammonia desorption, and improving power efficiency through an increased average electric field, surpassing the performance of single-metal catalysts and plasma alone. Additionally, the study by Gorky *et al* [240] explored the effects of catalyst size by using SiO$_2$ to support Ni nanoparticles with average sizes of 5.6 nm and 13.5 nm. They found that smaller particles synthesized ammonia at least twice as fast as the larger ones and bulk nickel under equimolar conditions. Catalysts in M/C form not only provide active sites and increase the activation efficiency but also create pores to protect generated NH$_3$ from reverse reactions. Wang *et al* [220] effectively used mesoporous MCM-41 to support a Ni catalyst, achieving over 5% ammonia yield and 1.5 g kWh^{-1} energy yield. This effect was facilitated by an enhanced plasma-catalyst interaction due to active nickel sites on the MCM-41 surface, and the protective mesopores that prevented NH$_3$ decomposition, thereby effectively promoting the reaction (figure 12(b)).
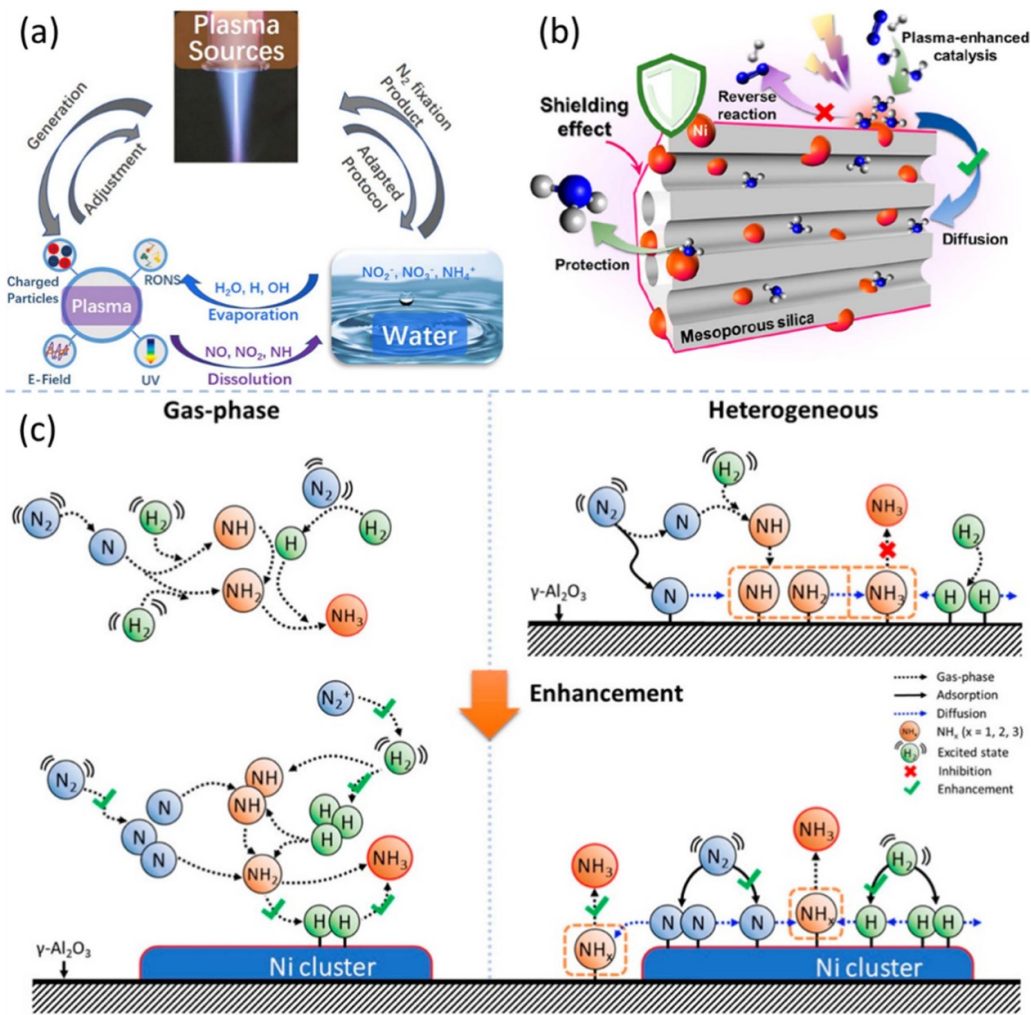
Figure 12. (a) Plasma sources, plasma, water and their interrelationship enable the effective plasma-water-based nitrogen fixation [219]. John Wiley & Sons. © 2022 Wiley-VCH GmbH; (b) Schematic of the proposed mechanism for the plasma-assisted surface reaction and the 'shielding protection' effect of mesoporous MCM-41. Reproduced from [220]. CC BY 4.0. (c) Proposed mechanism for the enhancement of ammonia synthesis by Ni/Al$_2$O$_3$ catalyst. Reproduced from [221]. CC BY 4.0.

3.3.2.2. N$_2$–H$_2$O reaction system. Traditional ammonia synthesis relies on hydrogen gas, often produced by CO$_2$-emitting methods like methane reforming or the energy-intensive process of water electrolysis. In contrast, using water as a hydrogen source in the system is safer and greener, due to the safety risks and purity demands associated with hydrogen gas. Additionally, it is more energy-efficient than the H–B process, in which deriving H$_2$ from CH$_4$ is the most energy-demanding step [241].

The plasma system consisting of N$_2$ and H$_2$O not only generates ammonia, but also produces by-products such as nitrogen oxides, hydrogen peroxide, and H$^+$ [242]. The reaction mechanism between N$_2$ and H$_2$O in plasma is complex as N$_2$ undergoes both oxidation and reduction reactions. When H$_2$O is exposed to the plasma, it undergoes decomposition into H atoms and OH radicals through two modes: electron impact and ultraviolet radiation, represented by equations (R25) and (R26) [241]. The presence of OH radicals is a crucial aspect of the reaction system, which significantly alters the type of active particles in the system and,

thus, affects the reaction pathway and final products [243]. Additionally, Sakakura *et al* [241] suggested that active nitrogen species, such as N atoms, N$_2^*$, and N$_2^+$, can react directly with H$_2$O to produce OH and NH radicals,

$$H_2O + e \rightarrow OH + H + e \quad (R25)$$

$$H_2O \xrightarrow{h\nu} OH + H. \quad (R26)$$
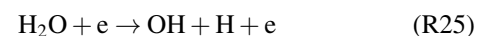
The NTP-assisted synthesis mechanism of NH$_3$ from N$_2$ and H$_2$O is generally by the mutual reaction of active nitrogen species with H atoms, OH radicals, or H$_2$O molecules to generate NH radicals, which are then gradually hydrogenated to produce NH$_3$ [244, 245]. Obviously, the generation of OH radicals is inevitable and vital in reactions involving water, with their strong oxidizing nature contributing to the production of nitrogen compounds like NO$_x$ [219] (figure 12(a)). Gromov *et al* [243] studied the dynamics of OH radicals and their impact on NO radical synthesis, finding that NO and OH radicals behaved similarly, and the production of NO is primarily

J. Phys. D: Appl. Phys. **57** (2024) 503002

Topical Review

driven by OH radicals. However, the role of O atoms in this process is relatively minor.

There are two ways of introducing water into the reaction system which have been discussed in section 2.1.4. One of the ways is that H_2O reacts with the N_2 plasma in the gas phase in the form of vapor or liquid droplet aerosols. The other way is that H_2O directly reacts with the N_2 plasma at the interface between the plasma and liquid phase, and this type is also known as a plasma/liquid (P/L) reaction. Depending on the reaction type used, there are variations in the reaction pathways and mechanisms for the synthesis of ammonia and nitrogen oxides.

Toth *et al* [246] used both atomized water droplets and water vapor to react with N_2 in a DBD reactor, and collected the products with water afterward. The results showed that ammonia was produced through gas-phase chemistry, and the liquid phase may not have played an important role. In addition, the mechanism of NH_3 production may be similar to the mechanism in which H_2O vapor is decomposed into H atoms and OH radicals. Similarly, Gorbanev *et al* [245] used a plasma jet reactor at the plasma-water interface and added water vapor to N_2 gas, marking the H_2O from two different sources, water vapor and liquid phase, using isotope labeling. The results showed that the water vapor added to the N_2 was the main source of NH_3 production and water vapor contents affect the reaction mechanism. During the reaction of dry N_2 with liquid-phase H_2O, NH_3, and H_2O_2 were produced in roughly equal amounts, which suggested that N atoms reacted with H_2O to generate NH and OH. The OH then combined to form H_2O_2, illustrating the ability of plasmas to interact with H_2O molecules in the liquid phase. Under conditions where the water vapor concentration was between 2% and 10%, the reaction was highly selective towards ammonia, and no H_2O_2 was detected in the product, indicating that it may contain O_2. However, when the water vapor reached saturation, the product contained both ammonia and NO_3^- and NO_2^-. Pattyn *et al* [247] used a similar plasma jet apparatus to control the H_2O content in N_2. This reactor involves both HER and oxygen evolution reaction, and H atoms may also combine to produce hydrogen gas. The supply of oxidative species (O_2, OH) and reductive species (H_2, H) involved in the reaction largely depends on the water vapor content in the gas phase, and an increase in the water vapor content in the gas phase is beneficial for the excitation of N_2 vibration and is also significantly correlated with the production of NO and H_2. In addition, since the ionization energies between nitrogen (15.58 eV) and water (12.62 eV) are notably different, the water vapor content also has a complex effect on discharge characteristics in many ways, such as affecting non-elastic collision mechanisms, electron density, and electron energy distribution functions.

In the P/L reaction for ammonia synthesis, several discharge types are commonly used, including plasma jet, GA discharge, rotating arc discharge, and underwater spark discharge. For example, Hawtof *et al* [248] used a plasma jet reactor, similar to the electrochemical method but with a plasma jet generated in the gap between a stainless steel nozzle and the solution surface replacing the metal cathode. H_2SO_4 was added to provide protons for N_2 reduction and captured NH_3. The selectivity for NH_3 production was 100% at low currents (1–2 mA) but decreased significantly at 3 mA or higher due to the increased number of electrons consuming protons at the plasma–liquid interface. Indumathy *et al* [249] employed GA discharge to generate a plasma plume at the interface between the liquid and plasma phases. Upon contact with water, the tip of the plasma plume exhibited vibrations and rotational excitations, and this method achieved a high ammonia yield of 0.68 mg h^{-1}. However, the energy efficiency of this approach is relatively low but can improve with longer reaction times. The aforementioned reaction types have limited contact area, whereas utilizing bubbles as interfaces can enhance the reaction area by increasing the contact surface. Peng *et al* [250] utilized an underwater bubble discharge to synthesize ammonia and achieved a nitrogen conversion rate of 11.2 μmol min^{-1}.

In comparison to the plasma synthesis of ammonia using N_2 and H_2 as reactants, there have been fewer studies on the catalytic synergy of N_2 and H_2O in plasma. The placement of the catalyst is relatively flexible and can be in either the gas or liquid phase. Lamichhane *et al* [251] investigated the plasma-assisted synthesis of ammonia using a plasma jet reactor with metal catalysts including zinc (Zn), magnesium (Mg), aluminum (Al), and copper (Cu) in the liquid phase. The metals reduced H^+ ions to H atoms and were used to regulate pH and increase the NH_3 reaction rate, with Mg being the most effective catalyst, improving the reaction rate by 2.6 times compared to using plasma alone. Lamichhane *et al* [251] used a RGA with swirling N_2 flow and a cooling water film to regulate the arc. The ionization of the water film by high-energy electrons and active nitrogen species produced H and OH/O radicals, which reacted with nitrogen radicals to generate NO_x. The authors then injected the resultant NO and H_2 into a plasma reactor coupled with a Pd/γ-Al_2O_3 catalyst, leading to a high selectivity for NH_3 of up to 95%. Zhang *et al* [49] used four different DBD configurations, including water-grounded double DBD (DDBD), water-grounded single DBD, DDBD-water cooling, and single DBD-water cooling. The discharge zone was filled with Ru catalysts with various supports such as Al_2O_3, SiO_2, and MgO, and their findings showed that MgO with its strong alkalinity and electron-providing capabilities, enhanced molecular dissociation on the catalyst surface and reduced the dissociation barrier of N_2 and H_2O, eventually resulting in a high ammonia yield of up to 2.67 mmol h^{-1}.

3.3.3. Summary. Research in plasma-assisted nitrogen fixation has focused on producing NO_x and ammonia. NTP offers a more energy-efficient approach for NO_x production compared to traditional methods, with the activation of N_2 via vibrational excited N_2^* being particularly efficient. GA discharge with relatively higher temperatures, is gaining attention for its high energy efficiency. For ammonia synthesis, plasma reactors combined with catalysts, especially DBD packed catalyst reactors, are extensively studied. The choice of catalysts, including mono, supported, and promoted types, significantly

J. Phys. D: Appl. Phys. **57** (2024) 503002

Topical Review

affects the process. Attempts to use alternative feedstocks like H_2O are also explored to improve energy efficiency.

However, plasma-assisted nitrogen fixation still lags behind the H–B process in terms of energy consumption and yield. Future research should aim to achieve lower energy consumption and higher production concentration, focusing on plasma reactor improvements and plasma-catalysis interaction. Selecting effective catalysts and exploring pulsed energization, like high frequency nanosecond pulsing, could optimize efficiency and yield. Integrating renewable energy sources and designing efficient power supply systems and large-scale reactors are critical. Challenges include product separation, absorption, overall process design, and scaling up the technology. Emerging markets with low ammonia capacity and high demand, such as in Africa, present opportunities for small-scale, decentralized plasma-assisted nitrogen fixation applications, leveraging local renewable resources. Therefore, concurrent techno-economic and sustainability evaluations are necessary to guide the process towards practical applications.

4. Hybrid technologies for gas conversion

Coupling of plasmas with other technologies for gas conversion, such as photocatalysis, electrocatalysis and biocatalysis, is a highly topical research area. When these technologies are employed individually, the energy efficiency and yield for gas conversions remain relatively low. However, when combined with the plasma in a synergistic manner, the energy efficiency and yield can be significantly enhanced [216].

4.1. Plasma-photocatalysis

Among these hybrid forms, photocatalysis combined with plasma is commonly utilized and mainly for decomposition of pollutants (e.g. VOCs) [252]. In the application of ammonia synthesis, the use of VUV/UV irradiation in photocatalytic processes can facilitate the progression of ammonia synthesis reactions by dissociating water molecules into H atoms and OH radicals. For instance, Sakakura *et al* [241, 253] studied the P/L reaction mechanism at the interface of the excited gas phase and water phase (figure 13(a)). The results showed that the P/L reaction dominated by N_2^* and N_2^+ as reaction particles was the main reaction when the P/L reaction site was irradiated with ultraviolet light, and the production of nitrogen-containing compounds increased. This finding suggests that under ultraviolet radiation, H_2O decomposes into H and OH, and N_2^+ and N_2^* are more likely to react with water molecules. However, when the content of N atoms is high, ultraviolet irradiation does not promote the reaction, indicating that the reactivity of N atoms with H_2O is high in the absence of photocatalysis. Peng *et al* [244] used a spray jet plasma and employed UV irradiation to excite vapor and liquid water molecules to promote nitrogen fixation, significantly increasing the yield of nitrate, nitrite, and ammonium, with the highest synthesis rates of 15.1 mmol min^{-1}, 40.3 mmol min^{-1}, and 2.5 mmol min^{-1}, respectively. Moreover, study by Mei *et al* [131], suggests that the UV emissions generated by the CO_2

DBD have a minimal impact on the activation of $BaTiO_3$ and TiO_2 catalysts in the plasma-photocatalytic conversion of CO_2. The synergistic effect observed in plasma-catalysis for CO_2 conversion is primarily attributed to the physical influence resulting from the presence of catalyst pellets within the discharge and the dominant surface reaction driven by the plasma-induced photocatalysis.

In plasma-photocatalysis, major challenges involve effectively combining plasma technology with photocatalysis and fine-tuning this integration for various reactions and catalysts. Ensuring efficient light absorption and distribution within the system is critical, necessitating innovative reactor and light source designs. Stability and durability of photocatalysts in plasma environments are also key concerns. Future research should focus on developing photocatalysts specifically for plasma compatibility and refining reactor designs for optimal interaction between light, plasma, and photocatalysts. Additionally, studies are needed to determine how plasma settings and light properties affect the efficiency and specificity of reactions, including plasma parameters, light intensity, and wavelength.

4.2. Plasma-electrocatalysis

The electrocatalytic coupling of plasmas for gas conversions, especially for ammonia synthesis, has been a research direction of great interest to scientists. Although plasmas have numerous advantages, the key challenges that need to be overcome are effective nitrogen fixation and suppressing the occurrence of reverse reactions [238]. Therefore, there is a need to develop more active catalysts under the plasma action and to design better-performing reactors to address these issues. Electrochemical catalysis is limited by the competition of the HER with the main reaction, the high energy barrier of the triple bond in nitrogen molecules, leading to the lower reaction rates, lower Faraday efficiencies, and lower product selectivity [254]. Therefore, the hybrid method involving the plasma activation and electrocatalysis has been proposed. Plasmas are used for nitrogen activation, and electrocatalysis is used to provide co-reactants, which has achieved good results.

Kumali *et al* [255] designed a device that combines a plasma jet and electrochemistry, using a quad-electrode to ensure that both plasma and electrochemical reactions occur at appropriate voltages. Liquid water is circulated through the anode chamber, while N_2/He gas is introduced into the cathode chamber through the plasma jet electrode. A proton exchange membrane electrolyzer assisted by the plasma is employed, enabling protons (H^+) produced by electrocatalysis to move from the anode to the cathode, where they react with the activated nitrogen species to produce ammonia. The results show that when a bias voltage of about 3.5 V is applied to both ends of the electrolyzer, 47% more ammonia is produced by the plasma than by the electrochemical reaction alone. Sharma *et al* [256] used a variety of catalysts for the ammonia synthesis, exposing catalysts to the plasma and coupling electrochemical and thermal catalysis. They utilized radiofrequency discharge and designed a N_2 plasma-assisted proton-conductive solid oxide electrolyzer (H-SOEC). The H-SOEC
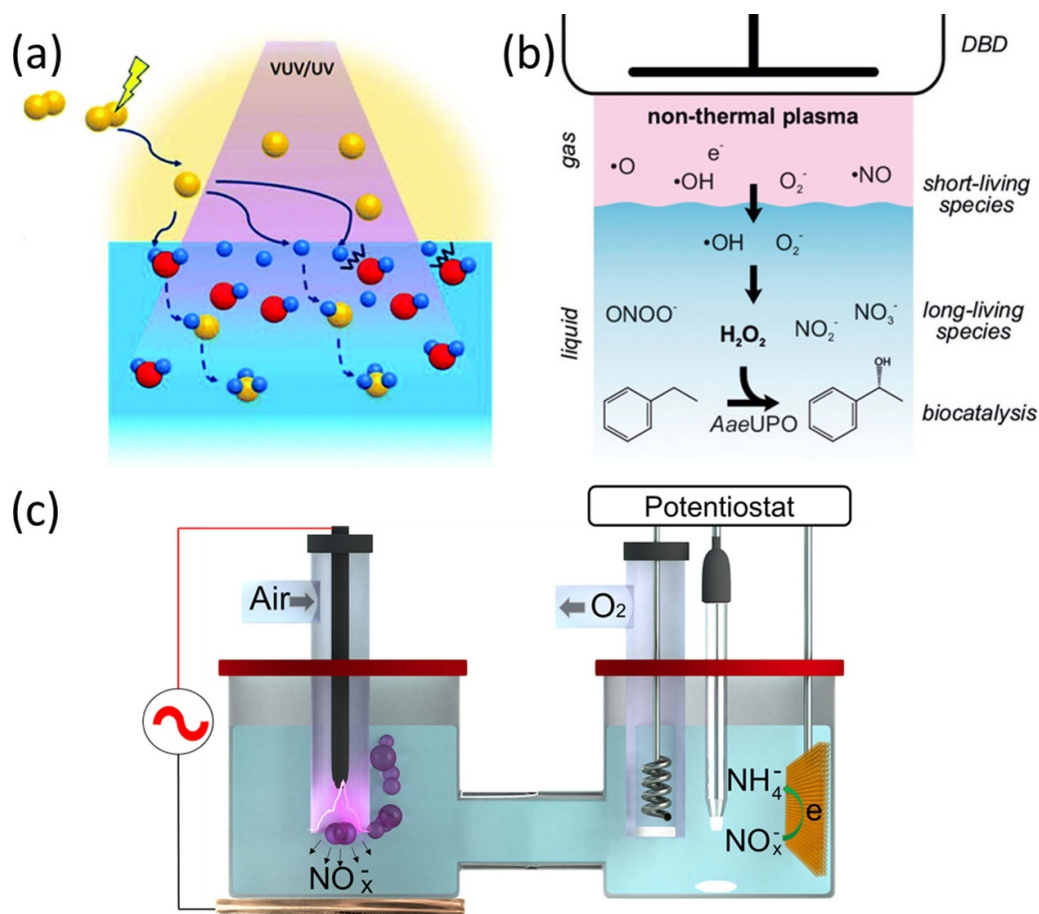
J. Phys. D: Appl. Phys. **57** (2024) 503002

Topical Review

Figure 13. (a) Water irradiated with UV light after which the interfacial reaction between the N-plasma and water phase was carried out for specified reaction times. Reproduced from [253] with permission from the Royal Society of Chemistry. (b) Scheme of plasma-driven biocatalysis: non-thermal plasma, created by dielectric barrier discharge, forms reactive species in liquid, facilitating hydrogen peroxide generation for biocatalysis. Enzyme immobilization minimizes plasma-related side effects, enabling the production of pure (R)-1-phenylethanol with plasma-generated H_2O_2 and AaeUPO. Reproduced from [261]. CC BY 4.0. (c) A schematic showing integrated plasma bubbles with an electrochemical system: plasma activation of air, producing NO_x dissolved in water as an intermediary for the electrochemical synthesis of ammonium. Reproduced from [216] with permission from the Royal Society of Chemistry.

is based on a half-cell supported Ni-BCZY/BCZY battery and platinum cathode. The platinum catalyst has a microporous structure, facilitating effective diffusion of the reactant gases and creating a high surface area. The ammonia production rate and Faraday efficiency of this method are 26.8 nmol·s^{-1}·cm^{-2} and 88% respectively. More recently, Sun *et al* [216] introduced a new hybrid technology which integrates NTP-driven NO_x production with its electrocatalytic reduction, thus facilitating green ammonia production under ambient conditions (figure 13(b)).

This approach overcomes the challenges of low solubility and intrinsic non-reactivity associated with atmospheric dinitrogen. The energy efficiency is enhanced through a NTP bubble column reactor, featuring a dual reactor configuration, multiple discharge schemes, and bubble dynamic control to generate NO_x intermediaries at an energy efficiency of 3.8 kWh mol^{-1}. These intermediaries were successfully converted to ammonia at a significant rate of 23.2 mg h^{-1}, using a scalable electrolyzer operated at a low cell voltage of 1.4 V. Further study has been conducted on this sustainable method to produce NH$_3$ directly from air using the

plasma-electrocatalysis system via the N_2–NO_x–NH_3 pathway [57], and the study of electrocatalysts has been significantly deepened and enhanced. Wu *et al* [257] used a RGA plasma jet as the initial step, followed by employing a cobalt single-atom electrocatalyst for ammonia synthesis at a yield rate of 1.43 mg cm^{-2} h^{-1} with almost 100% Faradaic efficiency. The distinctive electronic properties of isolated active sites enhanced proton/electron transfer and reduced HER. Zheng *et al* [258] engineered a defective N-MoS$_2$/VGs electrocatalyst (VG stands for vertically oriented graphene), which incorporates metallic 1 T-MoS$_2$ phase, N doping, and S vacancies through a one-step plasma engraving process. Via a plasma tandem-electrocatalysis system for NH$_3$ synthesis directly from air, they achieved an impressive NH$_3$ production rate of 7.3 mg h^{-1} cm^{-2} with an energy efficiency of 2.4 MJ mol^{-1}. Liu *et al* [259] developed amorphous Ni(OH)$_x$/Cu electrocatalysts that interact with hydrated K$^+$ in the double layer through noncovalent interactions and accelerate the activation of water, enriching adsorbed hydrogen species that can readily react with N-containing intermediates, with the NH$_3$ yield rate of approximately 21.25 mg h^{-1} cm^{-2} sustained over 100 h using

pure air as the intake. Kong *et al* [260] develop a plasma-electrochemical cascade pathway powered by electricity for sustainable hydroxylamine synthesis directly from ambient air and water at mild conditions. The faradaic efficiency for hydroxylamine reached 81.0% at -1.0 V versus a reversible hydrogen electrode, with a high hydroxylamine yield rate of 23.53 mg cm^{-2} h^{-1} and a selectivity of 95.8%.

The current approach to coupling plasma and electrocatalysis is mainly a two-step process, posing scalability challenges when transitioning from laboratory demonstrations to industrial applications, particularly in maintaining system efficiency and stability. A significant issue of one-step coupling process is the interaction between plasma and electrode materials, which can lead to material erosion or degradation, thereby affecting operational lifespan and performance of processing systems. Future work in plasma-electrocatalysis involves developing advanced electrode materials resistant to plasma-induced degradation and researching the integration of plasma and electrocatalytic systems for efficient and scalable operations.

4.3. Plasma-biocatalysis

Plasma biocatalysis, an emerging field at the intersection of plasma physics and biotechnology, leverages the unique properties of plasma to enhance or enable biochemical reactions [262]. This innovative approach involves the use of plasma, an ionized gas with reactive species, to influence enzymatic activities, offering new possibilities for industrial biocatalysis. This approach focuses on generating reactive species like hydrogen peroxide (H_2O_2) *in situ*, which play a crucial role in various enzymatic processes.

Yayci *et al* [261] have proposed an innovative technique employing DBD plasma for the *in-situ* generation of H_2O_2, a breakthrough in biocatalysis involving peroxidases and peroxygenases (figure 13(b)). This approach addresses the sensitivity of the enzymes to peroxide substrates, enabling controlled H_2O_2 production for more efficient enzymatic processes. The application of this method with horseradish peroxidase and fungal peroxygenase underscores the potential of technical plasmas for noninvasive and eco-friendly peroxide-based biotransformations, though direct plasma contact may impact enzyme activity. Yayci *et al* [263] explored the capabilities of a microscale APPJ (μAPPJ) in biocatalysis, noting its superior ability to produce H_2O_2 compared to DBD, particularly in processing larger reaction volumes. The efficacy of μAPPJ was validated using recombinant unspecific peroxygenase from Agrocybe aegerita (rAaeUPO), yielding high turnover rates without adverse side reactions from other plasma-generated species. This study positions μAPPJ as an effective plasma source for biocatalysis, preserving enzyme activity even after prolonged plasma treatment. Addressing the needs of fatty acid peroxygenase OleTJE, another research team [264] utilized the Cooperation in Science and Technology (COST)-Jet, an atmospheric pressure plasma jet. This method gradually generates H_2O_2 *in situ*, preventing OleTJE from overoxidation. The operation of COST-Jet using a helium-water mixture was shown to enhance enzyme turnover, surpassing traditional hydrogen peroxide treatments and demonstrating its advantage in delivering a regulated amount of H_2O_2 for OleTJE's functionality.

Although some research has explored the roles of other reactive oxygen and nitrogen species (RONS) such as peroxynitrite ($ONOO^-$) and superoxide (O_2^-) [265], these studies are relatively few and do not provide comprehensive discussions. Additionally, there is a notable absence of a comparative analysis between plasma-based hydrogen peroxide (H_2O_2) production and other *in-situ* methods like electrocatalysis or photocatalysis, leaving a gap in understanding the unique benefits of the plasma-based approach. For future research, it is essential to gain insights into the detailed roles and effects of various RONS in plasma biocatalysis. Understanding these roles could reveal unique advantages of plasma technology over other methods, contributing significantly to the advancement of this field.

5. Summary and outlook

PP2X, a distinctive thrust within the P2X approach, is an interdisciplinary field involving electrical engineering, physics, nanotechnology, and chemistry. It promises to enhance traditional catalysis through the efficient generation of chemicals, fuels and materials using NTPs. With its adaptable 'on-demand' capability, PP2X seamlessly accommodates the intermittency and variability of renewable energy sources like wind and solar power, while simultaneously mitigating CO_2 emissions from fossil fuel combustion. This review highlights recent trends and innovations in NTP technology applicable to renewable P2X, exploring CO_2 conversion, CH_4 conversion, and N_2 fixation. It also discusses the potential of hybrid technologies that blend plasmas with other renewable solutions.

Although research highlights the clear benefits of the PP2X approach, its practical implementation faces several notable challenges. Most of the research is still in the experimental stage, primarily using single-reactor setups. This presents difficulties in scaling up and integrating these processes, necessitating the development of new types of reactors and more effective plasma initiators. The high reactivity of plasma leads to complex competitive reactions, which demand advanced separation technologies. These technologies may incur additional financial and energy costs. Moreover, while combining plasma with catalysts appears to enhance reaction efficiency and initiate reactant activation, the detailed mechanisms and interactions between plasma and catalysts remain underexplored. This includes the effects of various excited states, both electronic and vibrational, on the catalyst surface and their impact on product formation. Energy consumption, a key factor for commercial viability, also presents a challenge. PP2X approach currently falls short of industrial production standards. Furthermore, existing studies tend to focus on the energy used in the reactions, neglecting the energy used by related equipment like plasma generators and gas systems. This oversight is critical and needs addressing. Lastly,

the energy efficiency and conversion rate of PP2X approach hinge on the appropriate selection of plasma sources and catalysts. Achieving the right balance between these two elements is frequently challenging.

To advance the industrial use of PP2X approach, it is crucial to enhance control precision, conversion rate, and energy efficiency in producing target products, often through catalyst introduction. The focus should be on designing multifunctional catalysts with strong adsorption and selective rearrangement capabilities. A combination of experimental, theoretical, and modeling techniques is essential for understanding complex multi-unit cascade plasma catalytic reactions, aiming for selective high-value product formation. The importance of a collaborative effort in a multi-scale, multi-phase computational study on various PP2X applications becomes even more crucial as complex hybrid systems are introduced to capitalize on the benefits of energy efficiency. A deeper insight into the fundamental mechanisms is essential to fully realize the capabilities of P2X approach. Advanced *in-situ* characterization and isotope tracing are key to uncovering plasma catalysis mechanisms, particularly in understanding reactant activation pathways and the role of transient species. It is also vital to tailor plasma-catalyst materials to the specific excitation characteristics of reactants and target product attributes. Additionally, integrating plasma reactors with renewable energy and developing process flow models for energy and material consumption are important. This includes piloting small-scale reactors compatible with distributed renewable energy, alongside feasibility and techno-economic studies for PP2X approach. It is essential to establish a standardized approach for estimating energy consumption in research related to PP2X application. This will offer comprehensive guidance for both economic and social policies throughout the lifecycle of new energy utilization.

PP2X stands at the intersection of various disciplines, making multidisciplinary collaboration vital. It offers opportunities in clean energy and green chemistry, potentially impacting energy grid stabilization and peak demand management. Modular plants and decentralized chemical production facilities represent future developments. This technology can significantly contribute to CO_2 emission reduction and sustainable energy landscapes. We aim for this article to spark further discussion and collaborative efforts in this dynamic field of research and technological innovation.

Data availability statement

No new data were created or analyzed in this study.

Acknowledgments

Declaration of interests

Authors P J is associated with PlasmaLeap Technologies, a company with interests in plasma-driven Power-to-X commercial activities.

ORCID iDs

Jing Sun https://orcid.org/0000-0002-9820-5754
Zhongping Qu https://orcid.org/0009-0000-0268-4766
Dingxin Liu https://orcid.org/0000-0003-0910-2903
Xin Tu https://orcid.org/0000-0002-6376-0897
Danhua Mei https://orcid.org/0000-0002-3024-3551
Zhi Fang https://orcid.org/0000-0001-9116-5449
Chuanlong Ma https://orcid.org/0000-0002-2847-1635
Liguang Dou https://orcid.org/0000-0002-7894-957X
Shuai Zhang https://orcid.org/0000-0002-5350-4048
Tao Shao https://orcid.org/0000-0002-5738-1241
Dawei Liu https://orcid.org/0000-0003-3503-2099
Xinpei Lu https://orcid.org/0000-0003-0676-9585
Zheng Bo https://orcid.org/0000-0001-9308-7624
Wei-Hung Chiang https://orcid.org/0000-0002-6350-6696
Michael Keidar https://orcid.org/0000-0003-0869-4310
Anton Nikiforov https://orcid.org/0000-0002-2255-6419
Ali Rouhollah Jalili https://orcid.org/0000-0003-3851-0818
Volker Hessel https://orcid.org/0000-0002-9494-1519
Annemie Bogaerts https://orcid.org/0000-0001-9875-6460
Anthony B Murphy https://orcid.org/0000-0002-2820-2304
Renwu Zhou https://orcid.org/0000-0003-1773-7095
Kostya (Ken) Ostrikov https://orcid.org/0000-0001-8672-9297

References

[1] Buttler A and Spliethoff H 2018 Current status of water electrolysis for energy storage, grid balancing and sector coupling via power-to-gas and power-to-liquids: a review *Renew. Sustain. Energy Rev.* **82** 2440–54

[2] Daiyan R, MacGill I and Amal R 2020 *Opportunities and Challenges for Renewable Power-to-X* (ACS Publications)

[3] Burre J, Bongartz D, Brée L, Roh K and Mitsos A 2020 Power-to-X: between electricity storage, e-production, and demand side management *Chem. Ing. Tech.* **92** 74–84

[4] Zhang Q, Bedford N M, Pan J, Lu X and Amal R 2019 A fully reversible water electrolyzer cell made up from FeCoNi (oxy) hydroxide atomic layers *Adv. Energy Mater.* **9** 1901312

[5] Liu J, Duan S, Shi H, Wang T, Yang X, Huang Y, Wu G and Li Q 2022 Rationally designing efficient electrocatalysts for direct seawater splitting: challenges, achievements, and promises *Angew. Chem.* **134** e202210753

[6] Wan Y, Xu J and Lv R 2019 Heterogeneous electrocatalysts design for nitrogen reduction reaction under ambient conditions *Mater. Today* **27** 69–90

[7] Yang J *et al* 2022 Potential-driven restructuring of Cu single atoms to nanoparticles for boosting the electrochemical reduction of nitrate to ammonia *J. Am. Chem. Soc.* **144** 12062–71

[8] Möller T, Ju W, Bagger A, Wang X, Luo F, Thanh T N, Varela A S, Rossmeisl J and Strasser P 2019 Efficient CO_2 to CO electrolysis on solid Ni–N–C catalysts at industrial current densities *Energy Environ. Sci.* **12** 640–7

[9] Ma W, Xie S, Zhang X-G, Sun F, Kang J, Jiang Z, Zhang Q, Wu D-Y and Wang Y 2019 Promoting electrocatalytic CO_2 reduction to formate via sulfur-boosting water activation on indium surfaces *Nat. Commun.* **10** 892

[10] Andersen S Z *et al* 2019 A rigorous electrochemical ammonia synthesis protocol with quantitative isotope measurements *Nature* **570** 504–8

[11] Goldston R J 2020 *Introduction to Plasma Physics* (CRC Press)

[12] Conrads H and Schmidt M 2000 Plasma generation and plasma sources *Plasma Sources Sci. Technol.* **9** 441

[13] Seo D H, Rider A E, Han Z J, Kumar S and Ostrikov K 2013 Plasma break-down and Re-build: same functional vertical graphenes from diverse natural precursors *Adv. Mater.* **25** 5638–42

[14] Pho Q H, Lin L, Rebrov E V, Sarafraz M M, Tran T T, Tran N N, Losic D and Hessel V 2023 Process intensification for gram-scale synthesis of N-doped carbon quantum dots immersing a microplasma jet in a gas-liquid reactor *Chem. Eng. J.* **452** 139164

[15] Xiao L, Zheng Q, Zhou R, Liu S, Zhao Y, Zhao Y, Zhou R and Ostrikov K K 2024 Plasma-assisted synthesis of porous bismuth nanosheets for electrocatalytic CO_2-to-formate reduction *J. Energy Chem.* **94** 19–28

[16] Coad B R, Favia P, Vasilev K and Griesser H J 2022 Plasma polymerization for biomedical applications: a review *Plasma Process. Polym.* **19** 2200121

[17] Zhou R, Zhao Y, Zhou R, Zhang T, Cullen P, Zheng Y, Dai L and Ostrikov K 2023 Plasma-electrified up-carbonization for low-carbon clean energy *Carbon Energy* **5** e260

[18] Zamri A A, Ong M Y, Nomanbhay S and Show P L 2021 Microwave plasma technology for sustainable energy production and the electromagnetic interaction within the plasma system: a review *Environ. Res.* **197** 111204

[19] Snoeckx R and Bogaerts A 2017 Plasma technology–a novel solution for CO_2 conversion? *Chem. Soc. Rev.* **46** 5805–63

[20] Vertongen R and Bogaerts A 2023 How important is reactor design for CO_2 conversion in warm plasmas? *J. CO_2 Util.* **72** 102510

[21] Bogaerts A, Neyts E C, Guaitella O and Murphy A B 2022 Foundations of plasma catalysis for environmental applications *Plasma Sources Sci. Technol.* **31** 053002

[22] Li T, Gao Y, Zhou R, Zhang T and Ostrikov K K 2024 Outlook for improving energy efficiency, conversion rates, and selectivity of plasma-assisted CO_2 conversion *Curr. Opin. Green Sustain. Chem.* **47** 100915

[23] Ray D, Ye P, Jimmy C Y and Song C 2023 Recent progress in plasma-catalytic conversion of CO_2 to chemicals and fuels *Catal. Today* **423** 113973

[24] Kondratenko E V, Mul G, Baltrusaitis J, Larrazábal G O and Pérez-Ramírez J 2013 Status and perspectives of CO_2 conversion into fuels and chemicals by catalytic, photocatalytic and electrocatalytic processes *Energy Environ. Sci.* **6** 3112–35

[25] Qiao J, Liu Y, Hong F and Zhang J 2014 A review of catalysts for the electroreduction of carbon dioxide to produce low-carbon fuels *Chem. Soc. Rev.* **43** 631–75

[26] Kumar B, Llorente M, Froehlich J, Dang T, Sathrum A and Kubiak C P 2012 Photochemical and photoelectrochemical reduction of CO_2 *Annu. Rev. Phys. Chem.* **63** 541–69

[27] Verma S, Kim B, Jhong H R M, Ma S and Kenis P J 2016 A gross-margin model for defining technoeconomic benchmarks in the electroreduction of CO_2 *ChemSusChem* **9** 1972–9

[28] Albo J, Alvarez-Guerra M, Castaño P and Irabien A 2015 Towards the electrochemical conversion of carbon dioxide into methanol *Green Chem.* **17** 2304–24

[29] Zhao Y, Gao W, Li S, Williams G R, Mahadi A H and Ma D 2019 Solar-versus thermal-driven catalysis for energy conversion *Joule* **3** 920–37

[30] Galadima A and Muraza O 2019 Catalytic thermal conversion of CO_2 into fuels: perspective and challenges *Renew. Sustain. Energy Rev.* **115** 109333

[31] Izumi Y 2013 Recent advances in the photocatalytic conversion of carbon dioxide to fuels with water and/or hydrogen using solar energy and beyond *Coord. Chem. Rev.* **257** 171–86

[32] Das S and Daud W W 2014 A review on advances in photocatalysts towards CO_2 conversion *RSC Adv.* **4** 20856–93

[33] Smestad G P and Steinfeld A 2012 photochemical and thermochemical production of solar fuels from H_2O and CO_2 using metal oxide catalysts *Ind. Eng. Chem. Res.* **51** 11828–40

[34] Roy S C, Varghese O K, Paulose M and Grimes C A 2010 Toward solar fuels: photocatalytic conversion of carbon dioxide to hydrocarbons *ACS Nano* **4** 1259–78

[35] Schenk P M, Thomas-Hall S R, Stephens E, Marx U C, Mussgnug J H, Posten C, Kruse O and Hankamer B 2008 Second generation biofuels: high-efficiency microalgae for biodiesel production *Bioenergy Res.* **1** 20–43

[36] Brennan L and Owende P 2010 Biofuels from microalgae—a review of technologies for production, processing, and extractions of biofuels and co-products *Renew. Sustain. Energy Rev.* **14** 557–77

[37] Halim R, Danquah M K and Webley P A 2012 Extraction of oil from microalgae for biodiesel production: a review *Biotechnol. Adv.* **30** 709–32

[38] Shen Y 2014 Carbon dioxide bio-fixation and wastewater treatment via algae photochemical synthesis for biofuels production *RSC Adv.* **4** 49672–722

[39] Fridman A, Chirokov A and Gutsol A 2005 Non-thermal atmospheric pressure discharges *J. Phys. D: Appl. Phys.* **38** R1

[40] Kogelschatz U 2003 Dielectric-barrier discharges: their history, discharge physics, and industrial applications *Plasma Chem. Plasma Process.* **23** 1–46

[41] Rad R H, Khani M R, Mehdikia H, Shafiei M and Shokri B 2019 Decomposition of high concentration benzene (produced in paper and painting industries) and its byproducts, methane and carbon dioxide, using plate gliding arc *J. Environ. Health Sci. Eng.* **17** 549–60

[42] Mousavi S A, Piavis W and Turn S 2019 Reforming of biogas using a non-thermal, gliding-arc, plasma in reverse vortex flow and fate of hydrogen sulfide contaminants *Fuel Process. Technol.* **193** 378–91

[43] Kalra C S, Kossitsyn M, Iskenderova K, Chirokov A, Cho Y I, Gutsol A and Fridman A 2003 Electrical discharges in the reverse vortex flow–tornado discharges *Electronic Proc. 16th Int. Symp. on Plasma Chemistry* (*Taormina, Italy*)

[44] Bogaerts A and Centi G 2020 Plasma technology for CO_2 conversion: a personal perspective on prospects and gaps *Front. Energy Res.* **8** 111

[45] Foster J E 2017 Plasma-based water purification: challenges and prospects for the future *Phys. Plasmas* **24** 055501

[46] Laroussi M 2015 Low-temperature plasma jet for biomedical applications: a review *IEEE Trans. Plasma Sci.* **43** 703–12

[47] Chokradjaroen C, Wang X, Niu J, Fan T and Saito N 2022 Fundamentals of solution plasma for advanced materials synthesis *Mater. Today Adv.* **14** 100244

[48] Zhou R, Zhang T, Zhou R, Wang S, Mei D, Mai-Prochnow A, Weerasinghe J, Fang Z, Ostrikov K K and Cullen P J 2021 Sustainable plasma-catalytic bubbles for hydrogen peroxide synthesis *Green Chem.* **23** 2977–85

[49] Zhang T, Zhou R, Zhang S, Zhou R, Ding J, Li F, Hong J, Dou L, Shao T and Murphy A B 2023 Sustainable ammonia synthesis from nitrogen and water by one-step plasma catalysis *Energy Environ. Mater.* **6** e12344

[50] Rumbach P, Xu R and Go D B 2016 Electrochemical production of oxalate and formate from CO_2 by solvated electrons produced using an atmospheric-pressure plasma *J. Electrochem. Soc.* **163** F1157

[51] Bruggeman P *et al* 2016 Plasma–liquid interactions: a review and roadmap *Plasma Sources Sci. Technol.* **25** 053002

[52] Starikovskiy A, Yang Y, Cho Y I and Fridman A 2011 Non-equilibrium plasma in liquid water: dynamics of generation and quenching *Plasma Sources Sci. Technol.* **20** 024003

[53] Mededovic S and Locke B 2007 Primary chemical reactions in pulsed electrical discharge channels in water *J. Phys. D: Appl. Phys.* **40** 7734

[54] Zhang T, Zhou R, Wang P, Mai-Prochnow A, McConchie R, Li W, Zhou R, Thompson E W, Ostrikov K K and Cullen P J 2021 Degradation of cefixime antibiotic in water by atmospheric plasma bubbles: performance, degradation pathways and toxicity evaluation *Chem. Eng. J.* **421** 127730

[55] Zhou R, Zhou R, Wang P, Luan B, Zhang X, Fang Z, Xian Y, Lu X, Ostrikov K K and Bazaka K 2019 Microplasma bubbles: reactive vehicles for biofilm dispersal *ACS Appl. Mater. Interfaces* **11** 20660–9

[56] Zhang T *et al* 2023 Catalyst-free carbon dioxide conversion in water facilitated by pulse discharges *J. Am. Chem. Soc.* **145** 28233–9

[57] Sun J *et al* 2024 Sustainable ammonia production via nanosecond-pulsed plasma oxidation and electrocatalytic reduction *Appl. Catal.* B **342** 123426

[58] Wang S *et al* 2023 Violet phosphorus-Fe_3O_4 as a novel photocatalysis-self-Fenton system coupled with underwater bubble plasma to efficiently remove norfloxacin in water *Chem. Eng. J.* **452** 139481

[59] Zhou R, Zhou R, Prasad K, Fang Z, Speight R, Bazaka K and Ostrikov K K 2018 Cold atmospheric plasma activated water as a prospective disinfectant: the crucial role of peroxynitrite *Green Chem.* **20** 5276–84

[60] Puliyalil H, Jurković D L, Dasireddy V D and Likozar B 2018 A review of plasma-assisted catalytic conversion of gaseous carbon dioxide and methane into value-added platform chemicals and fuels *RSC Adv.* **8** 27481–508

[61] Eliasson B and Kogelschatz U 1991 Nonequilibrium volume plasma chemical processing *IEEE Trans. Plasma Sci.* **19** 1063–77

[62] Feng J, Sun X, Li Z, Hao X, Fan M, Ning P and Li K 2022 Plasma-assisted reforming of methane *Adv. Sci.* **9** 2203221

[63] Wanten B, Maerivoet S, Vantomme C, Slaets J, Trenchev G and Bogaerts A 2022 Dry reforming of methane in an atmospheric pressure glow discharge: confining the plasma to expand the performance *J. CO_2 Util.* **56** 101869

[64] Kado S, Urasaki K, Sekine Y and Fujimoto K 2003 Direct conversion of methane to acetylene or syngas at room temperature using non-equilibrium pulsed discharge☆ *Fuel* **82** 1377–85

[65] Gomez E, Rani D A, Cheeseman C, Deegan D, Wise M and Boccaccini A 2009 Thermal plasma technology for the treatment of wastes: a critical review *J. Hazard. Mater.* **161** 614–26

[66] Tang L, Huang H, Hao H and Zhao K 2013 Development of plasma pyrolysis/gasification systems for energy efficient and environmentally sound waste disposal *J. Electrost.* **71** 839–47

[67] Carreon M L 2019 Plasma catalytic ammonia synthesis: state of the art and future directions *J. Phys. D: Appl. Phys.* **52** 483001

[68] Li D, Rohani V, Fabry F, Ramaswamy A P, Sennour M and Fulcheri L 2020 Direct conversion of CO_2 and CH_4 into liquid chemicals by plasma-catalysis *Appl. Catal.* B **261** 118228

[69] Michiels R, Engelmann Y and Bogaerts A 2020 Plasma catalysis for CO_2 hydrogenation: unlocking new pathways toward CH_3OH *J. Phys. Chem.* C **124** 25859–71

[70] Stere C E, Anderson J A, Chansai S, Delgado J J, Goguet A, Graham W G, Hardacre C, Taylor S R, Tu X and Wang Z 2017 Non-thermal plasma activation of gold-based catalysts for low-temperature water–gas shift catalysis *Angew. Chem., Int. Ed.* **56** 5579–83

[71] Neyts E C, Ostrikov K, Sunkara M K and Bogaerts A 2015 Plasma catalysis: synergistic effects at the nanoscale *Chem. Rev.* **115** 13408–46

[72] Zhou D, Zhou R, Zhou R, Liu B, Zhang T, Xian Y, Cullen P J, Lu X and Ostrikov K K 2021 Sustainable ammonia production by non-thermal plasmas: status, mechanisms, and opportunities *Chem. Eng. J.* **421** 129544

[73] Devins J C and Burton M 1954 Formation of hydrazine in electric discharge decomposition of ammonia1, 2 *J. Am. Chem. Soc.* **76** 2618–26

[74] Mizuno A, Chakrabarti A and Okazaki K 1993 Application of corona technology in the reduction of greenhouse gases and other gaseous pollutants *Non-Thermal Plasma Techniques for Pollution Control: Part B: Electron Beam and Electrical Discharge Processing* (Springer) pp 165–85

[75] Sheng Z, Kim H-H, Yao S and Nozaki T 2020 Plasma-chemical promotion of catalysis for CH_4 dry reforming: unveiling plasma-enabled reaction mechanisms *Phys. Chem. Chem. Phys.* **22** 19349–58

[76] Tu X and Whitehead J 2012 Plasma-catalytic dry reforming of methane in an atmospheric dielectric barrier discharge: understanding the synergistic effect at low temperature *Appl. Catal.* B **125** 439–48

[77] Hensel K 2009 Microdischarges in ceramic foams and honeycombs *Eur. Phys. J.* D **54** 141–8

[78] Kraus M, Eliasson B, Kogelschatz U and Wokaun A 2001 CO_2 reforming of methane by the combination of dielectric-barrier discharges and catalysis *Phys. Chem. Chem. Phys.* **3** 294–300

[79] Schmidt-Szałowski K, Górska A and Młotek M 2006 Plasma-catalytic conversion of methane by DBD and gliding discharges *J. Adv. Oxid. Technol.* **9** 215–9

[80] Lee H and Sekiguchi H 2011 Plasma–catalytic hybrid system using spouted bed with a gliding arc discharge: CH_4 reforming as a model reaction *J. Phys. D: Appl. Phys.* **44** 274008

[81] Wang Q, Cheng Y and Jin Y 2009 Dry reforming of methane in an atmospheric pressure plasma fluidized bed with Ni/γ-Al_2O_3 catalyst *Catal. Today* **148** 275–82

[82] Wang S, Liu Z, Pang B, Gao Y, Luo S, Li Q, Chen H and Kong M G 2022 Highly synergetic effect for norfloxacin degradation by coupling underwater bubble plasma

J. Phys. D: Appl. Phys. **57** (2024) 503002

Topical Review

formation with a Fe (III)–S (IV) system *Chem. Eng. J.*
433 134570

[83] Bogaerts A *et al* 2020 The 2020 plasma catalysis roadmap *J. Phys. D: Appl. Phys.* **53** 443001

[84] Loenders B, Michiels R and Bogaerts A 2023 Is a catalyst always beneficial in plasma catalysis? Insights from the many physical and chemical interactions *J. Energy Chem.* **85** 501–33

[85] Stere C, Adress W, Burch R, Chansai S, Goguet A, Graham W and Hardacre C 2015 Probing a non-thermal plasma activated heterogeneously catalyzed reaction using *in situ* DRIFTS-MS *ACS Catal.* **5** 956–64

[86] Rivallan M, Fourré E, Aiello S, Tatibouët J M and Thibault-Starzyk F 2012 Insights into the mechanisms of isopropanol conversion on γ-Al₂O₃ by dielectric barrier discharge *Plasma Process. Polym.* **9** 850–4

[87] Liu L, Dai J, Das S, Wang Y, Yu H, Xi S, Zhang Z and Tu X 2023 Plasma-catalytic CO₂ reforming of toluene over hydrotalcite-derived NiFe/(Mg, Al) Oₓ catalysts *JACS Au* **3** 785–800

[88] Sun Y *et al* 2022 Plasma-catalytic CO₂ hydrogenation over a Pd/ZnO catalyst: *in situ* probing of gas-phase and surface reactions *JACS Au* **2** 1800–10

[89] Khosravi Z, Hinze A and Klages C-P 2012 *In-situ* FTIR-ATR spectroscopic investigations of atmospheric-pressure plasma modification of polyolefin thin films *Int. Conf. on Plasma Surface Engineering* pp 239–42

[90] Labbaye T *et al* 2014 *In situ* Raman spectroscopy for growth monitoring of vertically aligned multiwall carbon nanotubes in plasma reactor *Appl. Phys. Lett.* **105** 213109

[91] Sun J *et al* 2023 Insights into plasma-catalytic nitrogen fixation from catalyst microanalysis and chemical kinetics modelling *Chem. Eng. J.* **469** 143841

[92] Wang W, Patil B, Heijkers S, Hessel V and Bogaerts A 2017 Nitrogen fixation by gliding arc plasma: better insight by chemical kinetics modelling *ChemSusChem* **10** 2145–57

[93] Arakoni R, Stafford D S, Babaeva N Y and Kushner M J 2005 O₂ (Δ1) production in flowing He∕O₂ plasmas. II. Two-dimensional modeling *J. Appl. Phys.* **98** 073304

[94] Lietz A M and Kushner M J 2016 Air plasma treatment of liquid covered tissue: long timescale chemistry *J. Phys. D: Appl. Phys.* **49** 425204

[95] Pancheshnyi S, Eismann B, Hagelaar G and Pitchford L 2008 Computer code ZDPlasKin (University of Toulouse, Laplace, cnrs-ups-inp, Toulouse) (available at: www. zdplaskin.laplace.univ-tlse.fr)

[96] Hagelaar G and Pitchford L C 2005 Solving the Boltzmann equation to obtain electron transport coefficients and rate coefficients for fluid models *Plasma Sources Sci. Technol.* **14** 722

[97] Hong J, Pancheshnyi S, Tam E, Lowke J J, Prawer S and Murphy A B 2017 Kinetic modelling of NH₃ production in N₂–H₂ non-equilibrium atmospheric-pressure plasma catalysis *J. Phys. D: Appl. Phys.* **50** 154005

[98] Ramakers M, Trenchev G, Heijkers S, Wang W and Bogaerts A 2017 Gliding arc plasmatron: providing an alternative method for carbon dioxide conversion *ChemSusChem* **10** 2642–52

[99] Bonitz M, Filinov A, Abraham J-W, Balzer K, Kählert H, Pehlke E, Bronold F X, Pamperin M, Becker M and Loffhagen D 2019 Towards an integrated modeling of the plasma-solid interface *Front. Chem. Sci. Eng.* **13** 201–37

[100] Hong J, Zhang T, Zhou R, Dou L, Zhang S, Zhou R, Ashford B, Shao T, Murphy A B and Ostrikov K K 2022 Green chemical pathway of plasma synthesis of ammonia from nitrogen and water: a comparative kinetic study with a N₂/H₂ system *Green Chem.* **24** 7458–68

[101] Cui Z *et al* 2022 Plasma-catalytic methanol synthesis from CO₂ hydrogenation over a supported Cu cluster catalyst:

insights into the reaction mechanism *ACS Catal.* **12** 1326–37

[102] Han Y, Wang J-G, Cheng D-G and Liu C-J 2006 Density functional theory study of methanol conversion via cold plasmas *Ind. Eng. Chem. Res.* **45** 3460–7

[103] Kim D-Y *et al* 2022 Cooperative catalysis of vibrationally excited CO₂ and alloy catalyst breaks the thermodynamic equilibrium limitation *J. Am. Chem. Soc.* **144** 14140–9

[104] Mehta P, Barboun P, Herrera F A, Kim J, Rumbach P, Go D B, Hicks J C and Schneider W F 2018 Overcoming ammonia synthesis scaling relations with plasma-enabled catalysis *Nat. Catal.* **1** 269–75

[105] Nozaki T, Chen X, Kim D-Y and Zhan C 2023 Combination of DBD and catalysts for CH₄ and CO₂ conversion: basics and applications *Plasma Chem. Plasma Process.* **43** 1–26

[106] Ueta H, Chen L, Beck R D, Colón-Dìaz I and Jackson B 2013 Quantum state-resolved CH₄ dissociation on Pt (111): coverage dependent barrier heights from experiment and density functional theory *Phys. Chem. Chem. Phys.* **15** 20526–35

[107] Kruszelnicki J, Engeling K W, Foster J E, Xiong Z and Kushner M J 2016 Propagation of negative electrical discharges through 2-dimensional packed bed reactors *J. Phys. D: Appl. Phys.* **50** 025203

[108] Wang W, Kim H-H, Van Laer K and Bogaerts A 2018 Streamer propagation in a packed bed plasma reactor for plasma catalysis applications *Chem. Eng. J.* **334** 2467–79

[109] Wang W, Mei D, Tu X and Bogaerts A 2017 Gliding arc plasma for CO₂ conversion: better insights by a combined experimental and modelling approach *Chem. Eng. J.* **330** 11–25

[110] Zhang Q-Z and Bogaerts A 2018 Plasma streamer propagation in structured catalysts *Plasma Sources Sci. Technol.* **27** 105013

[111] Adamovich I *et al* 2022 The 2022 plasma roadmap: low temperature plasma science and technology *J. Appl. Phys.* **55** 373001

[112] Van Laer K and Bogaerts A 2015 Fluid modelling of a packed bed dielectric barrier discharge plasma reactor *Plasma Sources Sci. Technol.* **25** 015002

[113] Van Laer K and Bogaerts A 2017 Influence of gap size and dielectric constant of the packing material on the plasma behaviour in a packed bed DBD reactor: a fluid modelling study *Plasma Process. Polym.* **14** 1600129

[114] Van Laer K and Bogaerts A 2017 How bead size and dielectric constant affect the plasma behaviour in a packed bed plasma reactor: a modelling study *Plasma Sources Sci. Technol.* **26** 085007

[115] Zhang Q-Z and Bogaerts A 2018 Propagation of a plasma streamer in catalyst pores *Plasma Sources Sci. Technol.* **27** 035009

[116] Hensel K, Katsura S and Mizuno A 2005 DC microdischarges inside porous ceramics *IEEE Trans. Plasma Sci.* **33** 574–5

[117] Hensel K, Martišovitš V, Machala Z, Janda M, Leštinský M, Tardiveau P and Mizuno A 2007 Electrical and optical properties of AC microdischarges in porous ceramics *Plasma Process. Polym.* **4** 682–93

[118] Matera S, Schneider W F, Heyden A and Savara A 2019 Progress in accurate chemical kinetic modeling, simulations, and parameter estimation for heterogeneous catalysis *ACS Catal.* **9** 6624–47

[119] Pan J, Liu Y, Zhang S, Hu X, Liu Y and Shao T 2023 Deep learning-assisted pulsed discharge plasma catalysis modeling *Energy Convers. Manage.* **277** 116620

[120] Ashford B and Tu X 2017 Non-thermal plasma technology for the conversion of CO₂ *Curr. Opin. Green Sustain. Chem.* **3** 45–49

J. Phys. D: Appl. Phys. **57** (2024) 503002

Topical Review

[121] Mierczynski P, Mierczynska-Vasilev A, Szynkowska-Jóźwik M I, Ostrikov K and Vasilev K 2023 Plasma-assisted catalysis for CH_4 and CO_2 conversion *Catal. Commun.* **180** 106709

[122] Xu S, Chen H, Hardacre C and Fan X 2021 Non-thermal plasma catalysis for CO_2 conversion and catalyst design for the process *J. Appl. Phys.* **54** 233001

[123] Zhu X, Liu J-H, Li X-S, Liu J-L, Qu X and Zhu A-M 2017 Enhanced effect of plasma on catalytic reduction of CO_2 to CO with hydrogen over Au/CeO_2 at low temperature *J. Energy Chem.* **26** 488–93

[124] Paulussen S, Verheyde B, Tu X, De Bie C, Martens T, Petrovic D, Bogaerts A and Sels B 2010 Conversion of carbon dioxide to value-added chemicals in atmospheric pressure dielectric barrier discharges *Plasma Sources Sci. Technol.* **19** 034015

[125] Mei D, Zhu X, He Y-L, Yan J D and Tu X 2014 Plasma-assisted conversion of CO_2 in a dielectric barrier discharge reactor: understanding the effect of packing materials *Plasma Sources Sci. Technol.* **24** 015011

[126] Chen G, Godfroid T, Britun N, Georgieva V, Delplancke-Ogletree M-P and Snyders R 2017 Plasma-catalytic conversion of CO_2 and CO_2/H_2O in a surface-wave sustained microwave discharge *Appl. Catal.* B **214** 114–25

[127] Chen G, Britun N, Godfroid T, Georgieva V, Snyders R and Delplancke-Ogletree M-P 2017 An overview of CO_2 conversion in a microwave discharge: the role of plasma-catalysis *J. Phys. D: Appl. Phys.* **50** 084001

[128] Berthelot A and Bogaerts A 2017 Modeling of CO_2 splitting in a microwave plasma: how to improve the conversion and energy efficiency *J. Phys. Chem.* C **121** 8236–51

[129] Li L, Zhang H, Li X, Kong X, Xu R, Tay K and Tu X 2019 Plasma-assisted CO_2 conversion in a gliding arc discharge: improving performance by optimizing the reactor design *J. CO_2 Util.* **29** 296–303

[130] Wang W, Berthelot A, Kolev S, Tu X and Bogaerts A 2016 CO_2 conversion in a gliding arc plasma: 1D cylindrical discharge model *Plasma Sources Sci. Technol.* **25** 065012

[131] Mei D, Zhu X, Wu C, Ashford B, Williams P T and Tu X 2016 Plasma-photocatalytic conversion of CO_2 at low temperatures: understanding the synergistic effect of plasma-catalysis *Appl. Catal.* B **182** 525–32

[132] Snoeckx R, Zeng Y, Tu X and Bogaerts A 2015 Plasma-based dry reforming: improving the conversion and energy efficiency in a dielectric barrier discharge *RSC Adv.* **5** 29799–808

[133] Mei D and Tu X 2017 Conversion of CO_2 in a cylindrical dielectric barrier discharge reactor: effects of plasma processing parameters and reactor design *J. CO_2 Util.* **19** 68–78

[134] Aerts R, Somers W and Bogaerts A 2015 Carbon dioxide splitting in a dielectric barrier discharge plasma: a combined experimental and computational study *ChemSusChem* **8** 702–16

[135] Mei D, He Y-L, Liu S, Yan J and Tu X 2016 Optimization of CO_2 conversion in a cylindrical dielectric barrier discharge reactor using design of experiments *Plasma Process. Polym.* **13** 544–56

[136] Rad R H, Brüser V, Schiorlin M, Schäfer J and Brandenburg R 2023 Enhancement of CO_2 splitting in a coaxial dielectric barrier discharge by pressure increase, packed bed and catalyst addition *Chem. Eng. J.* **456** 141072

[137] Brandenburg R, Schiorlin M, Schmidt M, Höft H, Pipa A V and Brüser V 2023 Plane parallel barrier discharges for carbon dioxide splitting: influence of discharge arrangement on carbon monoxide formation *Plasma* **6** 162–80

[138] Van Laer K and Bogaerts A 2015 Improving the conversion and energy efficiency of carbon dioxide splitting in a zirconia-packed dielectric barrier discharge reactor *Energy Technol.* **3** 1038–44

[139] Mei D and Tu X 2017 Atmospheric pressure non-thermal plasma activation of CO_2 in a packed-bed dielectric barrier discharge reactor *ChemPhysChem* **18** 3253–9

[140] Wang L, Du X, Yi Y, Wang H, Gul M, Zhu Y and Tu X 2020 Plasma-enhanced direct conversion of CO_2 to CO over oxygen-deficient Mo-doped CeO_2 *Chem. Commun.* **56** 14801–4

[141] Zhang H, Li L, Xu R, Huang J, Wang N, Li X and Tu X 2020 Plasma-enhanced catalytic activation of CO_2 in a modified gliding arc reactor *Waste Dispos. Sustain. Energy* **2** 139–50

[142] Zeng Y and Tu X 2017 Plasma-catalytic hydrogenation of CO_2 for the cogeneration of CO and CH_4 in a dielectric barrier discharge reactor: effect of argon addition *J. Phys. D: Appl. Phys.* **50** 184004

[143] Benrabbah R, Cavaniol C, Liu H, Ognier S, Cavadias S, Gálvez M E and Da Costa P 2017 Plasma DBD activated ceria-zirconia-promoted Ni-catalysts for plasma catalytic CO_2 hydrogenation at low temperature *Catal. Commun.* **89** 73–76

[144] Zeng Y and Tu X 2015 Plasma-catalytic CO_2 hydrogenation at low temperatures *IEEE Trans. Plasma Sci.* **44** 405–11

[145] Farahani M D, Zeng Y and Zheng Y 2022 The application of nonthermal plasma in methanol synthesis via CO_2 hydrogenation *Energy Sci. Eng.* **10** 1572–83

[146] Wang W, Wang S, Ma X and Gong J 2011 Recent advances in catalytic hydrogenation of carbon dioxide *Chem. Soc. Rev.* **40** 3703–27

[147] Porosoff M D, Yan B and Chen J G 2016 Catalytic reduction of CO_2 by H_2 for synthesis of CO, methanol and hydrocarbons: challenges and opportunities *Energy Environ. Sci.* **9** 62–73

[148] Ginés M, Marchi A and Apesteguía C 1997 Kinetic study of the reverse water-gas shift reaction over $CuO/ZnO/Al_2O_3$ catalysts *Appl. Catal.* A **154** 155–71

[149] Chen C-S, Cheng W-H and Lin S-S 2000 Mechanism of CO formation in reverse water–gas shift reaction over Cu/Al_2O_3 catalyst *Catal. Lett.* **68** 45–48

[150] Zhang Z, Ding H, Zhou Q, Pan W, Qiu K, Mu X, Ma J, Zhang K and Zhao Y 2023 Research progress and the prospect of CO_2 hydrogenation with dielectric barrier discharge plasma technology *Carbon Lett.* **33** 1–15

[151] Wang L, Yi Y, Guo H and Tu X 2018 Atmospheric pressure and room temperature synthesis of methanol through plasma-catalytic hydrogenation of CO_2 *ACS Catal.* **8** 90–100

[152] Men Y-L, Liu Y, Wang Q, Luo Z-H, Shao S, Li Y-B and Pan Y-X 2019 Highly dispersed Pt-based catalysts for selective CO_2 hydrogenation to methanol at atmospheric pressure *Chem. Eng. Sci.* **200** 167–75

[153] Jwa E, Lee S, Lee H and Mok Y 2013 Plasma-assisted catalytic methanation of CO and CO_2 over Ni–zeolite catalysts. *Fuel processing technology* **108** 89–93

[154] Whitehead J C 2016 Plasma–catalysis: the known knowns, the known unknowns and the unknown unknowns *J. Phys. D: Appl. Phys.* **49** 243001

[155] Ahmad F, Lovell E C, Masood H, Cullen P J, Ostrikov K K, Scott J A and Amal R 2020 Low-temperature CO_2 methanation: synergistic effects in plasma-Ni hybrid catalytic system *ACS Sustain. Chem. Eng.* **8** 1888–98

[156] Biset-Peiró M, Guilera J, Zhang T, Arbiol J and Andreu T 2019 On the role of ceria in $Ni-Al_2O_3$ catalyst for CO_2 plasma methanation *Appl. Catal.* A **575** 223–9

J. Phys. D: Appl. Phys. **57** (2024) 503002

Topical Review

[157] Lee C J, Lee D H and Kim T 2017 Enhancement of methanation of carbon dioxide using dielectric barrier discharge on a ruthenium catalyst at atmospheric conditions *Catal. Today* **293** 97–104

[158] Rui N *et al* 2021 Highly active Ni/CeO$_2$ catalyst for CO$_2$ methanation: preparation and characterization *Appl. Catal. B* **282** 119581

[159] Chen G, Silva T, Georgieva V, Godfroid T, Britun N, Snyders R and Delplancke-Ogletree M P 2015 Simultaneous dissociation of CO$_2$ and H$_2$O to syngas in a surface-wave microwave discharge *Int. J. Hydrog. Energy* **40** 3789–96

[160] Snoeckx R, Ozkan A, Reniers F and Bogaerts A 2017 The quest for value-added products from carbon dioxide and water in a dielectric barrier discharge: a chemical kinetics study *ChemSusChem* **10** 409–24

[161] Ma X, Li S, Ronda-Lloret M, Chaudhary R, Lin L, Van Rooij G, Gallucci F, Rothenberg G, Raveendran Shiju N and Hessel V 2019 Plasma assisted catalytic conversion of CO$_2$ and H$_2$O over Ni/Al$_2$O$_3$ in a DBD reactor *Plasma Chem. Plasma Process.* **39** 109–24

[162] Zhao B, Liu Y, Zhu Z, Guo H and Ma X 2018 Highly selective conversion of CO$_2$ into ethanol on Cu/ZnO/Al$_2$O$_3$ catalyst with the assistance of plasma *J. CO$_2$ Util.* **24** 34–39

[163] Knezevic J *et al* 2024 Long-chain hydrocarbons from nonthermal plasma-driven biogas upcycling *J. Am. Chem. Soc.* **146** 12601–8

[164] Indarto A, Yang D R, Choi J-W, Lee H and Song H K 2007 Gliding arc plasma processing of CO$_2$ conversion *J. Hazard. Mater.* **146** 309–15

[165] Nunnally T, Gutsol K, Rabinovich A, Fridman A, Gutsol A and Kemoun A 2011 Dissociation of CO$_2$ in a low current gliding arc plasmatron *J. Phys. D: Appl. Phys.* **44** 274009

[166] Verheyen C, Silva T, Guerra V and Bogaerts A 2020 The effect of H$_2$O on the vibrational populations of CO$_2$ in a CO$_2$/H$_2$O microwave plasma: a kinetic modelling investigation *Plasma Sources Sci. Technol.* **29** 095009

[167] Baldissarelli V Z, Benetoli L O D B, Cassini F A, Souza I G D and Debacher N A 2014 Plasma-assisted production of carbon black and carbon nanotubes from methane by thermal plasma reform *J. Braz. Chem. Soc.* **25** 126–32

[168] Li T, Rehmet C, Cheng Y, Jin Y and Cheng Y 2017 Experimental comparison of methane pyrolysis in thermal plasma *Plasma Chem. Plasma Process.* **37** 1033–49

[169] Ghanbari M, Binazadeh M, Zafarnak S, Taghvaei H and Rahimpour M R 2020 Hydrogen production via catalytic pulsed plasma conversion of methane: effect of Ni–K$_2$O/Al$_2$O$_3$ loading, applied voltage, and argon flow rate *Int. J. Hydrog. Energy* **45** 13899–910

[170] Khalifeh O, Taghvaei H, Mosallanejad A, Rahimpour M R and Shariati A 2016 Extra pure hydrogen production through methane decomposition using nanosecond pulsed plasma and Pt–Re catalyst *Chem. Eng. J.* **294** 132–45

[171] Zhang H, Du C, Wu A, Bo Z, Yan J and Li X 2014 Rotating gliding arc assisted methane decomposition in nitrogen for hydrogen production *Int. J. Hydrog. Energy* **39** 12620–35

[172] Wang L, Yi Y, Wu C, Guo H and Tu X 2017 One-step reforming of CO$_2$ and CH$_4$ into high-value liquid chemicals and fuels at room temperature by plasma-driven catalysis *Angew. Chem.* **129** 13867–71

[173] Tu X and Whitehead J C 2014 Plasma dry reforming of methane in an atmospheric pressure AC gliding arc discharge: co-generation of syngas and carbon nanomaterials *Int. J. Hydrog. Energy* **39** 9658–69

[174] Long H, Shang S, Tao X, Yin Y and Dai X 2008 CO$_2$ reforming of CH$_4$ by combination of cold plasma jet and Ni/γ-Al$_2$O$_3$ catalyst *Int. J. Hydrog. Energy* **33** 5510–5

[175] Zeng Y, Zhu X, Mei D, Ashford B and Tu X 2015 Plasma-catalytic dry reforming of methane over γ-Al$_2$O$_3$ supported metal catalysts *Catal. Today* **256** 80–87

[176] Zeng Y, Wang L, Wu C, Wang J, Shen B and Tu X 2018 Low temperature reforming of biogas over K-, Mg-and Ce-promoted Ni/Al$_2$O$_3$ catalysts for the production of hydrogen rich syngas: understanding the plasma-catalytic synergy *Appl. Catal. B* **224** 469–78

[177] Wang H, Zhao B, Qin L, Wang Y, Yu F and Han J 2020 Non-thermal plasma-enhanced dry reforming of methane and CO$_2$ over Ce-promoted Ni/C catalysts *Mol. Catal.* **485** 110821

[178] Mei D, Sun M, Liu S, Zhang P, Fang Z and Tu X 2023 Plasma-enabled catalytic dry reforming of CH$_4$ into syngas, hydrocarbons and oxygenates: insight into the active metals of γ-Al$_2$O$_3$ supported catalysts *J. CO$_2$ Util.* **67** 102307

[179] Aghamir F M, Matin N S, Jalili A H, Esfarayeni M, Khodagholi M and Ahmadi R 2004 Conversion of methane to methanol in an ac dielectric barrier discharge *Plasma Sources Sci. Technol.* **13** 707

[180] Sorensen S, Karawajczyk A, Strömholm C and Kirm M 1995 Dissociative photoexcitation of CH$_4$ and CD$_4$ *Chem. Phys. Lett.* **232** 554–60

[181] Nozaki T, Hattori A and Okazaki K 2004 Partial oxidation of methane using a microscale non-equilibrium plasma reactor *Catal. Today* **98** 607–16

[182] Sushkevich V L, Palagin D, Ranocchiari M and Van Bokhoven J A 2017 Selective anaerobic oxidation of methane enables direct synthesis of methanol *Science* **356** 523–7

[183] Zuo Z, Ramírez P J, Senanayake S D, Liu P and Rodriguez J A 2016 Low-temperature conversion of methane to methanol on CeO$_x$/Cu$_2$O catalysts: water controlled activation of the C–H bond *J. Am. Chem. Soc.* **138** 13810–3

[184] Chawdhury P, Ray D, Vinodkumar T and Subrahmanyam C 2019 Catalytic DBD plasma approach for methane partial oxidation to methanol under ambient conditions *Catal. Today* **337** 117–25

[185] Zhu X, Liu X, Lian H-Y, Liu J-L and Li X-S 2019 Plasma catalytic steam methane reforming for distributed hydrogen production *Catal. Today* **337** 69–75

[186] Liu J-L, Snoeckx R and Cha M S 2018 Steam reforming of methane in a temperature-controlled dielectric barrier discharge reactor: the role of electron-induced chemistry versus thermochemistry *J. Phys. D: Appl. Phys.* **51** 385201

[187] Montoro-Damas A M, Gómez-Ramírez A, Gonzalez-Elipe A R and Cotrino J 2016 Isotope labelling to study molecular fragmentation during the dielectric barrier discharge wet reforming of methane *J. Power Sources* **325** 501–5

[188] Rosca V, Duca M, de Groot M T and Koper M T M 2009 Nitrogen cycle electrocatalysis *Chem. Rev.* **109** 2209–44

[189] Hasan M H, Mahlia T M I, Mofijur M, Rizwanul Fattah I, Handayani F, Ong H C and Silitonga A 2021 A comprehensive review on the recent development of ammonia as a renewable energy carrier *Energies* **14** 3732

[190] Han K, Luo J, Chen J, Chen B, Xu L, Feng Y, Tang W and Wang Z L 2021 Self-powered ammonia synthesis under ambient conditions via N$_2$ discharge driven by Tesla turbine triboelectric nanogenerators *Microsyst. Nanoeng.* **7** 7

[191] MacFarlane D R, Cherepanov P V, Choi J, Suryanto B H, Hodgetts R Y, Bakker J M, Vallana F M F and Simonov A N 2020 A roadmap to the ammonia economy *Joule* **4** 1186–205

J. Phys. D: Appl. Phys. **57** (2024) 503002

Topical Review

[192] Patil B S, Hessel V, Seefeldt L C, Dean D R, Hoffman B M, Cook B J and Murray L J 2000 Nitrogen fixation *Ullmann's Encyclopedia of Industrial Chemistry* pp 1–21

[193] Hessel V, Anastasopoulou A, Wang Q, Kolb G and Lang J 2013 Energy, catalyst and reactor considerations for (near)-industrial plasma processing and learning for nitrogen-fixation reactions *Catal. Today* **211** 9–28

[194] Osorio-Tejada J, Van't Veer K, Long N V D, Tran N N, Fulcheri L, Patil B S, Bogaerts A and Hessel V 2022 Sustainability analysis of methane-to-hydrogen-to-ammonia conversion by integration of high-temperature plasma and non-thermal plasma processes *Energy Convers. Manage.* **269** 116095

[195] Anastasopoulou A, Keijzer R, Patil B, Lang J, van Rooij G and Hessel V 2020 Environmental impact assessment of plasma-assisted and conventional ammonia synthesis routes *J. Ind. Ecol.* **24** 1171–85

[196] Osorio-Tejada J L, Rebrov E and Hessel V 2023 Internalisation of environmental costs of decentralised nitrogen fertilisers production *Int. J. Life Cycle Assess.* **28** 1–14

[197] Tran N N *et al* 2021 Economic optimization of local Australian ammonia production using plasma technologies with green/turquoise hydrogen *ACS Sustain. Chem. Eng.* **9** 16304–15

[198] Rouwenhorst K H, Jardali F, Bogaerts A and Lefferts L 2021 From the Birkeland–Eyde process towards energy-efficient plasma-based NO$_X$ synthesis: a techno-economic analysis *Energy Environ. Sci.* **14** 2520–34

[199] Li S, Medrano J A, Hessel V and Gallucci F 2018 Recent progress of plasma-assisted nitrogen fixation research: a review *Processes* **6** 248

[200] Qu Z, Zhou R, Sun J, Gao Y, Li Z, Zhang T, Zhou R, Liu D, Tu X and Cullen P 2024 Plasma-assisted sustainable nitrogen-to-ammonia fixation: mixed-phase, synergistic processes and mechanisms *ChemSusChem* **17** e202300783

[201] Patil B S, Cherkasov N, Srinath N V, Lang J, Ibhadon A O, Wang Q and Hessel V 2021 The role of heterogeneous catalysts in the plasma-catalytic ammonia synthesis *Catal. Today* **362** 2–10

[202] Patil B S, Peeters F, van Rooij G J, Medrano J, Gallucci F, Lang J, Wang Q and Hessel V 2018 Plasma assisted nitrogen oxide production from air: using pulsed powered gliding arc reactor for a containerized plant *AlChE J.* **64** 526–37

[203] Patil B S, Van Kaathoven A S, Peeters F J, Cherkasov N, Lang J, Wang Q and Hessel V 2020 Deciphering the synergy between plasma and catalyst support for ammonia synthesis in a packed dielectric barrier discharge reactor *J. Phys. D: Appl. Phys.* **53** 144003

[204] Rusanov V, Fridman A and Sholin G 1981 The physics of a chemically active plasma with nonequilibrium vibrational excitation of molecules *Sov. Phys. - Usp.* **24** 447

[205] Marinov D, Guaitella O, Rousseau A and Ionikh Y 2010 Production of molecules on a surface under plasma exposure: example of NO on pyrex *J. Phys. D: Appl. Phys.* **43** 115203

[206] Zhang S, Zong L, Zeng X, Zhou R, Liu Y, Zhang C, Pan J, Cullen P J, Ostrikov K K and Shao T 2022 Sustainable nitrogen fixation with nanosecond pulsed spark discharges: insights into free-radical-chain reactions *Green Chem.* **24** 1534–44

[207] Wandell R J, Wang H, Bulusu R K, Gallan R O and Locke B R 2019 Formation of nitrogen oxides by nanosecond pulsed plasma discharges in gas–liquid reactors *Plasma Chem. Plasma Process.* **39** 643–66

[208] Pei X, Gidon D, Yang Y-J, Xiong Z and Graves D B 2019 Reducing energy cost of NO$_x$ production in air plasmas *Chem. Eng. J.* **362** 217–28

[209] Kelly S and Bogaerts A 2021 Nitrogen fixation in an electrode-free microwave plasma *Joule* **5** 3006–30

[210] Vervloessem E, Aghaei M, Jardali F, Hafezkhiabani N and Bogaerts A 2020 Plasma-based N$_2$ fixation into NO$_x$: insights from modeling toward optimum yields and energy costs in a gliding arc plasmatron *ACS Sustain. Chem. Eng.* **8** 9711–20

[211] Jardali F, Van Alphen S, Creel J, Eshtehardi H A, Axelsson M, Ingels R, Snyders R and Bogaerts A 2021 NO$_x$ production in a rotating gliding arc plasma: potential avenue for sustainable nitrogen fixation *Green Chem.* **23** 1748–57

[212] Van Alphen S, Eshtehardi H A, O'Modhrain C, Bogaerts J, Van Poyer H, Creel J, Delplancke M-P, Snyders R and Bogaerts A 2022 Effusion nozzle for energy-efficient NO$_x$ production in a rotating gliding arc plasma reactor *Chem. Eng. J.* **443** 136529

[213] Tsonev I, O'Modhrain C, Bogaerts A and Gorbanev Y 2023 Nitrogen fixation by an arc plasma at elevated pressure to increase the energy efficiency and production rate of NO$_x$ *ACS Sustain. Chem. Eng.* **11** 1888–97

[214] Abdelaziz A A and Kim H-H 2020 Temperature-dependent behavior of nitrogen fixation in nanopulsed dielectric barrier discharge operated at different humidity levels and oxygen contents *J. Phys. D: Appl. Phys.* **53** 114001

[215] Vervloessem E, Gorbanev Y, Nikiforov A, De Geyter N and Bogaerts A 2022 Sustainable NO$_x$ production from air in pulsed plasma: elucidating the chemistry behind the low energy consumption *Green Chem.* **24** 916–29

[216] Sun J, Alam D, Daiyan R, Masood H, Zhang T, Zhou R, Cullen P J, Lovell E C, Jalili A R and Amal R 2021 A hybrid plasma electrocatalytic process for sustainable ammonia production *Energy Environ. Sci.* **14** 865–72

[217] Patil B, Cherkasov N, Lang J, Ibhadon A, Hessel V and Wang Q 2016 Low temperature plasma-catalytic NO$_x$ synthesis in a packed DBD reactor: effect of support materials and supported active metal oxides *Appl. Catal.* B **194** 123–33

[218] Rouwenhorst K H, Engelmann Y, Van't Veer K, Postma R S, Bogaerts A and Lefferts L 2020 Plasma-driven catalysis: green ammonia synthesis with intermittent electricity *Green Chem.* **22** 6258–87

[219] Huang Z, Xiao A, Liu D, Lu X and Ostrikov K 2022 Plasma-water-based nitrogen fixation: status, mechanisms, and opportunities *Plasma Process. Polym.* **19** 2100198

[220] Wang Y, Yang W, Xu S, Zhao S, Chen G, Weidenkaff A, Hardacre C, Fan X, Huang J and Tu X 2022 Shielding protection by mesoporous catalysts for improving plasma-catalytic ambient ammonia synthesis *J. Am. Chem. Soc.* **144** 12020–31

[221] Wang Y, Craven M, Yu X, Ding J, Bryant P, Huang J and Tu X 2019 Plasma-enhanced catalytic synthesis of ammonia over a Ni/Al$_2$O$_3$ catalyst at near-room temperature: insights into the importance of the catalyst surface on the reaction mechanism *ACS Catal.* **9** 10780–93

[222] Peng P, Li Y, Cheng Y, Deng S, Chen P and Ruan R 2016 Atmospheric pressure ammonia synthesis using non-thermal plasma assisted catalysis *Plasma Chem. Plasma Process.* **36** 1201–10

[223] Gómez-Ramírez A, Montoro-Damas A M, Cotrino J, Lambert R M and González-Elipe A R 2017 About the enhancement of chemical yield during the atmospheric plasma synthesis of ammonia in a ferroelectric packed bed reactor *Plasma Process. Polym.* **14** 1600081

[224] van 't Veer K, Engelmann Y, Reniers F and Bogaerts A 2020 Plasma-catalytic ammonia synthesis in a DBD plasma: role of microdischarges and their afterglows *J. Phys. Chem.* C **124** 22871–83

J. Phys. D: Appl. Phys. **57** (2024) 503002

Topical Review

[225] Bayer B N, Bruggeman P J and Bhan A 2023 Species, pathways, and timescales for NH_3 formation by low-temperature atmospheric pressure plasma catalysis *ACS Catal.* **13** 2619–30

[226] Suzuki A and Asahina S 2013 Stable molecules in N_2–H_2 plasmas measured using a quartz sensor *Jpn. J. Appl. Phys.* **52** 11NC04

[227] Mizushima T, Matsumoto K, Sugoh J-I, Ohkita H and Kakuta N 2004 Tubular membrane-like catalyst for reactor with dielectric-barrier-discharge plasma and its performance in ammonia synthesis *Appl. Catal.* A **265** 53–59

[228] Xie D, Sun Y, Zhu T, Fan X, Hong X and Yang W 2016 Ammonia synthesis and by-product formation from H_2O, H_2 and N_2 by dielectric barrier discharge combined with an Ru/Al_2O_3 catalyst *RSC Adv.* **6** 105338–46

[229] Nakajima J and Sekiguchi H 2008 Synthesis of ammonia using microwave discharge at atmospheric pressure *Thin Solid Films* **516** 4446–51

[230] Peng P *et al* 2018 A review on the non-thermal plasma-assisted ammonia synthesis technologies *J. Clean. Prod.* **177** 597–609

[231] Zhou R, Zhou D, Liu B, Nie L, Xian Y, Zhang T, Zhou R, Lu X, Ostrikov K K and Cullen P J 2023 Controlling energy transfer in plasma-driven ammonia synthesis by adding helium gas *ACS Sustain. Chem. Eng.* **11** 1828–36

[232] Hong J, Prawer S and Murphy A B 2014 Production of ammonia by heterogeneous catalysis in a packed-bed dielectric-barrier discharge: influence of argon addition and voltage *IEEE Trans. Plasma Sci.* **42** 2338–9

[233] Zijlmans R, Gabriel O, Welzel S, Hempel F, Röpcke J, Engeln R and Schram D 2006 Molecule synthesis in an Ar–CH_4–O_2–N_2 microwave plasma *Plasma Sources Sci. Technol.* **15** 564

[234] De Castro A, Alegre D and Tabarés F 2017 Influence of residence time and helium addition in the ammonia formation on tungsten walls in N_2H_2 glow discharge plasmas *Nucl. Mater. Energy* **12** 399–404

[235] Gorbanev Y, Engelmann Y, Van't Veer K, Vlasov E, Ndayirinde C, Yi Y, Bals S and Bogaerts A 2021 Al_2O_3-supported transition metals for plasma-catalytic NH_3 synthesis in a DBD plasma: metal activity and insights into mechanisms *Catalysts* **11** 1230

[236] Engelmann Y, Van't Veer K, Gorbanev Y, Neyts E C, Schneider W F and Bogaerts A 2021 Plasma catalysis for ammonia synthesis: a microkinetic modeling study on the contributions of Eley–Rideal reactions *ACS Sustain. Chem. Eng.* **9** 13151–63

[237] Ndayirinde C, Gorbanev Y, Ciocarlan R-G, De Meyer R, Smets A, Vlasov E, Bals S, Cool P and Bogaerts A 2023 Plasma-catalytic ammonia synthesis: packed catalysts act as plasma modifiers *Catal. Today* **419** 114156

[238] Iwamoto M, Horikoshi M, Hashimoto R, Shimano K, Sawaguchi T, Teduka H and Matsukata M 2020 Higher activity of Ni/γ-Al_2O_3 over Fe/γ-Al_2O_3 and Ru/γ-Al_2O_3 for catalytic ammonia synthesis in nonthermal atmospheric-pressure plasma of N_2 and H_2 *Catalysts* **10** 590

[239] Liu Y, Wang C-W, Xu X-F, Liu B-W, Zhang G-M, Liu Z-W, Chen Q and Zhang H-B 2022 Synergistic effect of Co–Ni bimetal on plasma catalytic ammonia synthesis *Plasma Chem. Plasma Process.* **42** 267–82

[240] Gorky F, Best A, Jasinski J, Allen B J, Alba-Rubio A C and Carreon M L 2021 Plasma catalytic ammonia synthesis on Ni nanoparticles: the size effect *J. Catal.* **393** 369–80

[241] Sakakura T, Murakami N, Takatsuji Y, Morimoto M and Haruyama T 2019 Contribution of discharge excited atomic N, N_2^*, and N_2^+ to a plasma/liquid interfacial reaction as suggested by quantitative analysis *ChemPhysChem* **20** 1467–74

[242] Sakakura T, Murakami N, Takatsuji Y and Haruyama T 2020 Nitrogen fixation in a plasma/liquid interfacial reaction and its switching between reduction and oxidation *J. Phys. Chem.* C **124** 9401–8

[243] Gromov M, Leonova K, Britun N, De Geyter N, Morent R, Snyders R and Nikiforov A 2022 Plasma nitrogen fixation in the presence of a liquid interface: role of OH radicals *React. Chem. Eng.* **7** 1047–52

[244] Peng P *et al* 2018 *In situ* plasma-assisted atmospheric nitrogen fixation using water and spray-type jet plasma *Chem. Commun.* **54** 2886–9

[245] Gorbanev Y, Vervloessem E, Nikiforov A and Bogaerts A 2020 Nitrogen fixation with water vapor by nonequilibrium plasma: toward sustainable ammonia production *ACS Sustain. Chem. Eng.* **8** 2996–3004

[246] Toth J R, Abuyazid N H, Lacks D J, Renner J N and Sankaran R M 2020 A plasma-water droplet reactor for process-intensified, continuous nitrogen fixation at atmospheric pressure *ACS Sustain. Chem. Eng.* **8** 14845–54

[247] Pattyn C, Maira N, Buddhadasa M, Vervloessem E, Iséni S, Roy N C, Remy A, Delplancke M-P, De Geyter N and Reniers F 2022 Disproportionation of nitrogen induced by DC plasma-driven electrolysis in a nitrogen atmosphere *Green Chem.* **24** 7100–12

[248] Hawtof R, Ghosh S, Guarr E, Xu C, Mohan Sankaran R and Renner J N 2019 Catalyst-free, highly selective synthesis of ammonia from nitrogen and water by a plasma electrolytic system *Sci. Adv.* **5** eaat5778

[249] Indumathy B, Ananthanarasimhan J, Rao L, Yugeswaran S and Ananthapadmanabhan P 2022 Catalyst-free production of ammonia by means of interaction between a gliding arc plasma and water surface *J. Appl. Phys.* **55** 395501

[250] Peng P *et al* 2019 Plasma *in situ* gas–liquid nitrogen fixation using concentrated high-intensity electric field *J. Phys. D: Appl. Phys.* **52** 494001

[251] Lamichhane P, Paneru R, Nguyen L N, Lim J S, Bhartiya P, Adhikari B C, Mumtaz S and Choi E H 2020 Plasma-assisted nitrogen fixation in water with various metals *React. Chem. Eng.* **5** 2053–7

[252] Khezami L, Nguyen-Tri P, Saoud W A, Bouzaza A, El Jery A, Nguyen D D, Gupta V K and Assadi A A 2021 Recent progress in air treatment with combined photocatalytic/plasma processes: a review *J. Environ. Manage.* **299** 113588

[253] Sakakura T, Uemura S, Hino M, Kiyomatsu S, Takatsuji Y, Yamasaki R, Morimoto M and Haruyama T 2018 Excitation of H_2O at the plasma/water interface by UV irradiation for the elevation of ammonia production *Green Chem.* **20** 627–33

[254] Meng Z, Yao J-X, Sun C-N, Kang X, Gao R, Li H-R, Bi B, Zhu Y-F, Yan J-M and Jiang Q 2022 Efficient ammonia production beginning from enhanced air activation *Adv. Energy Mater.* **12** 2202105

[255] Kumari S, Pishgar S, Schwarting M E, Paxton W F and Spurgeon J M 2018 Synergistic plasma-assisted electrochemical reduction of nitrogen to ammonia *Chem. Commun.* **54** 13347–50

[256] Sharma R K, Patel H, Mushtaq U, Kyriakou V, Zafeiropoulos G, Peeters F, Welzel S, van de Sanden M C M and Tsampas M N 2020 Plasma activated electrochemical ammonia synthesis from nitrogen and water *ACS Energy Lett.* **6** 313–9

[257] Wu A *et al* 2021 Direct ammonia synthesis from the air via gliding arc plasma integrated with single atom electrocatalysis *Appl. Catal.* B **299** 120667

J. Phys. D: Appl. Phys. **57** (2024) 503002

Topical Review

[258] Zheng J *et al* 2023 Enhanced NH$_3$ synthesis from air in a plasma tandem-electrocatalysis system using plasma-engraved N-doped defective MoS$_2$ *JACS Au* **3** 1328–36

[259] Liu W, Xia M, Zhao C, Chong B, Chen J, Li H, Ou H and Yang G 2024 Efficient ammonia synthesis from the air using tandem non-thermal plasma and electrocatalysis at ambient conditions *Nat. Commun.* **15** 3524

[260] Kong X, Ni J, Song Z, Yang Z, Zheng J, Xu Z, Qin L, Li H, Geng Z and Zeng J 2024 Synthesis of hydroxylamine from air and water via a plasma-electrochemical cascade pathway *Nat. Sustain.* **7** 1–9

[261] Yayci A, Baraibar Á G, Krewing M, Fueyo E F, Hollmann F, Alcalde M, Kourist R and Bandow J E 2020 Plasma-driven *in situ* production of hydrogen peroxide for biocatalysis *ChemSusChem* **13** 2072–9

[262] Wapshott-Stehli H L and Grunden A M 2021 *In situ* H$_2$O$_2$ generation methods in the context of enzyme biocatalysis *Enzyme Microb. Technol.* **145** 109744

[263] Yayci A, Dirks T, Kogelheide F, Alcalde M, Hollmann F, Awakowicz P and Bandow J E 2020 Microscale atmospheric pressure plasma jet as a source for plasma-driven biocatalysis *ChemCatChem* **12** 5893–7

[264] Wapshott-Stehli H L, Myers B G, Herrera Quesada M J, Grunden A and Stapelmann K 2022 Plasma-driven biocatalysis: *in situ* hydrogen peroxide production with an atmospheric pressure plasma jet increases the performance of OleTJE when compared to adding the same molar amount of hydrogen peroxide in bolus *Plasma Process. Polym.* **19** 2100160

[265] Schüttler S, Schöne A L, Jeß E, Gibson A R and Golda J 2024 Production and transport of plasma-generated hydrogen peroxide from gas to liquid *Phys. Chem. Chem. Phys.* **26** 8255–72